Molecular and Clinical Implications of *IDH1* and *EGFR* Mutations in Gliomas

Ya Gao

Molecular and Clinical Implications of *IDH1* and *EGFR* Mutations in Gliomas

-

Moleculaire en klinische implicaties van IDH1- en EGFR-mutaties in gliomen

Thesis

To obtain the degree of Doctor from the
Erasmus University Rotterdam
by the command of the
rector magnificus

Prof.dr. R.C.M.E. Engels

and in accordance with the decision of the Doctoral Board.
The public defense shall be held on
Wednesday, 13th February 2019 at 9:30

by Ya Gao

born in Jinan, Shandong, China

Erasmus University Rotterdam

DOCTORAL COMMITTEE

Promotor   Prof. Dr. P.A.E. Sillevis Smitt

Members   Prof. Dr. Ir. W. M. Martens
                Prof. Dr. R. Willemsen
                Prof. Dr. J.V.M.G.Bovée

Co-promotors   Dr. P. J. French
                Dr. M. L. Lamfers

TABLE OF CONTENTS

Chapter 1

General Introduction

1.   DIFFUSE GLIOMAS

Diffuse gliomas are the most common type of malignant brain tumors in adults, with an incidence of ~ 5 per 100 000 adults in the United States each year (1, 2). In the past decade, diffuse gliomas were classified into astrocytoma, oligodendroglioma and oligoastrocytoma based on histological features described by the World Health Organization (WHO) in 2007 (3). Diffuse gliomas are graded from II to IV. Grade II/III gliomas are classified as low grade gliomas (LGG) (3). Grade IV diffuse gliomas are the most aggressive form of gliomas, also known as glioblastoma multiforme (GBM). GBMs are further stratified into primary (those that arise de novo, and comprise $\sim 90\%$ of all GBMs) and secondary GBMs (those that progress from gliomas of lower grades).

Treatment decisions are dependent on the subtype of gliomas. Standard treatments for diffuse glioma patients include surgical resection followed by either radiotherapy (RT), chemotherapy (usually temozolomide or TMZ) or a combination thereof (4-6). However, current treatment strategy has limited improvement on the overall survival of patients (~ 6 month for RT and 3 months for TMZ in GBM) and almost all patients eventually die from disease progression (7-9).

A major problem of the WHO 2007 classification system based on histological appearance has been the significant intra- and inter-observer variation (10, 11). The technological advances in sequencing technology have led to the identification of almost all cancer genes in gliomas. Interestingly some of the genetic changes segregate in defined histological subtypes but correlate better with patient survival than the histological classification of gliomas (12-15). For example, *isocitrate dehydrogenase 1/2* (*IDH1/2*) mutations occur in 60-80% of Grade II/III gliomas. However, tumors with wildtype *IDH* have a significantly worse prognosis compared with *IDH*-mutated, even within tumors of identical grade (Fig. 1). Primary GBMs (pGBM), are mainly *IDH*-wildtype and they have a median overall survival of 9.9 months (16). Secondary GBMs (sGBM) account for 10% of GBMs and they often harbor mutations in *IDH* and have a better prognosis compared with the *IDH* wild-type GBMs, with a median overall survival of 24 months (16).

1p/19q co-deletion has been associated with oligodendroglial histological features and this patient group was more responsive to chemotherapy than those with intact 1p/19q (6, 17, 18). Molecular alterations in the *alpha thalassemia/mental retardation syndrome X-linked* (*ATRX*) or *tp53* gene have been identified in a more astrocytic-like subset of Grade II/III gliomas and are almost always mutually exclusive with 1p/19q co-deleted gliomas.
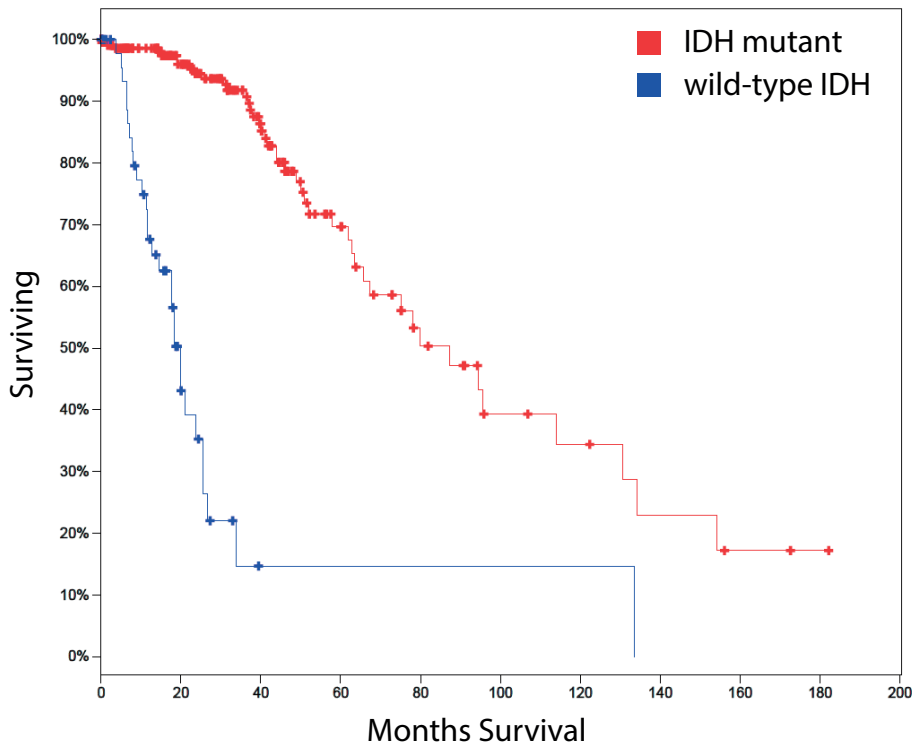
Figure 1. Diffuse glioma patients with mutations in IDH have a better prognosis than the ones with wild-type IDH (TCGA database_283 LGG samples).

The improvement in prognostic classification of gliomas by the molecular markers has led to an update of the WHO classification in 2016. In this update, gliomas are firstly divided into astrocytoma, oligoastrocytoma, oligodendroglioma and GBM based on histology. They are further classified using molecular markers including 1p/19q co-deletion, mutations in *IDH1/2* and *alpha thalassemia/mental retardation syndrome X-linked* (*ATRX*)/*TP53* (Fig. 2) (16). For example, the combination of mutations in both *IDH* and *TP53* defines a molecular astrocytic group of gliomas and the combination of *IDH* mutations and 1p/19q co-deletion defines a molecular oligodendritic group of gliomas. Within histologically identified GBMs, *IDH* mutational status separates pGBM from sGBM.

Besides the molecular markers incorporated in the WHO 2016 classification for central nervous system (CNS) tumors, other molecular markers have been identified that are significantly associated with classification and clinical outcome (15). For example, increased telomerase activity has been discovered in several malignancies including melanomas, liposarcomas and hepatocellular carcinomas (19-21). In diffuse gliomas,
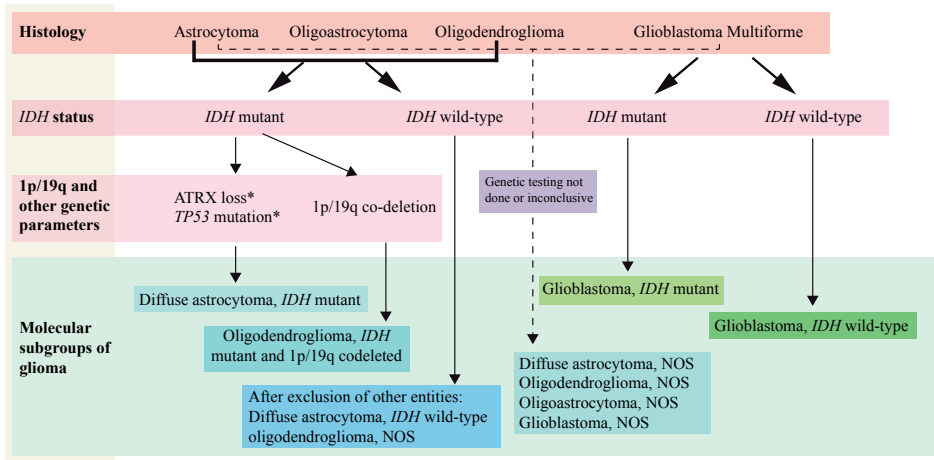
Figure 2. 2016 WHO classification for diffused gliomas using histological and genetic features (16).

mutations in two different genes result in an increased telomere length: mutations in the *ATRX* gene and in the *telomerase reverse transcriptase* (*TERT*) promoter. Mutations in the *TERT* promoter region are present in almost all GBMs and oligodendroglial tumors (28, 29).

Apart from the prognostic biomarkers listed above, there are only few biomarkers that predict response to treatment. Of those, MGMT-promoter methylation is the most robust and is predictive of response to TMZ. TMZ is a commonly used chemotherapy agent which catalyzes alkylation of thymine and guanine, leading to DNA damages and initiation of apoptosis (22). O6-methylguanine-DNA methyltransferase (MGMT) mediates DNA damage repair system by removing alkyl groups and thus prevents apoptosis (23). Therefore patients with MGMT loss showed relatively better responses to TMZ treatment (24). In diffuse gliomas, MGMT promoter methylation has been identified in about 80 % LGGs and 40 % GBMs (25).

2.   ISOCITRATE DEHYDROGENASE

Isocitrate dehydrogenase (IDH) catalyzes conversion of isocitrate to α-ketoglutarate (αKG) using NAD(P)$^+$ as a co-factor (Fig. 3, left panel) (26). IDH has three isozymes, IDH1, IDH2 and IDH3. Both IDH1 and IDH2 function as homodimers using NADP + as co-factors. They differ with respect to their subcellular localization with IDH1 being localized in the cytoplasm and peroxisomes and IDH2 in mitochondria. IDH3 func-

tions as a heterotetramer in the mitochondria using NAD^+ as its oxidizing agent and is involved in the citric acid cycle for ATP production (27).

In 2008, one of the first genomic sequencing projects in GBM identified mutations in *IDH1* in 12 % of these tumors (28). As mentioned, *IDH1* mutations correlated with better survival in GBM patients. Subsequent whole genome sequencing efforts have identified *IDH1/2* mutations in multiple malignancies including LGGs, acute myeloid leukemia (AML), chondrosarcomas and cholangiocarcinomas (29-32). *IDH* mutations are a hallmark of LGGs. In gliomas, most of the identified mutations in *IDH* are in *IDH1* and over 90 % of reported *IDH1* mutations are a missense mutation, where arginine at position 132 is replaced by a histidine (*IDH1^{R132H}*). Some patients in whom no mutations in *IDH1* were identified harbored mutations in the *IDH2* gene. Mutations in *IDH2* affect the amino acid R172, an amino acid that is analogous to R132 in IDH1 (29).

The *IDH1^{R132H}* mutations are mostly heterozygous and the generated mutant enzyme is likely to dimerize with the wildtype counterpart (Fig. 3, right panel). Mutant IDH1 uses αKG as a substrate to produce D-2hydroxyglutarate or D2HG (33). D2HG shares structural similarity with αKG and the accumulation of D2HG inhibits, via competitive inhibition, a number of αKG-dependent enzymes. As a cellular key component, αKG is involved in a wide range of pathways including regulating epigenetic modifications.
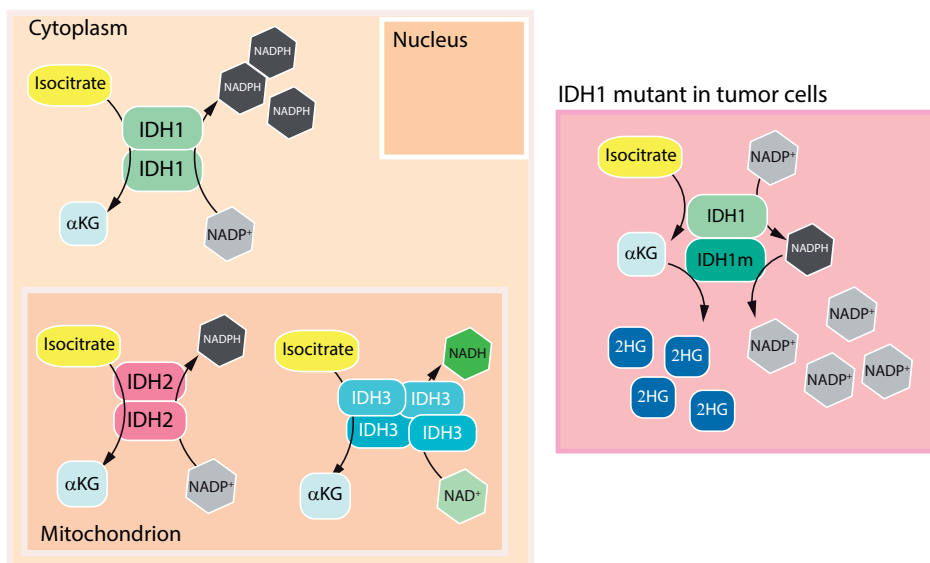

Figure 3. IDH in normal and tumor cells

Examples include Tet methylcytosine dioxygenase 2 (TET2) and Lysine Demethylase 4A (KDM4A)/JMJD2A, enzymes involved in the demethylation of DNA and histones (34-36). The increased level of D2HG also affects the hydroxylation of HIF-1α by inhibiting the Egl nine homolog 1 (EGLN1) prolyl hydroxylase (37), which leads to an upregulation of HIF1α-inducible genes including *vascular endothelial growth factor* (*VEGF*) (38, 39). It should be noted that, due to the different affinities for D2HG, the αKG-dependent enzymes are affected at various levels (35, 36). As a result of the competitive inhibition of αKG-dependent oxygenases by D2HG, *IDH1*-mutant cells ultimately remain in an undifferentiated state (40).

Since IDH1 is thought to play a role in oncogenesis and D2HG production is the key activity of mutant IDH1, several groups have tried to identify mutant IDH1 inhibitors. The first report came from *Popovici-Muller et al.* describing a series compounds with almost 90 % inhibition of D2HG production. The most promising compound also proved active in a U87 glioblastoma xenograft mouse model (41, 42). IDH1 and IDH2 inhibitors are currently being tested in clinical trials (43). A recent clinical trial for relapsed or refractory AML patients showed that treatment with IDH1 inhibitor, ivosidenib was correlated with persistent remission (44). Results of the trials for gliomas have not been reported yet.

However, targeting *IDH* mutations by decreasing D2HG production has been rising concerns and *in vitro* and *in vivo* studies have shown quite conflicting results. For example, some research groups showed decreased proliferation, less colony formation and increased differentiation after the inhibitor treatment to glioma, AML and chondrosarcoma cell lines and their corresponding xenograft models (45-47). On the other hand, in the sarcoma cell line H1060 that harbors an endogenous $IDH1^{R132C}$ mutation, inhibiting D2HG production did not affect the oncogenic properties such as proliferation or migration (48). Additionally, *Molenaar et al.* suggested that D2HG sensitizes tumor cells to ionizing radiation (IR) and inhibiting D2HG production resulted in decreased sensitivity to IR (49). Taken all studies together, other therapeutic targets or treatment strategies for *IDH*-mutated tumors remain to be characterized.

Understanding the molecular mechanism of gliomagenesis driven by *IDH* mutations is a key to seeking potential therapeutic targets. However, understanding the molecular mechanisms of mutant IDH1 has been hampered by the lack of good *in vitro* and *in vivo* model systems. It has been suggested that glioma cells with *IDH1* mutations cannot be propagated in a standard laboratory setting (50, 51), though few successful cultures have been reported (52).

To date, only few animal models have been described for *IDH* mutations in gliomas. One of the first attempts using a brain-specific *IDH1*-mutant knock-in mouse model was embryonically lethal due to D2HG-induced defects in collagen maturation (53). No glial tumors were formed in this model system.

In 2013, *Leenders et al.* reported on glioma xenografts using a patient derived high-grade oligodendroglioma cell line with $IDH1^{R132H}$ mutation (54). In a *Drosophila* model, UAS-Idh-R195H, an $IDH1^{R132H}$ mutation homologue, was induced, which resulted in activation of *tp53* expression and subsequently led to neuronal degeneration and defects in wing expansion (55). Nevertheless, none of the published *in vivo* model systems have generated gliomas by introducing CNS-specific expression of *IDH* mutations alone (53, 55-57).

3.   EPIDERMAL GROWTH FACTOR RECEPTOR

Epidermal growth factor receptor or EGFR, is a transmembrane receptor tyrosine kinase protein. The protein is activated following binding of ligands which include epidermal growth factor (EGF), transforming growth factor α (TGFα) and amphiregulin (58, 59). Activated EGFR triggers several signaling cascades including MAPK, AKT and STAT pathways. Activation of these pathways ultimately promote cell differentiation and proliferation (60, 61). Abnormal EGFR activities have been identified in several cancer types including gliomas and pulmonary adenocarcinoma (62, 63). *EGFR* amplification and mutations have been reported in about 57 % pGBM patients (64). High copy DNA amplification in gliomas is often seen as double-minutes (extrachromosomal copies of the gene). A subset of GBMs with EGFR amplification harbor additional mutations such as *EGFR variant III* (*EGFRvIII*, an intragenic deletion of exons 2-7). This mutation results in constitutive activation of the receptor (65). Targeted therapies for EGFR including monoclonal antibodies or tyrosine kinase inhibitors have been tested in multiple phase II clinical trials for pGBM patients but did not show significant improvement on overall survival (66, 67).

4.   SCOPE OF THIS THESIS

To improve the clinical outcome of glioma patients, there is considerable need to discover novel treatment options for patients. This firstly requires better understanding of the molecular mechanism of the driver mutations in each subgroup of gliomas.

In **Chapter 2 and 3**, we report on the creation of *in vitro* and *in vivo* model systems for understanding the function of driver mutation *IDH1* in LGG. This includes (a) a transgenic zebrafish model with CNS-specific expression of mutations in *IDH1* and (b) short-term primary glioma culture systems using gliomas with *IDH1* mutations. Both model systems showed increased levels of D2HG due to mutations in *IDH1* and can be used as drug screen model systems targeting mutations in *IDH1*. Our *in vivo* model suggests that expression of *IDH1* mutation alone at the early embryonic stage during zebrafish development is insufficient to promote gliomagenesis and even combining *IDH1* mutation with *Tp53* mutation did not increase the tumorigenesis incidences.

In **Chapters 4** and **5**, we further studied the molecular pathways affected by driver mutations in LGG and GBM. For both *IDH1* and *EGFR* mutations, we identified novel binding partners. We discovered that NF-kB, is a novel pathway affected by D2HG produced by mutant IDH1 enzyme, which ultimately may explain why *IDH*-mutated glioma cells keep on proliferating. To study tumor-specific effects of *EGFR* mutations in GBM, we made different *EGFR* clones harboring mutations that are either common to GBM or lung cancer. Our results suggest that each mutation has different binding partners and subsequent activation of downstream pathways. These results argue for the development of mutation specific inhibitors.

Surgical resection of recurrent GBMs is performed only in a minority of patients and treatment strategies using targeted-therapy are heavily dependent on the molecular data of primary tumors. In **Chapter 6** we showed that most of *EGFR* amplification in the primary tumor was retained at tumor recurrence therefore indicates that molecular data obtained in the primary tumor can be used to predict the *EGFR* status of the recurrent tumor. However, half of the *EGFRvIII* expression in the initial tumor is not retained in the recurrent tumor. A final chapter describes gene-expression analysis of samples included in the EORTC22033-26033 clinical trial. We showed that previously defined intrinsic glioma subtypes, subtypes based on unsupervised expression analysis of gene expression data, are prognostic for progression-free survival in EORTC22033-26033 clinical trial samples.

REFERENCES

1. Ostrom QT, Gittleman H, Liao P, Rouse C, Chen Y, Dowling J, et al. CBTRUS statistical report: primary brain and central nervous system tumors diagnosed in the United States in 2007-2011. Neuro Oncol. 2014;16 Suppl 4:iv1-63.

2. Schwartzbaum JA, Fisher JL, Aldape KD, Wrensch M. Epidemiology and molecular pathology of glioma. Nat Clin Pract Neurol. 2006;2:494-503; quiz 1 p following 16.

3. Louis DN, Ohgaki H, Wiestler OD, Cavenee WK, Burger PC, Jouvet A, et al. The 2007 WHO classification of tumours of the central nervous system. Acta Neuropathol. 2007;114:97-109.

4. Soffietti R, Baumert BG, Bello L, von Deimling A, Duffau H, Frenay M, et al. Guidelines on management of low-grade gliomas: report of an EFNS-EANO Task Force. Eur J Neurol. 2010;17:1124-33.

5. Stupp R, Mason WP, van den Bent MJ, Weller M, Fisher B, Taphoorn MJ, et al. Radiotherapy plus concomitant and adjuvant temozolomide for glioblastoma. N Engl J Med. 2005;352:987-96.

6. van den Bent MJ, Brandes AA, Taphoorn MJ, Kros JM, Kouwenhoven MC, Delattre JY, et al. Adjuvant procarbazine, lomustine, and vincristine chemotherapy in newly diagnosed anaplastic oligodendroglioma: long-term follow-up of EORTC brain tumor group study 26951. J Clin Oncol. 2013;31:344-50.

7. Mirimanoff RO, Gorlia T, Mason W, Van den Bent MJ, Kortmann RD, Fisher B, et al. Radiotherapy and temozolomide for newly diagnosed glioblastoma: recursive partitioning analysis of the EORTC 26981/22981-NCIC CE3 phase III randomized trial. J Clin Oncol. 2006;24:2563-9.

8. Buckner JC, Shaw EG, Pugh SL, Chakravarti A, Gilbert MR, Barger GR, et al. Radiation plus Procarbazine, CCNU, and Vincristine in Low-Grade Glioma. N Engl J Med. 2016;374:1344-55.

9. van den Bent MJ, Carpentier AF, Brandes AA, Sanson M, Taphoorn MJ, Bernsen HJ, et al. Adjuvant procarbazine, lomustine, and vincristine improves progression-free survival but not overall survival in newly diagnosed anaplastic oligodendrogliomas and oligoastrocytomas: a randomized European Organisation for Research and Treatment of Cancer phase III trial. J Clin Oncol. 2006;24:2715-22.

10. Muragaki Y, Chernov M, Maruyama T, Ochiai T, Taira T, Kubo O, et al. Low-grade glioma on stereotactic biopsy: how often is the diagnosis accurate? Minim Invasive Neurosurg. 2008;51:275-9.

11. Jackson RJ, Fuller GN, Abi-Said D, Lang FF, Gokaslan ZL, Shi WM, et al. Limitations of stereotactic biopsy in the initial management of gliomas. Neuro Oncol. 2001;3:193-200.

12. Phillips HS, Kharbanda S, Chen R, Forrest WF, Soriano RH, Wu TD, et al. Molecular subclasses of high-grade glioma predict prognosis, delineate a pattern of disease progression, and resemble stages in neurogenesis. Cancer Cell. 2006;9:157-73.

13. Verhaak RG, Hoadley KA, Purdom E, Wang V, Qi Y, Wilkerson MD, et al. Integrated genomic analysis identifies clinically relevant subtypes of glioblastoma characterized by abnormalities in PDGFRA, IDH1, EGFR, and NF1. Cancer Cell. 2010;17:98-110.

14. Freije WA, Castro-Vargas FE, Fang Z, Horvath S, Cloughesy T, Liau LM, et al. Gene expression profiling of gliomas strongly predicts survival. Cancer Res. 2004;64:6503-10.

15. Erdem-Eraslan L, Gravendeel LA, de Rooi J, Eilers PH, Idbaih A, Spliet WG, et al. Intrinsic molecular subtypes of glioma are prognostic and predict benefit from adjuvant procarbazine, lomustine, and vincristine chemotherapy in combination with other prognostic factors in anaplastic oligodendroglial brain tumors: a report from EORTC study 26951. J Clin Oncol. 2013;31:328-36.

16. Louis DN, Perry A, Reifenberger G, von Deimling A, Figarella-Branger D, Cavenee WK, et al. The 2016 World Health Organization Classification of Tumors of the Central Nervous System: a summary. Acta Neuropathol. 2016;131:803-20.

17. Jenkins RB, Blair H, Ballman KV, Giannini C, Arusell RM, Law M, et al. A t(1;19)(q10;p10) mediates the combined deletions of 1p and 19q and predicts a better prognosis of patients with oligodendroglioma. Cancer Res. 2006;66:9852-61.

18. Cairncross G, Wang M, Shaw E, Jenkins R, Brachman D, Buckner J, et al. Phase III trial of chemoradiotherapy for anaplastic oligodendroglioma: long-term results of RTOG 9402. J Clin Oncol. 2013;31:337-43.

19. Huang FW, Hodis E, Xu MJ, Kryukov GV, Chin L, Garraway LA. Highly recurrent TERT promoter mutations in human melanoma. Science. 2013;339:957-9.

20. Koelsche C, Renner M, Hartmann W, Brandt R, Lehner B, Waldburger N, et al. TERT promoter hotspot mutations are recurrent in myxoid liposarcomas but rare in other soft tissue sarcoma entities. J Exp Clin Cancer Res. 2014;33:33.

21. Chen YL, Jeng YM, Chang CN, Lee HJ, Hsu HC, Lai PL, et al. TERT promoter mutation in re-sectable hepatocellular carcinomas: a strong association with hepatitis C infection and absence of hepatitis B infection. Int J Surg. 2014;12:659-65.

22. Stevens MF, Hickman JA, Langdon SP, Chubb D, Vickers L, Stone R, et al. Antitumor activity and pharmacokinetics in mice of 8-carbamoyl-3-methyl-imidazo[5,1-d]-1,2,3,5-tetrazin-4(3H)-one (CCRG 81045; M & B 39831), a novel drug with potential as an alternative to dacarbazine. Cancer Res. 1987;47:5846-52.

23. Balmforth AJ, Ball SG, Freshney RI, Graham DI, McNamee HB, Vaughan PF. D-1 dopaminergic and beta-adrenergic stimulation of adenylate cyclase in a clone derived from the human astro-cytoma cell line G-CCM. J Neurochem. 1986;47:715-9.

24. van Nifterik KA, van den Berg J, van der Meide WF, Ameziane N, Wedekind LE, Steenbergen RDM, et al. Absence of the MGMT protein as well as methylation of the MGMT promoter predict the sensitivity for temozolomide. Brit J Cancer. 2010;103:29-35.

25. Cohen AL, Colman H. Glioma biology and molecular markers. Cancer Treat Res. 2015;163:15-30.

26. Muro-Pastor MI, Florencio FJ. NADP(+)-isocitrate dehydrogenase from the cyanobacterium Anabaena sp. strain PCC 7120: purification and characterization of the enzyme and cloning, sequencing, and disruption of the icd gene. J Bacteriol. 1994;176:2718-26.

27. Hartong DT, Dange M, Mcgee TL, Berson EL, Dryja TP, Colman RF. Insights from retinitis pigmentosa into the roles of isocitrate dehydrogenases in the Krebs cycle. Nature Genetics. 2008;40:1230-4.

28. Parsons DW, Jones S, Zhang X, Lin JC, Leary RJ, Angenendt P, et al. An integrated genomic analysis of human glioblastoma multiforme. Science. 2008;321:1807-12.

29. Yan H, Parsons DW, Jin G, McLendon R, Rasheed BA, Yuan W, et al. IDH1 and IDH2 muta-tions in gliomas. N Engl J Med. 2009;360:765-73.

30. Amary MF, Bacsi K, Maggiani F, Damato S, Halai D, Berisha F, et al. IDH1 and IDH2 mutations are frequent events in central chondrosarcoma and central and periosteal chondromas but not in other mesenchymal tumours. J Pathol. 2011;224:334-43.

31. Watanabe T, Nobusawa S, Kleihues P, Ohgaki H. IDH1 mutations are early events in the devel-opment of astrocytomas and oligodendrogliomas. Am J Pathol. 2009;174:1149-53.

32. Shang Z, Wang D, Xiao M, Geng Z, Wang HX, Wang J, et al. [Detection of isocitrate dehydrogenase 1 gene mutation in 205 AML patients and its clinical significance]. Zhongguo Shi Yan Xue Ye Xue Za Zhi. 2012;20:1307-11.

33. Dang L, White DW, Gross S, Bennett BD, Bittinger MA, Driggers EM, et al. Cancer-associated IDH1 mutations produce 2-hydroxyglutarate. Nature. 2009;462:739-44.

34. Figueroa ME, Abdel-Wahab O, Lu C, Ward PS, Patel J, Shih A, et al. Leukemic IDH1 and IDH2 mutations result in a hypermethylation phenotype, disrupt TET2 function, and impair hematopoietic differentiation. Cancer Cell. 2010;18:553-67.

35. Xu W, Yang H, Liu Y, Yang Y, Wang P, Kim SH, et al. Oncometabolite 2-hydroxyglutarate is a competitive inhibitor of alpha-ketoglutarate-dependent dioxygenases. Cancer Cell. 2011;19:17-30.

36. Chowdhury R, Yeoh KK, Tian YM, Hillringhaus L, Bagg EA, Rose NR, et al. The oncometabolite 2-hydroxyglutarate inhibits histone lysine demethylases. Embo Rep. 2011;12:463-9.

37. Koivunen P, Lee S, Duncan CG, Lopez G, Lu G, Ramkissoon S, et al. Transformation by the (R)-enantiomer of 2-hydroxyglutarate linked to EGLN activation. Nature. 2012;483:484-8.

38. Fu Y, Zheng S, Zheng Y, Huang R, An N, Liang A, et al. Glioma derived isocitrate dehydrogenase-2 mutations induced up-regulation of HIF-1alpha and beta-catenin signaling: possible impact on glioma cell metastasis and chemo-resistance. Int J Biochem Cell Biol. 2012;44:770-5.

39. Zhao S, Lin Y, Xu W, Jiang W, Zha Z, Wang P, et al. Glioma-derived mutations in IDH1 dominantly inhibit IDH1 catalytic activity and induce HIF-1alpha. Science. 2009;324:261-5.

40. Lu C, Ward PS, Kapoor GS, Rohle D, Turcan S, Abdel-Wahab O, et al. IDH mutation impairs histone demethylation and results in a block to cell differentiation. Nature. 2012;483:474-8.

41. Davis M, Pragani R, Popovici-Muller J, Gross S, Thorne N, Salituro F, et al. ML309: A potent inhibitor of R132H mutant IDH1 capable of reducing 2-hydroxyglutarate production in U87 MG glioblastoma cells. 2010.

42. Popovici-Muller J, Saunders JO, Salituro FG, Travins JM, Yan S, Zhao F, et al. Discovery of the First Potent Inhibitors of Mutant IDH1 That Lower Tumor 2-HG in Vivo. ACS Med Chem Lett. 2012;3:850-5.

43. Fujii T, Khawaja MR, DiNardo CD, Atkins JT, Janku F. Targeting isocitrate dehydrogenase (IDH) in cancer. Discov Med. 2016;21:373-80.

44. DiNardo CD, Stein EM, de Botton S, Roboz GJ, Altman JK, Mims AS, et al. Durable Remissions with Ivosidenib in IDH1-Mutated Relapsed or Refractory AML. N Engl J Med. 2018;378:2386-98.

45. Li L, Paz AC, Wilky BA, Johnson B, Galoian K, Rosenberg A, et al. Treatment with a Small Molecule Mutant IDH1 Inhibitor Suppresses Tumorigenic Activity and Decreases Production of the Oncometabolite 2-Hydroxyglutarate in Human Chondrosarcoma Cells. PLoS One. 2015;10:e0133813.

46. Rohle D, Popovici-Muller J, Palaskas N, Turcan S, Grommes C, Campos C, et al. An inhibitor of mutant IDH1 delays growth and promotes differentiation of glioma cells. Science. 2013;340:626-30.

47. Chaturvedi A, Cruz MMA, Jyotsana N, Sharma A, Yun HY, Gorlich K, et al. Mutant IDH1 promotes leukemogenesis in vivo and can be specifically targeted in human AML. Blood. 2013;122:2877-87.

48. Suijker J, Oosting J, Koornneef A, Struys EA, Salomons GS, Schaap FG, et al. Inhibition of mutant IDH1 decreases D-2-HG levels without affecting tumorigenic properties of chondrosarcoma cell lines. Oncotarget. 2015;6:12505-19.

49. Molenaar RJ, Botman D, Smits MA, Hira VV, van Lith SA, Stap J, et al. Radioprotection of IDH1-Mutated Cancer Cells by the IDH1-Mutant Inhibitor AGI-5198. Cancer Res. 2015;75:4790-802.

50. Piaskowski S, Bienkowski M, Stoczynska-Fidelus E, Stawski R, Sieruta M, Szybka M, et al. Glioma cells showing IDH1 mutation cannot be propagated in standard cell culture conditions. Brit J Cancer. 2011;104:968-70.

51. Balvers RK, Kleijn A, Kloezeman JJ, French PJ, Kremer A, van den Bent MJ, et al. Serum-free culture success of glial tumors is related to specific molecular profiles and expression of extracellular matrixassociated gene modules. Neuro-Oncology. 2013;15:1684-95.

52. Luchman HA, Stechishin OD, Dang NH, Blough MD, Chesnelong C, Kelly JJ, et al. An in vivo patient-derived model of endogenous IDH1-mutant glioma. Neuro Oncol. 2012;14:184-91.

53. Sasaki M, Knobbe CB, Itsumi M, Elia AJ, Harris IS, Chio, II, et al. D-2-hydroxyglutarate produced by mutant IDH1 perturbs collagen maturation and basement membrane function. Genes Dev. 2012;26:2038-49.

54. Navis AC, Niclou SP, Fack F, Stieber D, van Lith S, Verrijp K, et al. Increased mitochondrial activity in a novel IDH1-R132H mutant human oligodendroglioma xenograft model: in situ detection of 2-HG and alpha-KG. Acta Neuropathol Commun. 2013;1:18.

55. Reitman ZJ, Sinenko SA, Spana EP, Yan H. Genetic dissection of leukemia-associated IDH1 and IDH2 mutants and D-2-hydroxyglutarate in Drosophila. Blood. 2015;125:336-45.

56. Itsumi M, Inoue S, Elia AJ, Murakami K, Sasaki M, Lind EF, et al. Idh1 protects murine hepatocytes from endotoxin-induced oxidative stress by regulating the intracellular NADP/NADPH ratio. Cell Death Differ. 2015.

57. Bardella C, Al-Dalahmah O, Krell D, Brazauskas P, Al-Qahtani K, Tomkova M, et al. Expression of Idh1R132H in the Murine Subventricular Zone Stem Cell Niche Recapitulates Features of Early Gliomagenesis. Cancer Cell. 2016;30:578-94.

58. Moghal N, Sternberg PW. Multiple positive and negative regulators of signaling by the EGF-receptor. Curr Opin Cell Biol. 1999;11:190-6.

59. Barton CM, Hall PA, Hughes CM, Gullick WJ, Lemoine NR. Transforming growth factor alpha and epidermal growth factor in human pancreatic cancer. J Pathol. 1991;163:111-6.

60. Oda K, Matsuoka Y, Funahashi A, Kitano H. A comprehensive pathway map of epidermal growth factor receptor signaling. Mol Syst Biol. 2005;1:2005 0010.

61. Wells A. EGF receptor. Int J Biochem Cell Biol. 1999;31:637-43.

62. Lynch TJ, Bell DW, Sordella R, Gurubhagavatula S, Okimoto RA, Brannigan BW, et al. Activating mutations in the epidermal growth factor receptor underlying responsiveness of non-small-cell lung cancer to gefitinib. N Engl J Med. 2004;350:2129-39.

63. Barber TD, Vogelstein B, Kinzler KW, Velculescu VE. Somatic mutations of EGFR in colorectal cancers and glioblastomas. N Engl J Med. 2004;351:2883.

64. Brennan CW, Verhaak RG, McKenna A, Campos B, Noushmehr H, Salama SR, et al. The somatic genomic landscape of glioblastoma. Cell. 2013;155:462-77.

65. Wong AJ, Ruppert JM, Bigner SH, Grzeschik CH, Humphrey PA, Bigner DS, et al. Structural alterations of the epidermal growth factor receptor gene in human gliomas. Proc Natl Acad Sci U S A. 1992;89:2965-9.

66. van den Bent MJ, Brandes AA, Rampling R, Kouwenhoven MC, Kros JM, Carpentier AF, et al. Randomized phase II trial of erlotinib versus temozolomide or carmustine in recurrent glioblastoma: EORTC brain tumor group study 26034. J Clin Oncol. 2009;27:1268-74.

67. Sarkaria JN, Galanis E, Wu W, Peller PJ, Giannini C, Brown PD, et al. North Central Cancer Treatment Group Phase I trial N057K of everolimus (RAD001) and temozolomide in combination with radiation therapy in patients with newly diagnosed glioblastoma multiforme. Int J Radiat Oncol Biol Phys. 2011;81:468-75.

Chapter 2

IDH1-mutated transgenic zebrafish lines: an *in-vivo* model for drug screening and functional analysis

Ya Gao[1], Maurice de Wit[1], Eduard A. Struys[2], Herma C. Z. van der Linde[3], Gajja S. Salomons[2], Martine L. M. Lamfers[4], Rob Willemsen[3], Peter A.E. Sillevis Smitt[1] and Pim J. French[1]

[1]Department of Neurology, Erasmus MC, Rotterdam, the Netherlands
[2] Department of Clinical Chemistry, VU University Medical Center, Amsterdam the Netherlands
Departments of [3]Genetics and [4]Neurosurgery, Erasmus MC, Rotterdam, the Netherlands

ABSTRACT

Introduction

The gene encoding isocitrate dehydrogenase 1 (*IDH1*) is frequently mutated in several tumor types including gliomas. The most prevalent mutation in gliomas is a missense mutation leading to a substitution of arginine with histidine at the residue 132 (R132H). Wild type IDH1 catalyzes oxidative decarboxylation of isocitrate to α-ketoglutarate (α-KG) whereas mutant IDH1 converts α-KG into D2-hydroxyglutarate (D2HG). Unfortunately, there are few *in vivo* model systems for *IDH*-mutated tumors to study the effects of *IDH1* mutations in tumor development. We have therefore created transgenic zebrafish lines that express various *IDH1* mutants.

Materials and methods

IDH1 mutations ($IDH1^{R132H}$, $IDH1^{R132C}$ and loss-of-function mutation $IDH1^{G70D}$), $IDH1^{wildtype}$ or *eGFP* were cloned into constructs with several brain-specific promoters (*Nestin*, *Gfap* or *Gata2*). These constructs were injected into fertilized zebrafish eggs at the one-cell stage.

Results

In total more than ten transgenic zebrafish lines expressing various brain-specific *IDH1* mutations were created. A significant increase in the level of D2HG was observed in all transgenic lines expressing $IDH1^{R132C}$ or $IDH1^{R132H}$, but not in any of the lines expressing $IDH1^{wildtype}$, $IDH1^{G70D}$ or *eGFP*. No differences in 5-hydroxymethyl cytosine and mature collagen IV levels were observed between wildtype and mutant IDH1 transgenic fish. To our surprise, we failed to identify any strong phenotype, despite increased levels of the oncometabolite D2HG. No tumors were observed, even when backcrossing with *tp53*-mutant fish which suggests that additional transforming events are required for tumor formation. Elevated D2HG levels could be lowered by treatment of the transgenic zebrafish with an inhibitor of mutant IDH1 activity.

Conclusions

We have generated a transgenic zebrafish model system for mutations in *IDH1* that can be used for functional analysis and drug screening. Our model systems help understand the biology of *IDH1* mutations and its role in tumor formation.

INTRODUCTION

Somatic missense mutations in the gene encoding isocitrate dehydrogenase 1 (*IDH1*) or *IDH2* are frequently identified in various malignancies including gliomas, acute myeloid leukemia, cholangiocarcinoma, chondrosarcoma and sporadically in various other cancer types (1-8). In gliomas, *IDH1* mutations are one of the earliest genetic changes identified, preceding other common genetic aberrations such as *1p19q* co-deletion, and are therefore present in virtually all tumor cells (9-11). *IDH1* and *IDH2* mutations are almost always mutually exclusive. For glioma patients, presence of IDH mutations is of clinical relevance as patients harboring *IDH* mutated gliomas have a better survival compared to those with wildtype *IDH*. The prognostic significance of *IDH* mutations has led to its incorporation in the WHO 2016 update to classify gliomas (12). Mutations in *IDH1* are almost always heterozygous point mutations affecting the arginine at position 132 (R132). Approximately 90 % of these mutations in gliomas are *IDH1^{R132H}*.

Wildtype IDH1 is a cytoplasmic enzyme that catalyzes the oxidative decarboxylation of isocitrate to α-ketoglutarate (αKG) and uses $NADP^+$ as a co-factor (13, 14). The mutant enzyme however, uses αKG as a substrate to produce D-2-hydroxyglutarate (D2HG) with concomitant consumption of NADPH (15). The resulting accumulation of D2HG then competitively inhibits a spectrum of αKG-dependent enzymes including TET2, JMJD2 and various prolyl hydroxylases (16-18). This inhibition ultimately facilitates carcinogenesis by retaining cells in an undifferentiated and stem-like state. Because of the oncogenic role of mutant IDH1, several groups have developed compounds that specifically inhibit the activity of the mutant enzyme (19, 20). These inhibitors are currently being tested in clinical trials.

Several *IDH1^{R132H}* conditional knock-in (KI) mouse models were recently generated to further study the role of the mutant enzyme in an *in vivo* model system. Unfortunately most mice in which IDH1 mutations were conditionally expressed either died before birth or rapidly after induction of expression of the mutant enzyme (21). Nevertheless, expression of mutant IDH1 results in a retention of cells in an undifferentiated state or induces pre-cancerous lesions in cartilage or the SVZ (22-24). Despite these signs of early tumor formation, no gliomas in any of the three mouse models were thus-far identified, also not when backcrossing into a *Tp53* -mutant background (23, 25).

To further study the effects of IDH1 mutations in tumor development, we have generated transgenic zebrafish that express IDH1 mutants under the control of various CNS-specific promoters.

MATERIALS AND METHODS

Cloning

Human *pEGFP-IDH1^wildtype* and *pEGFP-IDH1^R132H* constructs were described as previous (26). *IDH1^R132C* and *IDH1^G70D* mutations were cloned by in-fusion PCR with two sets of primers, 5'-CTATCATCATAGGTTGTCATGCTTATGGGGATCAATAC-3' and 5'-CCATAAGCATGACAACCTATGATGATAGGTTTTAC-3' for *IDH1^R132C*; 5'-AGAAGCATAATGTTGACGTCAAATGTGCCAC-3' and 5'-GTGGCACATTT-GACGTCAACATTATGCTTCT-3' for *IDH1^G70D*. The whole construct was linearized and inserted into a miniTol2 vector (Addgene, plasmid #31829).

Generation of transgenic zebrafish

All experiments with zebrafish (Tupfel long fin or TL) were conducted according to the protocols approved by the Animal Experimentation Committee of the Erasmus Medical center and EU guidelines. To generate transgenic zebrafish lines expressing *GFP-IDH1^wildtype* and *GFP-IDH1^R132H* driven by different promoters (*Nestin*, *Gata2* and *Gfap*), we injected various constructs into the cells of fertilized zebrafish eggs at the one-cell stage. Embryos that showed GFP expression at 1 day post fertilization (dpf) were collected and raised to adulthood (3 months, F0) and then individually crossed with non-transgenic wildtype TL (F1). GFP expression in the F1 fish indicated that the constructs were integrated into the fish genome. The GFP-positive F1s were separately raised to adults and then interbred to generate homozygous F2. Although we did not actually test for homozygosity of our transgenic lines, we inferred this by the observation that all F2 inbred offspring expressed GFP. All F2 progenies were further inbred. The experiments were performed mainly on likely homozygous F4 zebrafish. *tp53* mutant fish (*tp53^M214K*) were described by Berghmans et al and obtained from ZFIN (ZFIN.org) (27).

Histology and Immunohistochemistry

Zebrafish embryos were fixed overnight in 4% paraformaldehyde (PFA) at 4°C and then embedded in paraffin for further histological analysis. Paraffin sections (6 μm) were stained with hematoxylin and eosin (HE). For immunohistochemistry (IHC), paraffin sections were dewaxed and hydrated followed by boiling in 10 mM sodium citrate for eight minutes and 2 times 3 minutes of boiling in a microwave oven. Prior to immunostaining, the endogenous peroxidase activity was blocked by 30% hydrogen peroxide and 12.5% sodiumazide in PBS for 30 minutes. The slides were washed in PBS and PBS+ which contained 0.5% g/ml protifar and 0.15% g/ml glycine and then incubated with primary antibody overnight at 4°C. The primary antibodies used were anti-GFP (1:2000) monoclonal antibody (Roche, Woerden, the Netherlands), 5hmC (1:

200, Active Motif, La Hulpe, Belgium) and anti-human IDH1^{R132H} (1:200) monoclonal antibody (Dianova, clone DIA H09, Huissen, the Netherlands), diluted in PBS + . The sections were then washed in PBS + and incubated with BrightVision Poly-HRP-Anti IgG (immunologic) for 60 minutes at room temperature (RT). The slides were washed in PBS + and PBS and then treated with 1:50 diluted DAB-substrate (DAKO Liquid DAB substrate-chromogen system) for 4-8 minutes, followed by counterstaining with haematoxylin and mounted in entellan. Histological images were captured using an Olympus BX40 camera.

Real-time PCR

To examine the expression of *IDH1* and *GFP* during envelopment, total RNA was extracted by dissolving embryos in 500 µl TRIzol® (Life technologies, Carlsbad, USA) and 100 µl chloroform followed by centrifugation at 12.000 g for 15 min at 4˚C. RNA in the aqueous phase was precipitated with 250 µl isopropanol and collected at 12 000 g for 10 minutes at 4˚C. The pellet was washed twice in 250 µl 75 % ethanol, centrifuged at 12 000 g for 5 minutes at 4˚C, dried and dissolved in 10 µl nuclease free water (Ambion, Thermo Scientific, Rochester, USA). For cDNA synthesis, each reaction contained 1000 ng RNA, 1 µl hexamers, 1 µl 10 mM dNTP's and milliQ water to 13 µl and was heated to 65˚C for 5 minutes and left on ice for at least 1 minute. The RNA was then treated with 4 µl 5x Firststrand buffer, 1 µl 0.1M DTT, 0.5 µl RNaseOUT and 0.5 µl DNase. The samples were heated to 37˚C for 40 minutes and further heated to 65˚C for 10 minutes. The RNAs were then reverse-transcribed by adding 1 µl Superscript III (Invitrogen, Breda, the Netherlands) and 0.5 µl RNase OUT followed by incubation at 25˚C for 5 minutes and 42˚C for one hour. 1 µl cDNA was used in a 15 µl reaction containing 7.5 µl Syber Select Mastermix (Life technologies), 1mM primers and MilliQ. The primer sequences are described in Supplementary Table 1. The reactions were performed in triplicate using a CFX96 Real-Time PCR System (Bio-Rad). The threshold cycle (Cq) for each reaction was obtained and the values were averaged. The standard deviation (SD) had to be below 0.2. The relative expression levels, of different time points in zebrafish life, were calculated. First the ΔCq of a sample was calculated; ΔCq = *IDH1* Cq mean- *β-actin* Cq mean. Then one time point was set as a reference (= 1.00) and the ΔΔCq was calculated as ΔΔCq = ΔCq reference - ΔCq unknown sample. To calculate the relative expression levels the formula 2^ ^{ΔΔCq} was used.

Protein extraction and immunoblotting

Zebrafish embryos were lysed in 500 µl HEPES-buffer containing 1x protease inhibitor (cOmplete, Thermo Scientific) and 3 µM DTT followed by homogenization by a PRO 200 homogenizer and incubated on ice for 30 minutes. 50 µg of protein was separated

by loading onto a precast SDS gel (Thermo Scientific) and electrophoresis at 150 V till loading buffer reached the bottom of the gel. Protein was then transferred to a nitrocellulose membrane in transfer buffer at 100 V, 380 mA, for 1 hour. The membrane was blocked with blocking buffer containing 1 % BSA in PBS for 1 hour at room temperature and incubated with primary antibody overnight at 4 °C with agitation. Primary antibodies used were anti-Collagen Type IV (1:1000, Abcam, Hilversum, The Netherlands) and 5hmC (1: 1000).

Microinjection of wildtype zebrafish embryos with *Gfap* constructs

20 µl of injection solution containing 350 ng of *Gfap* constructs, 30 ng/µl Tol2 transposase RNA and 0.1 % pheno-red was freshly prepared before injection. 4.2 nl of injection solution was injected into the cell of 1-cell stage embryos using a Pneumatic PicoPump (PV820, WPI). For each construct, injection was performed on 100 eggs in three independent experiments. The fertilization rate was calculated based on 30 uninjected embryos collected on the same day. The number of GFP$^+$, GFP$^-$, healthy and abnormal embryos were counted on 1dpf.

5hmC assay

Total DNA was extracted using whole fish embryos. A nitrocellulose membrane was pre-soaked in 20X SSC for 1 hour. 250 ng DNA was diluted in 150 l H2O and 150 l 20X SSC. The membrane and two layers of thick filter papers were placed on a manifold (manifold II slot-blot manifold, Cole-Parmer, Wertheim, Germany) and equilibrated with 10X SSC. DNA samples were then loaded and fixed on the membrane using a vacuum pump for 5 minutes. The membrane was air-dried and processed as described above in the immunoblotting section. Blots were stained using the 5hmC antibody (1:1000) and analyzed using ECL.

IDH1 mutant inhibitor test

Five transgenic zebrafish embryos from each line were screened for GFP expression at 1 or 2 dpf and removed from the chorion and raised in 2 ml tap water for 48 hours with either 10µM AGI-5198 (Xcess Biosciences, Inc.) in 0.1 % DMSO or 0.1 % DMSO. Zebrafish embryos were collected at 3 dpf in 25 µl of HBSS buffer for 2HG measurement.

Quantification of D/L2HG in zebrafish

To quantify the level of D- and L2HG in the zebrafish, five embryos were collected at 1, 2, 3, 5 and 6 dpf in HBSS buffer (5µl per embryo). The embryos were homogenized with a PRO 200 homogenizer and lysed with sonication before LC-MS/MS. The D and L forms of 2HG were separately measured and quantified as described previously (28).

Statistics

Differences in D- and L- 2HG levels between experimental conditions were evaluated using the students t-test. A Fisher's exact test was used to compare differences between frequencies.

RESULTS

Generation and characterization of transgenic zebrafish lines

We firstly generated transgenic lines for two constructs, *eGFP-IDH1^wildtype^* and *eGFP-IDH1^R132H^*, in which the transgene was expressed under control of a *Nestin* promoter. These constructs are referred to as Nes^{IDH1wt} and Nes^{R132H}. At least two independent lines per construct were generated to control for integration-site dependent effects.

Transgene expression was detected in the brain and spinal cord on 1, 3 and 6 days post fertilization (dpf) by fluorescent imaging (Fig. 1A and Fig. S1A) and by immunohisto-chemistry (Fig. 1B) using anti-GFP antibodies. Expression of Nes^{R132H} was confirmed using an IDH1^R132H^-mutant specific antibody (Fig. S2). As expected, this antibody did not show staining in the Nes^{IDH1wt}-fish. Expression of transgenes on 1, 2, 3 and 6 dpf was also detected on the RNA level by RT-QPCR (Fig. 1C). We then measured D2HG levels to monitor the activity of the neomorphic enzyme. Consistent with RNA and protein expression, the D2HG level in Nes^{R132H} mutant transgenic fish was elevated compared to controls (non-transgenic and Nes^{IDH1wt}) on 1-5 dpf (Fig. 1D). The increase in D2HG was virtually identical when using macro-dissected embryos (head region) compared to whole fish (Fig. S3). L2HG levels in all the transgenic lines were similar to the non-transgenic controls (Fig. 1E); indicating expression of *IDH1^R132H^* only affects D2HG levels. D2HG levels returned to normal by 21 dpf. These experiments demonstrate CNS-specific expression of *IDH1^wt^* or *IDH1^R132H^* in our transgenic zebrafish lines during development. This temporal expression pattern in the CNS is consistent with the *Nestin* promoter activity (29-31).

It has been reported that accumulation of D2HG results in DNA hypermethylation by inhibition of TET enzymes (32). In our transgenic fish, DNA methylation as determined by 5hmC antibody staining was however not affected (Fig. S4). We next screened for collagen maturation defects, as these were observed in an IDH1^R132H^-KI mouse model (21). However, western blot analysis failed to detect the presence of immature isoforms of collagen in our transgenic fish lines (Fig. S5). In summary, despite expression of the transgene (and the elevated levels of D2HG in lines expressing Nes^{R132H}), all of the
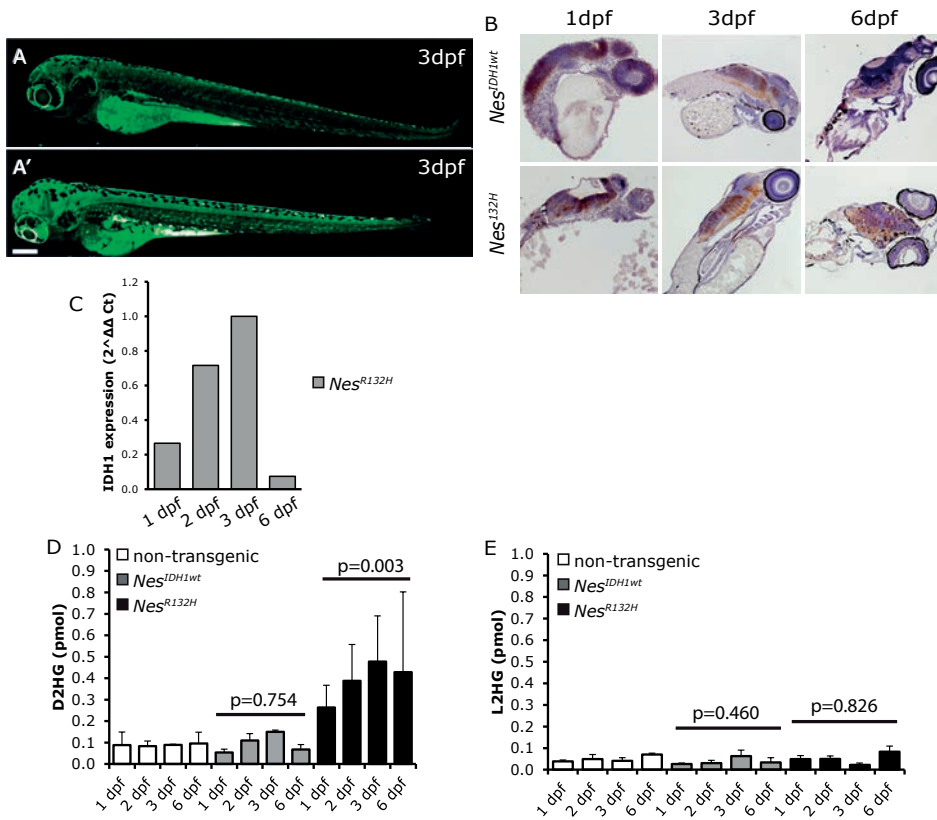
Figure 1. Characterization of Nes^{IDH1} zebrafish lines. Expression of the transgene was detected in the central nervous system (CNS) of zebrafish embryos using fluorescent imaging (A: non-transgenic wildtype zebrafish showing background auto-fluorescence staining, mainly in the yolk sac; A': Nes^{IDH1} show expression of the transgene in the CNS of 3dpf embryos). Expression was confirmed by immunochemistry staining using an anti-GFP antibody (B) and Q-PCR (C). D2HG only accumulated in Nes^{R132H} zebrafish (D, non-transgenic vs Nes^{IDH1wt}, p= 0.754, non-transgenic vs Nes^{R132H}, p= 0.003, student's t-test). L2HG levels in the transgenic lines showed no such increase (E). For Q-PCR experiments, we used a pool of five fish per time-point; D2HG and L2HG measurements were averages of two replicates using 5 fish per replicate. Scale bar: 200 μm.

zebrafish lines remained healthy without presenting any identifiable developmental abnormalities (Fig. S6).

Given the short temporal expression of *IDH1* constructs driven by the *Nestin* promoter, we cloned constructs under the control of a brain specific *Gata2* promoter. This promoter was previously used for constructing a transgenic zebrafish model for neurodegeneration (33). Three transgenic lines were generated, *pGata2-GFP-IDH1^{wt}*, *pGata2-GFP-IDH1^{R132H}* and *pGata2-GFP*. These constructs are referred to as *Gata^{IDH1wt}*, *Gata^{R132H}* and *Gata^{GFP}*. Unfortunately, we failed to observe any transgene expression in the developing (or adult) CNS in any of the lines generated. We did however observe

expression in the notochord from 1 for up to 5 dpf (Fig. S7), but, despite expression of a D2HG-producing IDH1 mutant, all fish were viable, developed normally and produced offspring. Similar to the Nes^{IDH1wt} and Nes^{R132H} fish, no gross abnormalities or (pre-) neoplastic lesions were observed. As we failed to observe expression in the CNS we did not further investigate these lines.

Because of the temporal limitations of the *Nestin* promoter and the lack of expression in the CNS using the *Gata2* promoter, we generated six additional lines, one for *eGFP-IDH1^{wildtype}*, *eGFP-IDH1^{R132H}*, *eGFP-IDH1^{G70D}* and e*GFP*, and two for *eGFP-IDH1^{R132C}*, in which the transgene was expressed under control of a *Gfap* promoter. Constructs used for these lines are referred to as *Gfap^{IDH1wt}*, *Gfap^{R132H}*, *Gfap^{R132C}*, *Gfap^{G70D}* and *Gfap^{GFP}*. The expression vector (*gfap:GFP*) has been demonstrated to have glial-specific expression in the zebrafish CNS, detectable during the embryonic stage (34). The *IDH1^{G70D}* mutation is an enzymatic null mutation that was included to serve as a non-D2HG-producing control (15, 35). The *IDH1^{R132C}* mutation was generated to study potential differences between *IDH1^{R132H}* and *IDH1^{R132C}*, and is a mutant with reportedly higher neomorphic enzymatic activity (36). Expression of the transgenes was confirmed using fluorescent imaging on 1, 3 and 5 dpf (Fig. 2A and S1B). GFP was observed in the brain and spinal cord in all the *Gfap* transgenic zebrafish lines. CNS-specific expression of the transgene was further confirmed by immunohistochemistry using anti-GFP antibodies (Fig. 2B). Expression of the transgene on the RNA level was confirmed by RT-QPCR till at least 20 dpf (Fig. 2C). There were no obvious differences in results from these assays between *IDH1^{R132H}* and *IDH1^{R132C}* transgenic zebrafish. The D2HG levels were markedly elevated in both *Gfap^{R132C}* zebrafish lines (line 84 and 85) on 3 dpf, which are about 8 and 18 times higher compared to the *Gfap^{GFP}* and *Gfap^{IDH1wt}* lines (line 73 and 92, Fig. 2D). D2HG levels in *Gfap^{G70D}* zebrafish remained similar as in *Gfap^{GFP}* and *Gfap^{IDH1wt}* lines. L2HG levels of all the IDH1 transgenic lines were similar to the *Gfap^{GFP}* control, confirming that expression of transgene only affects the D2HG level (Fig. 2E).When crossing *Gfap^{R132C}* line 85, an average of 21.1 % of generated embryos showed abnormal tail development on 1dpf, which was higher than in the *Gfap^{GFP}* (3 %) and *Gfap^{IDH1wt}* (0 %) control lines (Fig. 2F and 2G). The tail defects may be explained by the fact that the first detectable expression of *Gfap* is at 10 h post fertilization in the developing tail bud (34). However, no clear (pre-) cancerous lesion was observed in any of the zebrafish lines studies.

It is possible that *IDH1$^{R132H/R132C}$* induced a pathologic phenotype due to the site of integration of our transgene. To correct for potential integration site artifacts, we directly injected fertilized zebrafish eggs at the one-cell stage with various constructs and monitored zebrafish development. We specifically monitored tail development
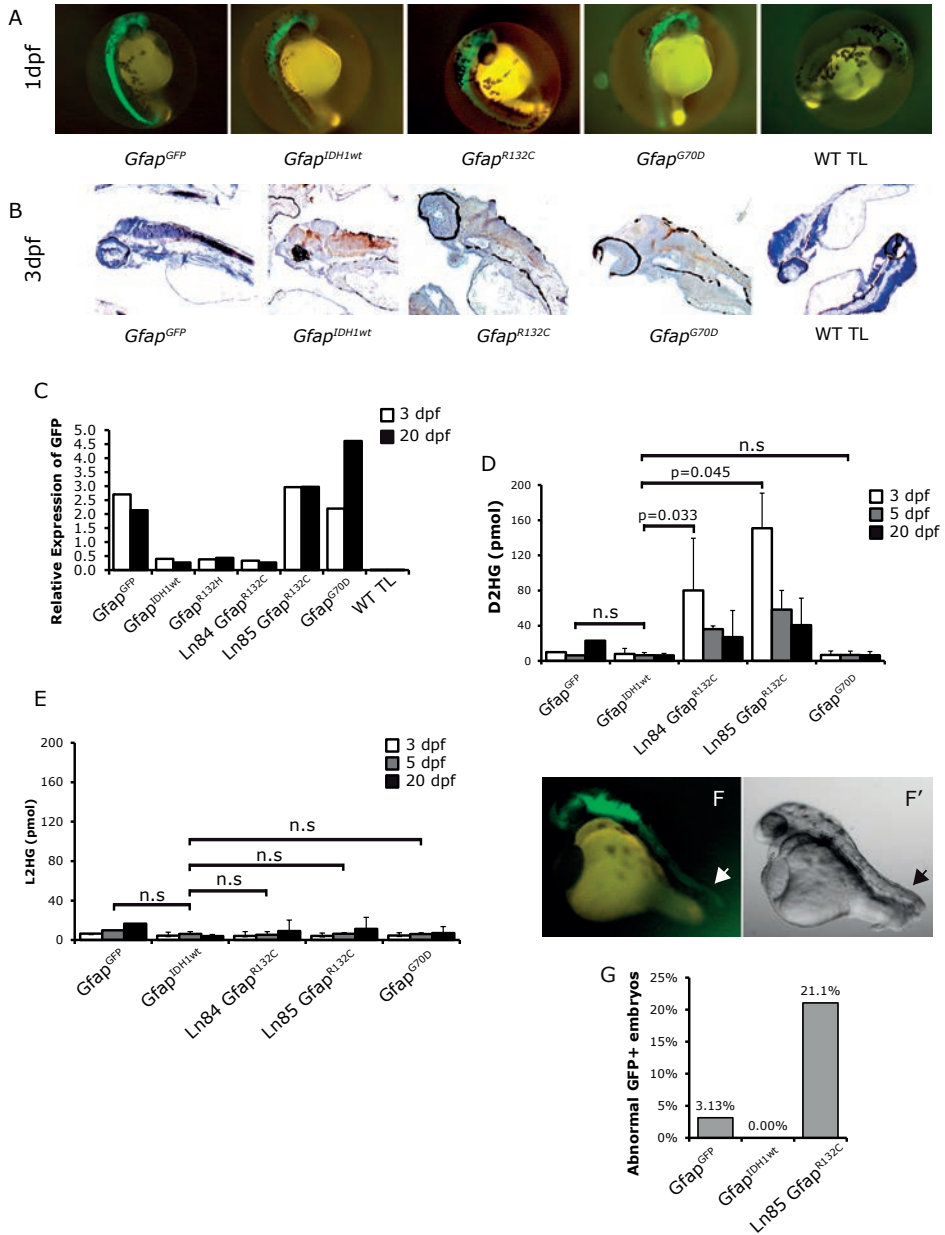
Figure 2. Characterization of *Gfap* zebrafish lines. Expression of transgene was detected using fluorescent imaging (A), immunohistochemistry with an anti-GFP antibody (B) and QPCR (C). Elevated levels of D2HG were only detected in *Gfap^R132C* lines (D). L2HG levels in the transgenic fish embryos were not affected (E). About 21% *Gfap^R132C* embryos showed defects in tail development on 1dpf (F and G). Arrow heads: the site of abnormal tail development in the *Gfap^R132C* embryos. For Q-PCR experiments, we used a pool of five (3dpf) or three (20 dpf) fish per time-point; D2HG and L2HG measurements were averages of two replicates using five (3 and 5 dpf) or three (20 dpf) fish per replicate. Scale bar: 500 μm.

in our transgenic fish. In three independent experiments, we injected fertilized eggs with $Gfap^{GFP}$, $Gfap^{IDH1wt}$ or $Gfap^{R132C}$ constructs. While most embryos injected with $Gfap^{GFP}$ remained healthy (n = 105/129, Fig. S8A and S8D), most embryos injected with the $Gfap^{R132C}$ construct were not (n = 75/85, P < 0.001, Fisher's exact test). In line with our transgenic lines, many showed an abnormal development of the tail on 1dpf. However, zebrafish embryos injected with $Gfap^{IDH1wt}$ constructs also sometimes had abnormal tail development, though the frequency was significantly lower than that of $Gfap^{R132C}$ (n = 13/24, P < 0.001).

tp53 deficient Transgenic zebrafish crossed with IDH1 mutant fish

TP53 mutations often co-occur in IDH1-mutated astrocytomas. To determine whether $Gfap^{R132C}$ affects tumor formation, we crossed the homozygous $tp53^{M214K}$ mutant transgenic zebrafish with our transgenic zebrafish lines. It was previously reported that homozygous *tp53* mutant zebrafish developed tumors (Schwannomas) at ∼ 8 months post fertilization with an incidence of 28 % (27). Although we find that heterozygous *tp53* mutant fish developed tumors (Table 1 and Fig. S9, incidence = 15 %, n = 2/13) with an average age of onset ∼ 1 year post fertilization, this incidence was not increased when the fish were crossed into a *pGfap:GFP-IDH1*^{R132H} (or ^{wt}) background, with incidence between 6 to 14.3 % regardless of the *IDH1* variants or *GFP* controls (P > 0.3 for all comparisons, Fisher's exact test). The non-CNS tumors we observe in our transgenic lines are most likely Schwannomas, as previously described (27). They are mainly in the abdominal cavity, an area where we do not see expression of our transgene. Our results therefore demonstrate that expression of mutant IDH1 does not promote tumor formation in *tp53* mutant zebrafish.

Table 1. Tumorigenesis incidence of *Gfap* fish after crossing with *Tp53* mutant

	# of generated fish	# of fish with tumor (over 1 year post fertilization)	Incidence of non-CNS-tumors (%)	Incidence of CNS-tumors (%)
Gfap^{GFP}	35	3	8.6	0
Gfap^{R132C}	30	3	10	0
Gfap^{G70D}	28	4	14.3	0
Gfap^{wt}	15	1	6	0
Heterozygous *Tp53* mutant	13	2	15	0

IDH1 mutated transgenic zebrafish as an in vivo model for drug screening

AGI-5198 is a specific inhibitor for the IDH1 mutant enzymatic activity (19). To determine whether this inhibitor also affects D2HG production *in vivo*, we applied it

to our transgenic zebrafish lines harboring different IDH1 variants under control of the *Nestin* and *Gfap* promoters at 1dpf for 48 hours. Dose-response analysis indicates maximal inhibition at 10µM AGI-5198 on the *Nes*[IDH1] transgenic zebrafish (Fig. S10). The inhibitor did not show any overt toxicity, even after prolonged (2 days) treatment. The accumulated D2HG in our *Nes*[R132H] transgenic zebrafish was decreased by 10 µM AGI-5198 to 41% of the levels prior to treatment whereas D2HG levels in the non-transgenic and *Nes*[IDH1wt] transgenic zebrafish were not affected (Fig. 3A). The D2HG levels were also markedly reduced in the *Gfap*[R132C] zebrafish line from 34.86 reduced to 8.77 pmol (25% of the D2HG level in the untreated fish (Fig. 3B)). Levels of D2HG in control transgenic lines remained low and were not affected by the inhibitor. The L2HG level in all of the treated transgenic lines was not altered (Fig. 3C and D). These data demonstrate that our transgenic zebrafish lines can be used to screen the efficacy and toxicity of drugs that inhibit IDH1 mutant enzyme activity.
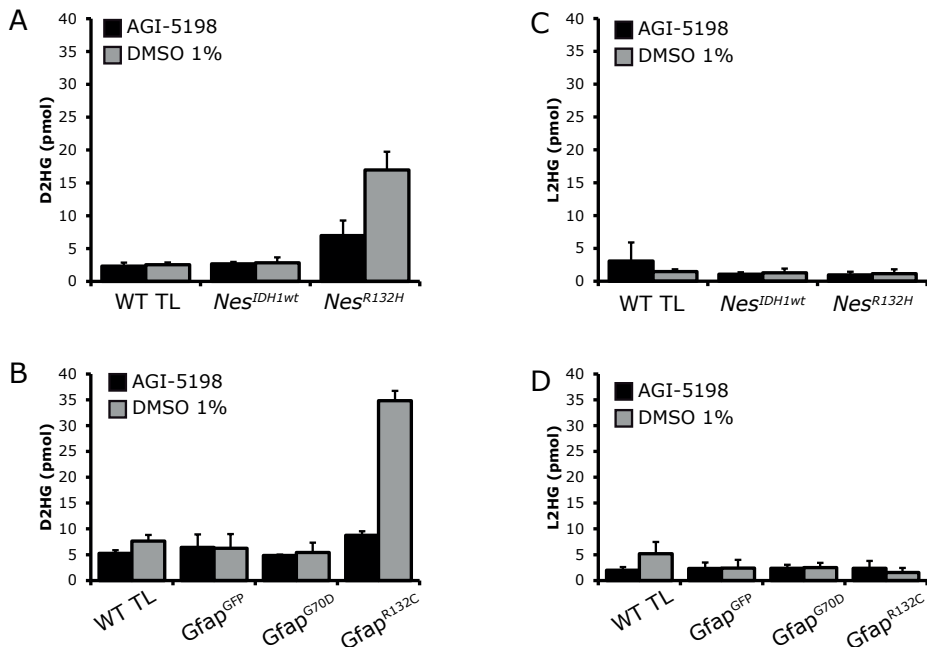
Figure 3. Treatment of transgenic zebrafish with 10µM IDH1 mutant inhibitor, AGI-5198, resulted in a reduction in the D2HG level in the IDH1 mutant zebrafish. D2HG level in *Nes*[R132H] transgenic zebrafish was reduced to 41% of untreated (A). D2HG level in *Gfap*[R132H] transgenic zebrafish was reduced to 25% of untreated (B) The L2HG level was not affected by AGI-5198 (C and D). D2HG and L2HG measurements were averages of two replicates using five fish per replicate.

DISCUSSION

Studying IDH1 mutations in gliomas has been hampered by the difficulty in generating appropriate model systems. For example, IDH-mutated gliomas are notoriously difficult to propagate *in vitro* (37) and mouse models for IDH1 mutations often have a lethal phenotype when $IDH1^{R132H}$ is expressed at early stages of development (21, 23, 25). Mice can survive when the mutant protein is expressed at later stages, but often with severe phenotypes (e.g. hydrocephalus). A *Drosophila* model with UAS-Idh-R195H resulted in defects in wing expansion (38). Here we report on transgenic zebrafish model systems for *IDH1* mutations, and show that expression of *IDH1* mutations and subsequent accumulation of D2HG does not overtly affect zebrafish development in the majority of offspring. However, tail development defects were observed in a subset of offspring in one line and also following direct injection of mutant constructs in wildtype zebrafish embryos (Fig. S8). Expression of mutant, but not wildtype *IDH1* may therefore affect the cells required for normal tail development.

In contrast to the *Nestin* or GFAP-R132H KI mouse models, we did not observe any overt phenotype in any of the Nes^{R132H} transgenic zebrafish and the majority of *Gfap* transgenic fish. In mice, the brain hemorrhage phenotype is caused by collagen maturation defects (caused by inhibition of prolyl hydroxylases by D2HG) (21). Alternatively, brain hemorrhages may be secondary to D2HG mediated coagulation defects (39). In our transgenic lines, we failed to detect signs of collagen maturation defects or brain hemorrhage, which may provide an explanation why our fish are able to survive into adulthood. The absence of collagen maturation defects in our fish may be related to the level of D2HG accumulation in our model system, the expression level of IDH1^{R132H} in our transgenic fish, and/or to the more limited temporal expression of our constructs. D2HG accumulation may also be limited as it is likely able to diffuse out of the fish into the water of the tank. This may explain that only a modest increase in the D2HG level was detected in the IDH1-mutated fish. We failed to detect changes in 5hmc levels in the IDH1-mutated embryos which may also be caused by insufficient accumulation of local D2HG within the fish. In addition, any potential effects on fish 'fitness' is selected against in the process of generating transgenic lines: only healthy fish (despite elevated D2HG levels) are used to generate stable lines.

We were unable to detect CNS-specific tumors in our transgenic zebrafish lines. This is in line with data from mouse models in which brain tumors were thus far not detected. This supports the notion that *IDH1* mutation alone may be insufficient to promote tumor formation and other genetic alterations are required (40). In most astrocytomas, *TP53* and *IDH* mutations often co-occur (41). However, the combination of *IDH1*

and *tp53* mutations did not induce gliomas in our zebrafish model. Similarly, *IDH1* mutations also did not increase tumor incidence in *Tp53* mutant mouse model, despite the observation that *IDH1* mutations induce pre-cancerous lesions such as proliferative subventricular nodules in one mouse model, but interestingly not in an almost identical other model (23, 25). Similarly, mutations in IDH1/2 in combination with *Tp53* deficiency were insufficient to induce gliomagenesis in RCAS/tva mouse models (40). Since mutations in *IDH* and *TP53* are the most common genetic alterations in astrocytomas, it remains unclear which additional mutations are required to induce glioma formation in our zebrafish model. Candidate genes should include oncogenic drivers ATRX and/or PDGFRA as they are present at significant frequency in lower grade gliomas. Of note, zebrafish has been appreciated as a valid model to study tumorigenesis, for example, *tp53*-mutant fish develop schwannomas and gliomas can also be generated in zebrafish by activating akt1 alone (42). Our data also show that D2HG can be present at high levels throughout the development of zebrafish without any overt signs of pathology (although a minority of our transgenic fish did show defects in tail development). These data are in line with the observation that some D2HG aciduria patients, which have high levels of D2HG due to mutations in *IDH2* or *D2HGDH*, do not have any overt phenotype. Moreover, D2HG aciduria patients do not have an increased incidence of brain tumors (43).

In conclusion, we developed various transgenic zebrafish models with CNS-specific expression of *IDH1* mutation. We identified tail defects in a subset of IDH1-mutant fish, but we thus-far failed to identify tumors. Nevertheless, our transgenic zebrafish are a suitable model to functionally study the *IDH1* mutation *in vivo* or to use as a drug screening model.

REFERENCE

1. Yan H, Parsons DW, Jin G, McLendon R, Rasheed BA, Yuan W, et al. IDH1 and IDH2 mutations in gliomas. N Engl J Med. 2009 Feb 19;360(8):765-73.

2. Balss J, Meyer J, Mueller W, Korshunov A, Hartmann C, von Deimling A. Analysis of the IDH1 codon 132 mutation in brain tumors. Acta Neuropathol. 2008 Dec;116(6):597-602.

3. Hartmann C, Meyer J, Balss J, Capper D, Mueller W, Christians A, et al. Type and frequency of IDH1 and IDH2 mutations are related to astrocytic and oligodendroglial differentiation and age: a study of 1,010 diffuse gliomas. Acta Neuropathol. 2009 Oct;118(4):469-74.

4. Cancer Genome Atlas Research N. Genomic and epigenomic landscapes of adult de novo acute myeloid leukemia. N Engl J Med. 2013 May 30;368(22):2059-74.

5. Meyer SC, Levine RL. Translational implications of somatic genomics in acute myeloid leukaemia. Lancet Oncol. 2014 Aug;15(9):e382-94.

6. Amary MF, Bacsi K, Maggiani F, Damato S, Halai D, Berisha F, et al. IDH1 and IDH2 mutations are frequent events in central chondrosarcoma and central and periosteal chondromas but not in other mesenchymal tumours. J Pathol. 2011 Jul;224(3):334-43.

7. Amary MF, Damato S, Halai D, Eskandarpour M, Berisha F, Bonar F, et al. Ollier disease and Maffucci syndrome are caused by somatic mosaic mutations of IDH1 and IDH2. Nat Genet. 2011 Dec;43(12):1262-5.

8. Pansuriya TC, van Eijk R, d'Adamo P, van Ruler MA, Kuijjer ML, Oosting J, et al. Somatic mosaic IDH1 and IDH2 mutations are associated with enchondroma and spindle cell hemangioma in Ollier disease and Maffucci syndrome. Nat Genet. 2011 Dec;43(12):1256-61.

9. Watanabe T, Nobusawa S, Kleihues P, Ohgaki H. IDH1 mutations are early events in the development of astrocytomas and oligodendrogliomas. Am J Pathol. 2009 Apr;174(4):1149-53.

10. Parsons DW, Jones S, Zhang X, Lin JC, Leary RJ, Angenendt P, et al. An integrated genomic analysis of human glioblastoma multiforme. Science. [Research Support, N.I.H., Extramural Research Support, Non-U.S. Gov't]. 2008 Sep 26;321(5897):1807-12.

11. Reitman ZJ, Yan H. Isocitrate dehydrogenase 1 and 2 mutations in cancer: alterations at a crossroads of cellular metabolism. J Natl Cancer Inst. 2010 Jul 7;102(13):932-41.

12. Louis DN, Perry A, Reifenberger G, von Deimling A, Figarella-Branger D, Cavenee WK, et al. The 2016 World Health Organization Classification of Tumors of the Central Nervous System: a summary. Acta Neuropathol. 2016 Jun;131(6):803-20.

13. Gabriel JL, Zervos PR, Plaut GW. Activity of purified NAD-specific isocitrate dehydrogenase at modulator and substrate concentrations approximating conditions in mitochondria. Metabolism. 1986 Jul;35(7):661-7.

14. Koh HJ, Lee SM, Son BG, Lee SH, Ryoo ZY, Chang KT, et al. Cytosolic NADP+-dependent isocitrate dehydrogenase plays a key role in lipid metabolism. J Biol Chem. 2004 Sep 17;279(38):39968-74.

15. Dang L, White DW, Gross S, Bennett BD, Bittinger MA, Driggers EM, et al. Cancer-associated IDH1 mutations produce 2-hydroxyglutarate. Nature. [Research Support, N.I.H., Extramural]. 2009 Dec 10;462(7274):739-44.

16. Zhu J, Zuo J, Xu Q, Wang X, Wang Z, Zhou D. Isocitrate dehydrogenase mutations may be a protective mechanism in glioma patients. Med Hypotheses. 2011 Apr;76(4):602-3.

17. Tefferi A. Novel mutations and their functional and clinical relevance in myeloproliferative neoplasms: JAK2, MPL, TET2, ASXL1, CBL, IDH and IKZF1. Leukemia. 2010 Jun;24(6):1128-38.

18. Prensner JR, Chinnaiyan AM. Metabolism unhinged: IDH mutations in cancer. Nat Med. 2011 Mar;17(3):291-3.

19. Rohle D, Popovici-Muller J, Palaskas N, Turcan S, Grommes C, Campos C, et al. An inhibitor of mutant IDH1 delays growth and promotes differentiation of glioma cells. Science. 2013 May 03;340(6132):626-30.

20. Brooks E, Wu X, Hanel A, Nguyen S, Wang J, Zhang JH, et al. Identification and Characterization of Small-Molecule Inhibitors of the R132H/R132H Mutant Isocitrate Dehydrogenase 1 Homodimer and R132H/Wild-Type Heterodimer. J Biomol Screen. 2014 Sep;19(8):1193-200.

21. Sasaki M, Knobbe CB, Itsumi M, Elia AJ, Harris IS, Chio, II, et al. D-2-hydroxyglutarate produced by mutant IDH1 perturbs collagen maturation and basement membrane function. Genes Dev. 2012 Sep 15;26(18):2038-49.

22. Hirata M, Sasaki M, Cairns RA, Inoue S, Puviindran V, Li WY, et al. Mutant IDH is sufficient to initiate enchondromatosis in mice. P Natl Acad Sci USA. 2015 Mar 3;112(9):2829-34.

23. Bardella C, Al-Dalahmah O, Krell D, Brazauskas P, Al-Qahtani K, Tomkova M, et al. Expression of Idh1R132H in the Murine Subventricular Zone Stem Cell Niche Recapitulates Features of Early Gliomagenesis. Cancer Cell. 2016 Oct 10;30(4):578-94.

24. Sasaki M, Knobbe CB, Munger JC, Lind EF, Brenner D, Brustle A, et al. IDH1(R132H) mutation increases murine haematopoietic progenitors and alters epigenetics. Nature. 2012 Aug 30;488(7413):656-9.

25. Pirozzi CJ, Carpenter AB, Waitkus MS, Wang CY, Zhu H, Hansen LJ, et al. Mutant IDH1 Disrupts the Mouse Subventricular Zone and Alters Brain Tumor Progression. Mol Cancer Res. 2017 May;15(5):507-20.

26. Bralten LB, Kloosterhof NK, Balvers R, Sacchetti A, Lapre L, Lamfers M, et al. IDH1 R132H decreases proliferation of glioma cell lines in vitro and in vivo. Ann Neurol. 2011 Mar;69(3):455-63.

27. Berghmans S, Murphey RD, Wienholds E, Neuberg D, Kutok JL, Fletcher CD, et al. tp53 mutant zebrafish develop malignant peripheral nerve sheath tumors. Proc Natl Acad Sci U S A. 2005 Jan 11;102(2):407-12.

28. Struys EA, Jansen EE, Verhoeven NM, Jakobs C. Measurement of urinary D- and L-2-hydroxyglutarate enantiomers by stable-isotope-dilution liquid chromatography-tandem mass spectrometry after derivatization with diacetyl-L-tartaric anhydride. Clin Chem. 2004 Aug;50(8):1391-5.

29. Lendahl U, Zimmerman LB, McKay RD. CNS stem cells express a new class of intermediate filament protein. Cell. 1990 Feb 23;60(4):585-95.

30. About I, Laurent-Maquin D, Lendahl U, Mitsiadis TA. Nestin expression in embryonic and adult human teeth under normal and pathological conditions. Am J Pathol. 2000 Jul;157(1):287-95.

31. Mahler J, Driever W. Expression of the zebrafish intermediate neurofilament Nestin in the developing nervous system and in neural proliferation zones at postembryonic stages. BMC Dev Biol. 2007 Jul 25;7:89.

32. Figueroa ME, Abdel-Wahab O, Lu C, Ward PS, Patel J, Shih A, et al. Leukemic IDH1 and IDH2 mutations result in a hypermethylation phenotype, disrupt TET2 function, and impair hematopoietic differentiation. Cancer Cell. 2010 Dec 14;18(6):553-67.

33. Tomasiewicz HG, Flaherty DB, Soria JP, Wood JG. Transgenic zebrafish model of neurodegeneration. J Neurosci Res. 2002 Dec 15;70(6):734-45.

34. Bernardos RL, Raymond PA. GFAP transgenic zebrafish. Gene Expression Patterns. 2006 Oct;6(8):1007-13.

35. Hemerly JP, Bastos AU, Cerutti JM. Identification of several novel non-p.R132 IDH1 variants in thyroid carcinomas. Eur J Endocrinol. 2010 Nov;163(5):747-55.

36. Pusch S, Schweizer L, Beck AC, Lehmler JM, Weissert S, Balss J, et al. D-2-Hydroxyglutarate producing neo-enzymatic activity inversely correlates with frequency of the type of isocitrate dehydrogenase 1 mutations found in glioma. Acta Neuropathol Commun. 2014 Feb 14;2:19.

37. Balvers RK, Kleijn A, Kloezeman JJ, French PJ, Kremer A, van den Bent MJ, et al. Serum-free culture success of glial tumors is related to specific molecular profiles and expression of extracellular matrix-associated gene modules. Neuro Oncol. 2013 Dec;15(12):1684-95.

38. Reitman ZJ, Sinenko SA, Spana EP, Yan H. Genetic dissection of leukemia-associated IDH1 and IDH2 mutants and D-2-hydroxyglutarate in Drosophila. Blood. 2015 Jan 08;125(2):336-45.

39. Unruh D, Schwarze SR, Khoury L, Thomas C, Wu M, Chen L, et al. Mutant IDH1 and thrombosis in gliomas. Acta Neuropathol. 2016 Dec;132(6):917-30.

40. Amankulor NM, Kim Y, Arora S, Kargl J, Szulzewsky F, Hanke M, et al. Mutant IDH1 regulates the tumor-associated immune system in gliomas. Genes Dev. 2017 Apr 15;31(8):774-86.

41. Draaisma K, Wijnenga MM, Weenink B, Gao Y, Smid M, Robe P, et al. PI3 kinase mutations and mutational load as poor prognostic markers in diffuse glioma patients. Acta Neuropathol Commun. 2015 Dec 23;3:88.

42. Jung IH, Leem GL, Jung DE, Kim MH, Kim EY, Kim SH, et al. Glioma is formed by active Akt1 alone and promoted by active Rac1 in transgenic zebrafish. Neuro Oncol. 2013 Mar;15(3):290-304.

43. Kranendijk M, Struys EA, Salomons GS, Van der Knaap MS, Jakobs C. Progress in understanding 2-hydroxyglutaric acidurias. J Inherit Metab Dis. 2012 Jul;35(4):571-87.

2
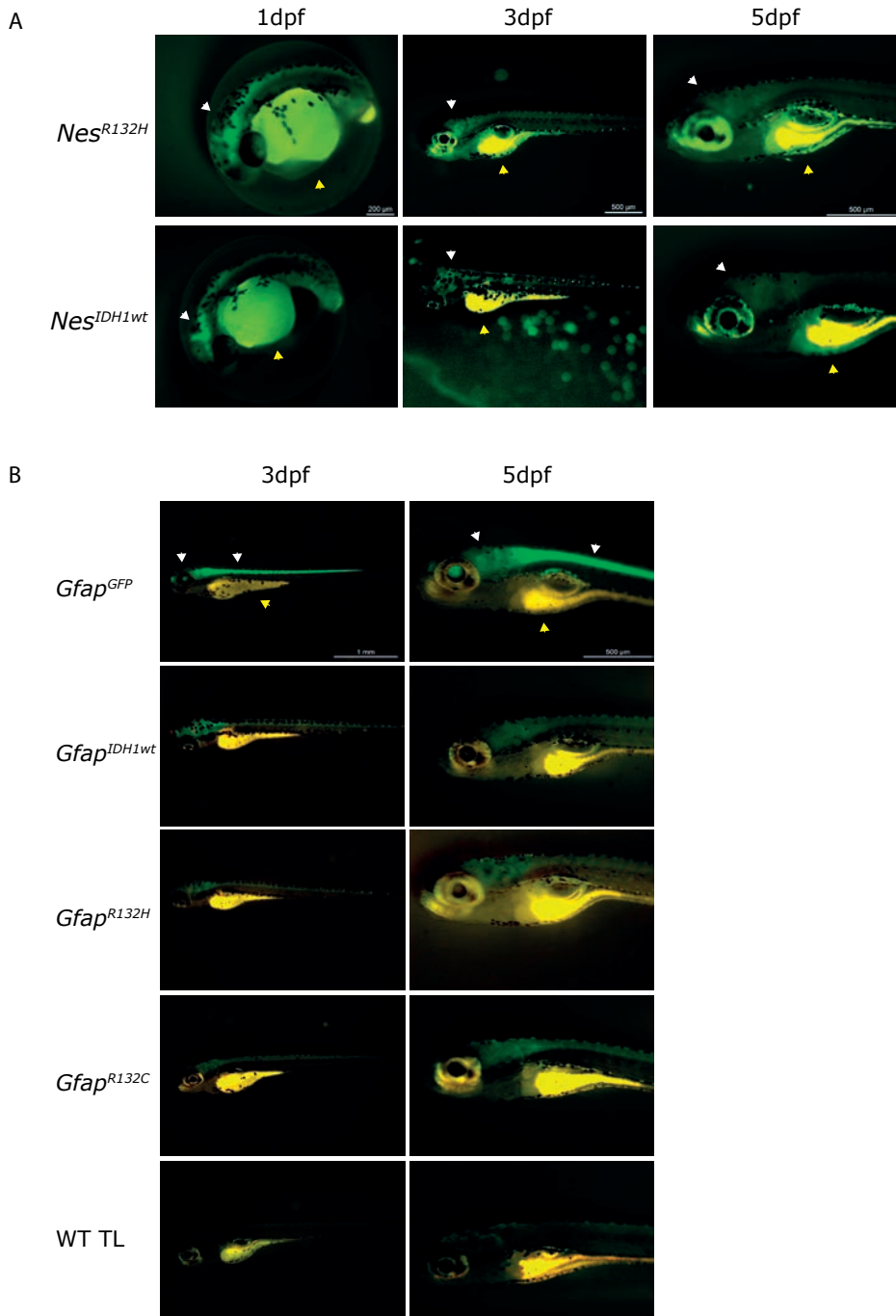
Supplementary Figure 1. Fluorescent imaging showed expression of transgene in the central nervous system of *Nestin* (A) and *Gfap* (B) transgenic zebrafish lines on 1, 3 and 5 dpf. White arrow head: CNS-specific GFP. Yellow arrow head: auto fluorescence in the yolk sac.
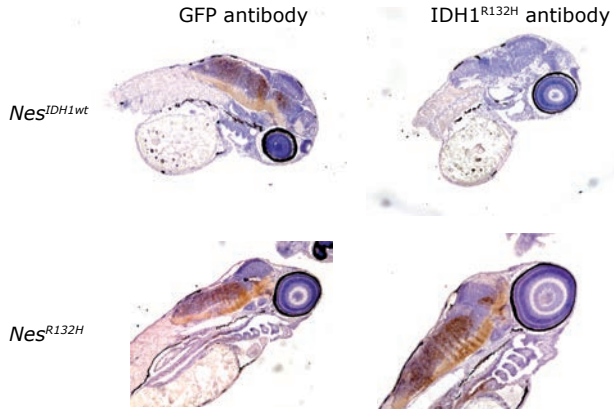
Supplementary Figure 2. Immunohistochemistry using anti-IDH1R132H antibody demonstrated expression of *IDH1^{R132H}* specific expression in Nestin zebrafish but not in *IDH1wt* transgenic fish.
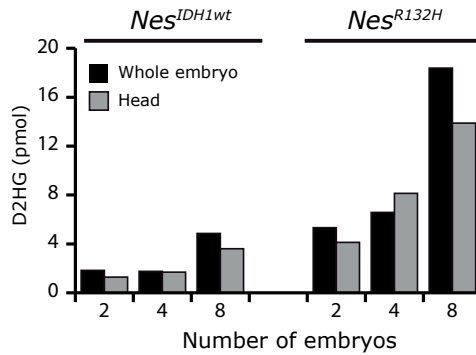
Supplementary Figure 3. D2HG measurement in *Nes^{IDH1wt}* and *Nes^{R132H}* transgenic fish. No differences in D2HG levels between macro-dissected and whole embryos were observed.

A

B
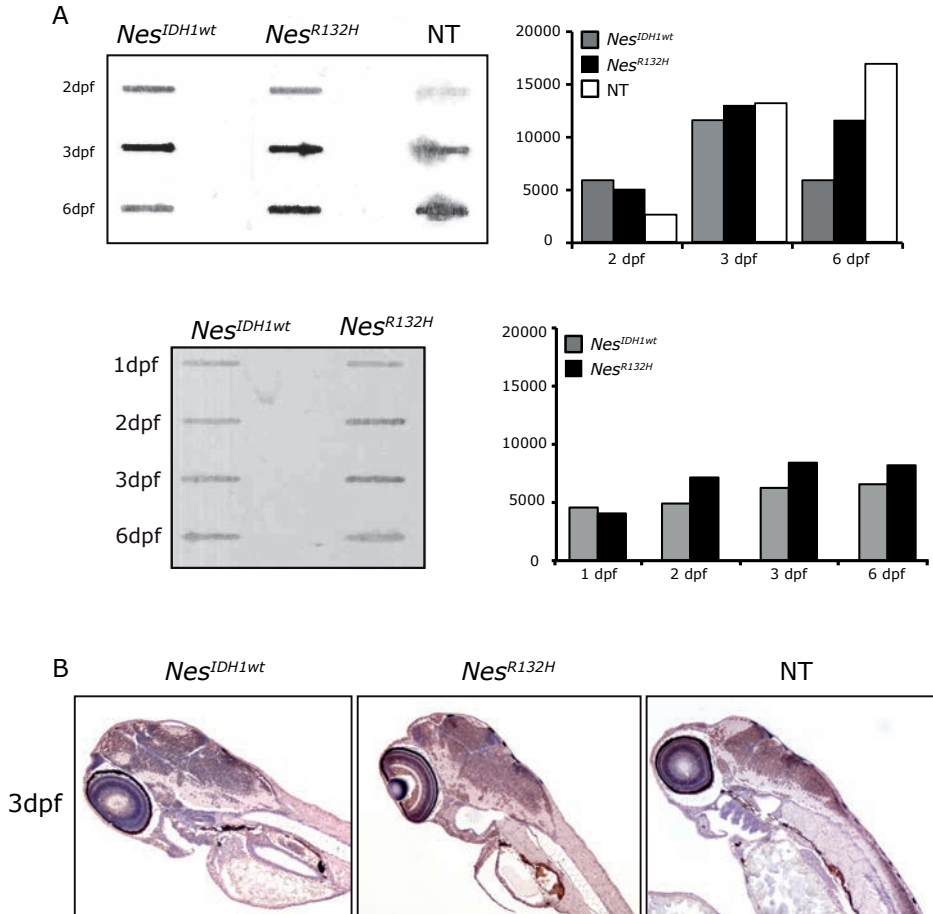
Supplementary Figure 4. 5hmC levels was not affected by high levels of D2HG in transgenic Nes^{R132H} mutant zebrafish. A. 5hmC levels in Nes^{IDH1wt}, Nes^{R132H} and non-transgenic zebrafish embryos were measured using slotblot stained with an 5hmC antibody (quantification of bands on the right panel). Similar results were obtained in three independent experiments one of which is shown below. B. Representative images showing 5-hmC immunostaining in Nes^{IDH1wt}, Nes^{R132H} transgenic and non-transgenic zebrafish embryo slices at 3dpf. NT: non-transgenic zebrafish.
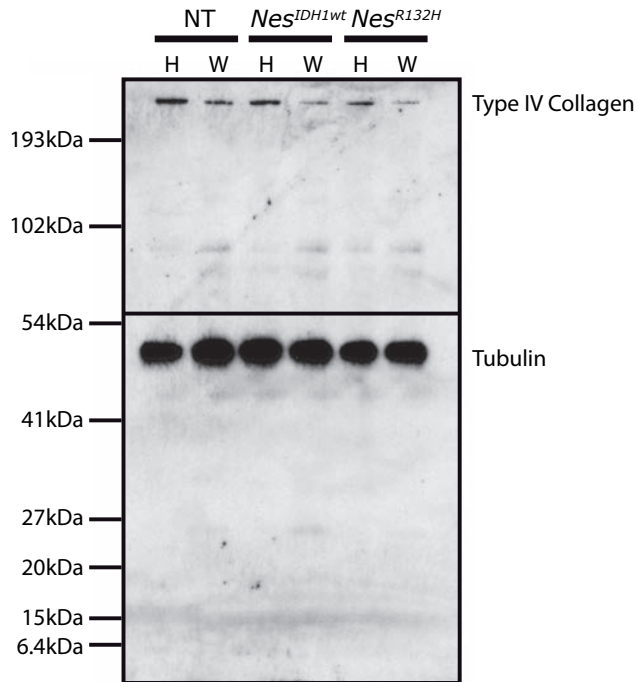
Supplementary Figure 5. Collagen maturation was not affected in Nes^{R132H} mutant zebrafish. Top half of the blot was stained for type IV Collagen, bottom half was stained for Tubulin (as loading control). Similar data were obtained in three independent experiments. NT: non-transgenic zebrafish. H: head of zebrafish embryos. W: whole embryo.
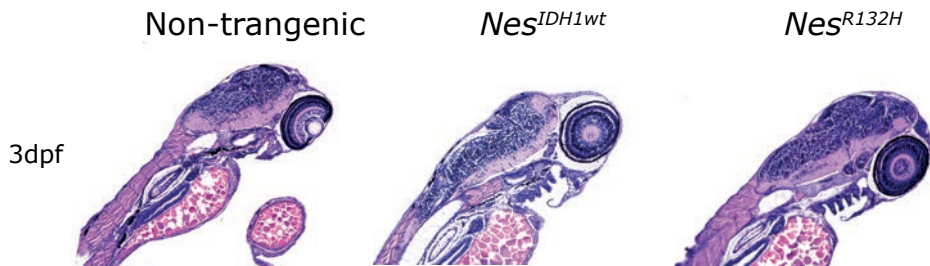
Supplementary Figure 6. Nes^{R132H} transgenic zebrafish with CNS-accumulation of D2HG showed no gross histological abnormalities on 3dpf on H&E staining.

Supplementary Figure 7. *Gata2^{GFP}* transgenic zebrafish shows expression in the notochord of zebrafish. Yellow arrow: In *Gata2^{IDHwt}* transgenic fish the transgene is expressed in non-CNS regions (yellow arrow) whereas *Gfap^{IDH1wt}* transgenic fish show CNS-specific expression of transgene (white arrow). The blue arrow shows an absence of GFP signal in non-transgenic fish.

2
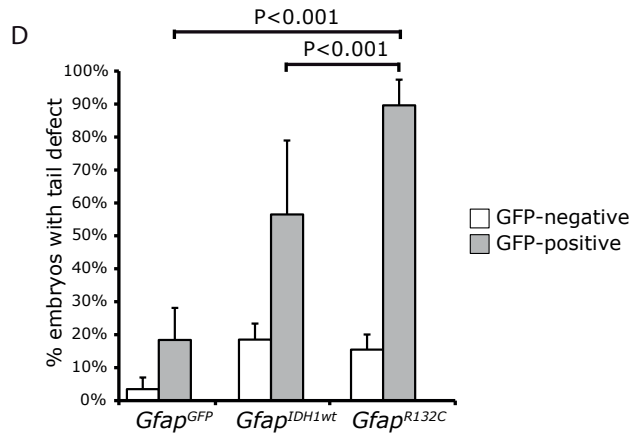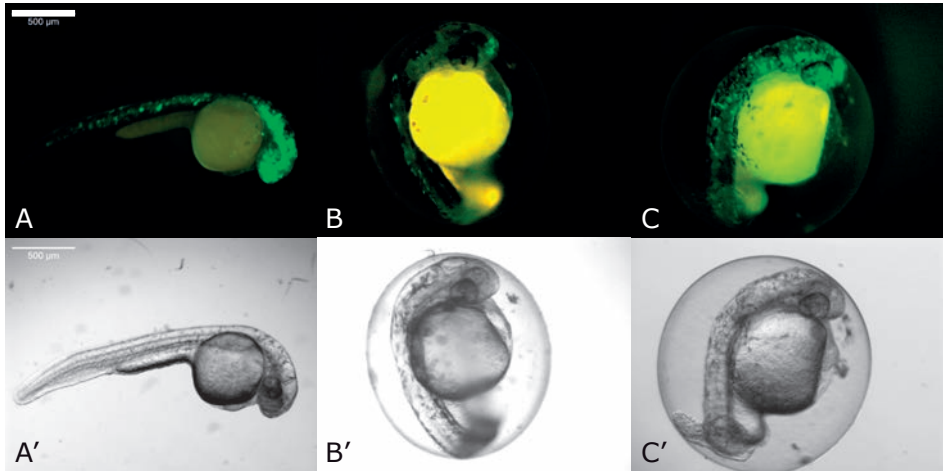
Supplementary Figure 8 Direct injection of fertilized zebrafish embryos with Gfap constructs showed mutant-specific tail defects. Fluorescent imaging showed CNS-specific expression of injected construct $Gfap^{GFP}$ (A), $Gfap^{IDH1wt}$ (B) and $Gfap^{R132C}$(C) and the corresponding bright-field images (A'-C'). D: the percentage of GFP-positive embryos with tail defects per construct. The ratio of injected embryos with tail defect were calculated based on results of three independent experiments (~100 eggs/construct/experiment). n.s: non-significant. Scale bar: 500µm.
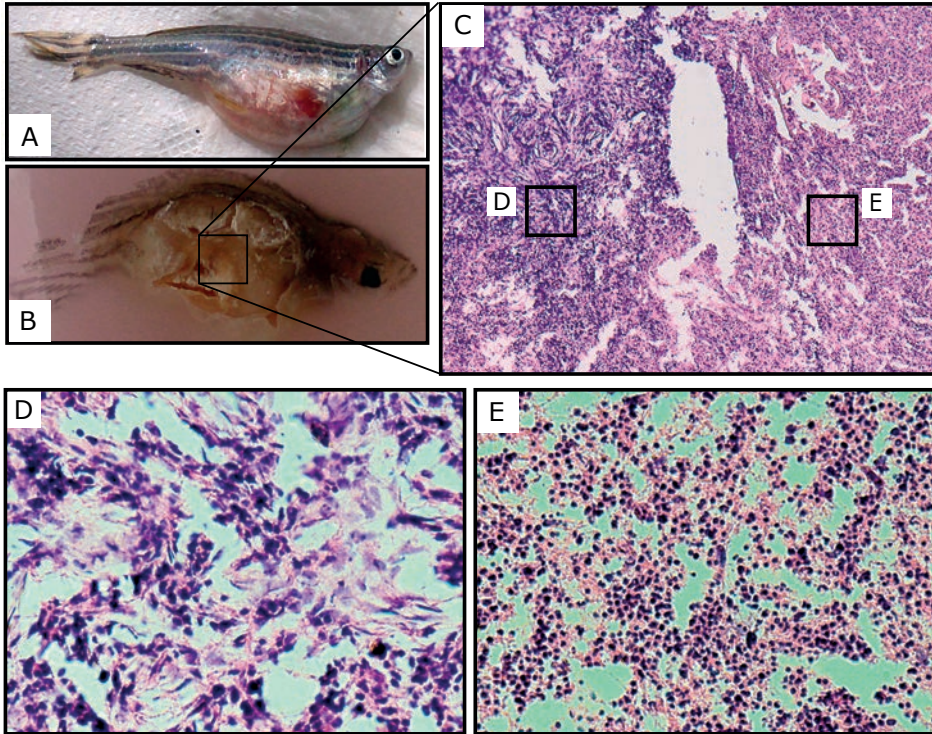
Supplementary Figure 9. An example of a schwannoma in tp53 deficient transgenic zebrafish crossed with IDH1 transgenic fish. Euthanized 1-year old fish with a distended abdominal cavity (A). Fish were fixed in paraffin blocks (B) and sectioned slides were stained with hematoxylin/eosin for histological examination (C). D and E: enlarged images of sections in C, histological feature of tumors were consistent with the schwannomas as previously demonstrated (36).
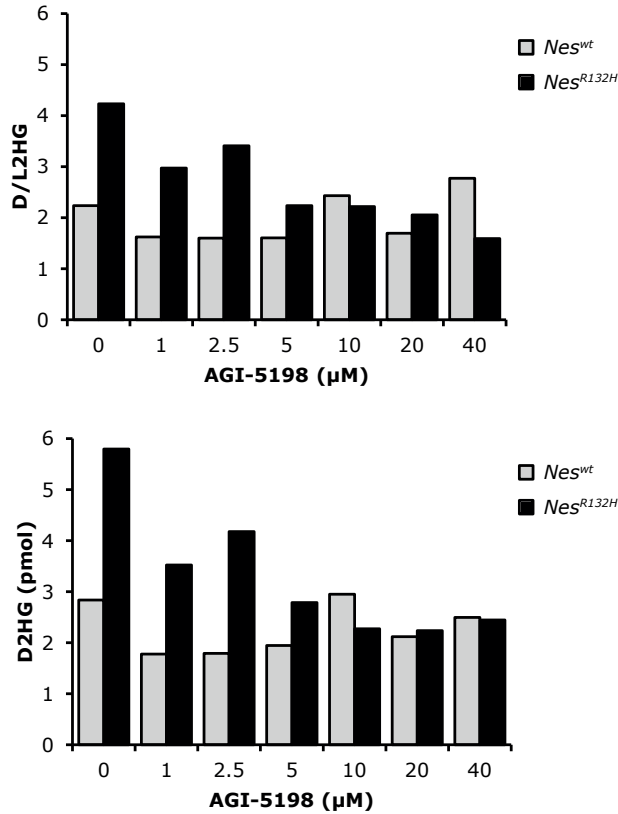
Supplementary Figure 10. Dose-response analysis of AGI-5198 on Nestin transgenic zebrafish. Maximal inhibition is reached at 10μM.

Supplementary Table 1. Primers used for the examination of IDH1 expression levels in zebrafish by QPCR.

Gene	Exon	Primer (5'-3')
IDH1	4	FW- CGACCAAGTCACCAAAGATGC
	4	RV- CCTCAACCCTCTTCTCATCAGG
B-actin	2	FW- CGTGCTGTCTTCCCATCCA
	3	RV-TCACCAACGTAGCTGTCTTTCTG

Chapter 3 & 4

Have been temporarily removed for copyright reasons

Chapter 5

Mutation specific functions of EGFR result in a mutation-specific downstream pathway activation

Lale Erdem-Eraslan[1][*], Ya Gao[1][*], Nanne K. Kloosterhof[1], Yassar Atlasi[2], Jeroen Demmers[3], Andrea Sacchetti[2], Johan M. Kros[2], Peter Sillevis Smitt[1], Joachim Aerts[4], Pim J. French[1]

Depts of [1]Neurology, [2]Pathology, [3]Proteomics Center, and [4]Pulmonary diseases, Erasmus Medical Center, Rotterdam, the Netherlands
[*] these authors contributed equally to this manuscript

ABSTRACT

Background

EGFR is frequently mutated in various types of cancer. Although all oncogenic mutations are considered activating, different tumor types have different mutation spectra. It is possible that functional differences underlie this tumor-type specific mutation spectrum.

Methods

We have determined whether specific mutations in EGFR (EGFR, EGFRvIII and EGFR-L858R) have differences in binding partners, differences in downstream pathway activation (gene expression and phosphoproteins), and have functional consequences on cellular growth and migration.

Results

Using biotin pulldown and subsequent mass spectrometry we were able to detect mutation specific binding partners for EGFR. Differential binding was confirmed using a proximity ligation assay and/or Western Blot for the dedicator of cytokinesis 4 (DOCK4), UDP-glucose glycoprotein glucosyltransferase 1 (UGGT1), MYC binding protein 2 (MYCBP2) and Smoothelin (SMTN). We also demonstrate that each mutation induces the expression of a specific set of genes, and that each mutation is associated with specific phosphorylation patterns. Finally, we demonstrate using stably expressing cell lines that EGFRvIII and EGFL858R display reduced growth and migration compared to EGFR wildtype expressing cells.

Conclusion

Our results indicate that there are distinct functional differences between different EGFR mutations. The functional differences between different mutations argue for the development of mutation specific targeted therapies.

INTRODUCTION

The epidermal growth factor receptor (EGFR) is a receptor tyrosine kinase that is a member of the ERBB protein family and is localised on the cell membrane. The receptor is activated by members of the pidermal growth factor (EGF) family (a.o. EGF, amphiregulin, TGF-a, HB-EGF and epiregulin) and binding of one such ligand results in receptor dimerisation which induces receptor phosphorylation, recruitment of adaptor proteins and subsequent activation of signal transduction cascades [1,2].

Somatic mutations in the EGFR gene are found in several types of cancer and the mutation spectrum includes gene amplifications, gene-fusions, deletions in the extracellular domain (e.g. EGFRvIII; a deletion of exons 2–7), deletions in the intracellular domain (e.g. EGFRvV; a deletion of exons 25–28) and mutations affecting the tyrosine kinase domain (mainly exon 19 and codon L858) [3–5]. These mutations result in a constitutively activated isoform of the protein and contribute to oncogenic transformation [5–8].

Although EGFR mutations are activating, there are marked differences in the spectrum of mutations between tumour types. For example, the c.2573T > G missense mutation, resulting in the L858R substitution, is found in _10–15 % of all pulmonary adenocarcinomas [4]. This mutation is the most frequent of all mutations in EGFR but has thus far never been identified in glioblastomas (GBMs) [3]. The most common mutations in GBMs affect the extracellular domain of EGFR, including EGFRvIII (~ 30 % of all GBMs) and the A289V and V598V missense mutations [3]. These extracellular domain mutations are not found in pulmonary adenocarcinomas [4]. One of the explanations for these tumour-type specific mutations is that each mutation invokes a unique signal transduction cascade. Indeed, EGFRvIII and EGFRwt have differential activation of the JNK, STAT and MAPK signalling pathways and induce the expression of a unique set of genes [9–13]. Because different tumour types may be dependent on the unique pathways that are activated by different EGFR mutations, studying these functional differences between mutations may identify novel, tumour type specific treatment targets. Here, we have further evaluated differential activation of signal transduction pathways by EGFR-wt, EGFR-L858R and EGFRvIII.

MATERIALS AND METHOD

EGFRvIII and EGFR-L858R cDNAs were obtained from Addgene (Cambridge, MA), EGFR wildtype was a gift from Ton van Agthoven and cloned into pcDNA3.1/CT-

GFP-TOPO (Invitrogen, Bleiswijk, the Netherlands). A biotin tag and eGFP were inserted C-terminal to the transmembrane domain of EGFR to retain the integrity of the C-terminal (intracellular) domain of EGFR. To demonstrate functionality, we transfected EGFRbio-GFP into ZR-75-1 cells. Normally, ZR-75-1 cells do not proliferate in the presence of tamoxifen [43]. However, ZR-75-1 cells expressing EGFR-bioGFP, cultured in the presence of tamoxifen, responded to EGF stimulation by an increase in cell proliferation, demonstrating the construct remained functional (not shown). Stably transfected HOG (human oligodendroglioma cells [44]) cell lines were created by transfection, geneticin selection and FACS sorting. Stable cell lines were derived from bulk culture and not form a single sorted cell followed by clonal propagation.

Migration and proliferation assays were performed using an Incucyte (Essen Bioscience, Ann Arbor, MI). For proliferation experiments, 50,000 cells/well were plated in a 24-well Greiner plate (Greiner Bio-One, Alphen a/d Rijn, the Netherlands). Growth curves were constructed using the Confluence v1.5 metric of the Incucyte software. For migration experiments, cells were grown to confluence in a 24-well Essen ImageLock-plate after which a cell-free zone (scratch) was created using a WoundMaker. Wells were then cultured in serum-free media.

Constructs containing EGFRwt-BG, EGFRvIII-BG and EGFRL858R-BG were transfected into HEK cell lines using Polyethylenimine 'Max' (Polysciences, Eppelheim, Germany). The EGFRwt-BG, EGFRvIII-BG and EGFRL858R-BG proteins were then isolated using Dynabeads (Life Technologies, Carlsbad, CA, United States of America (USA)) as described previously [39]. Purified proteins were washed and loaded on a SDS page gel. Nanoflow LC-MS/MS analysis was performed essentially as described by van den Berg et al. [45]. Candidate binding proteins that were present in a GFP control pulldown or identified in > 10 % of CRAPome experiments were omitted from the analysis [14]. We focused on candidate binding proteins that were identified with MASCOT scores > 300.

Western blots were performed as described [39]. Antibodies used were DOCK4 (1:100), UGGT1 (1:100), DDX21 (1:500) all from Sigma–Aldrich (Zwijndrecht, the Netherlands), EGFR (1:1000, Cell Signaling, Boston, MA) and GFP (1:5000, Abcam, Cambridge, United Kingdom (UK)).

Cells (HOG, U87MG, HEK) were cultured on glass slides for immunocytochemistry. Glioma samples were obtained from the Erasmus MC glioma tissue bank. Use of patient material for current study was approved by the Institutional Review Board. Antibodies used for immunocytochemistry and/or proximity ligation assays were

EGFR (1:200, DAKO, Heverlee, Belgium) and DOCK4 (1:100), MYCBP2 (1:200) and SMTN1 (1:100) all from Abcam. Proximity ligation assays were performed using a Duolink (Sigma–Aldrich) kit according to the manufacturer's instructions.

HEK cells were transiently transfected with EGFRbioGFP, EGFRL858R-bioGFP and EGFRvIII-bioGFP or BIO-eGFP constructs. Twenty hours after transfection, cells were FACS sorted to select for eGFP expressing cells. Cells were then snap frozen in liquid nitrogen and stored at _80 _C. RNA extraction was performed using TriZol (Invitrogen) and checked for RNA quality on a Bioanalyzer (Agilent, Amstelveen, the Netherlands). Gene expression was performed using HU133 plus2 arrays (Affymetrix, High Wycombe, UK) run by AROS Applied Biotechnology (Aarhus, Denmark). All experiments were performed in triplicate with each replicate experiment performed on separate days.

For reversed phase protein array (RPPA) analysis, stably transfected HOG cells were plated in six well plates and incubated in serum supplemented medium, or serum depleted medium (24 h depletion) $\pm$ 200 ng EGF for 5 min. RPPA arrays were performed by the MD Anderson RPPA core facility. Luciferase activity was measured by Dual–Luciferase Reporter Assay System (Promega). Pathway analysis was performed using Ingenuity (Redwood City, CA) and David [46].

RESULTS

We first generated constructs of wildtype EGFR and of two common mutations, EGFR-vIII and L858R, and inserted a biotinylation tag and eGFP in-frame and Cterminal to the transmembrane domain. Constructs are referred to as EGFRwt-BG, EGFRvIII-BG and EGFRL858R-BG respectively. Mass spectrometry following pulldown of biotinylated constructs identified over 3000 candidate binding partners for at least one of these constructs. When filtering for duplicate hits, and removal of proteins identified by a bio-eGFP control pulldown or present in > 10 % of crapome pulldown experiments [14], our list of candidate EGFR binding proteins included 87 unique proteins (Supplementary Table 1). Almost half (37/87) of these binding partners are known interactors of EGFR and include CBL, PIK3CA, PIK3R3, SHC1 and SOS1 [15–17].

Ingenuity pathway analysis indicated that the candidate EGFR associated proteins are involved in EGF signaling and Clathrin mediated endocytosis signalling. Candidate EGFR interacting proteins are enriched for proteins that are somatically mutated in GBMs. For example, 7/87 (8.0 %) genes are mutated at a population frequency > 1.5 %

(i.e. mutations found in at least 5/290 tumours) in the TCGA, a 3–4-fold enrichment compared to all genes mutated at this frequency in GBMs (485/_20.000 genes, 2.4 %, P = 0.007, Fishers' exact test).

Of the 87 candidate binding proteins, 22 showed selective association to one of the EGFR constructs (Table 1). Selective association was defined as a relative difference in mascot scores > 3, and an absolute difference in mascot scores > 500 between any of the three constructs. The strongest candidate proteins included DOCK4 (dedicator of cytokinesis 4) UGGT1 (UDPglucose glycoprotein glucosyltransferase 1), MYCBP2 (MYC binding protein 2, E3 ubiquitin protein ligase) and SMTN (Smoothelin).

Table 1. Proteins showing selective binding to one or more specific EGFR mutations

symbol	EGFR wt	EGFR V111	EGFR-p.L858R
AP1B1		961	
CRKL	561	740	229
DNM2	462	798	211
DOCK4	2725	2136	536
EXOC7	533	213	
IFI16	772	1079	
IPO5	1403	411	217
LAD1	106	669	1056
LMO7		340	1362
MYCBP2		1606	
MYO1E		156	503
NGLY1	353	1310	887
PIK3CA	147	902	86
PIK3CB	474	828	72
RTCB		558	341
SEL1L		604	174
SMTN			546
SPECC1L		69	909
SVIL		160	741
TNPO2	410	515	
UBE3C	157	828	280
UGGT1		1573	

Western blots on independent biotin pulldowns confirmed that DOCK4 binds preferentially to EGFRvIII-BG and EGFRwt-BG but not to EGFRL858R-BG (Fig. 1b, Western blot experiments in two independent experiments). The association was further confirmed using a proximity ligation assay (PLA, Fig. 1c). OCK4 also associates with
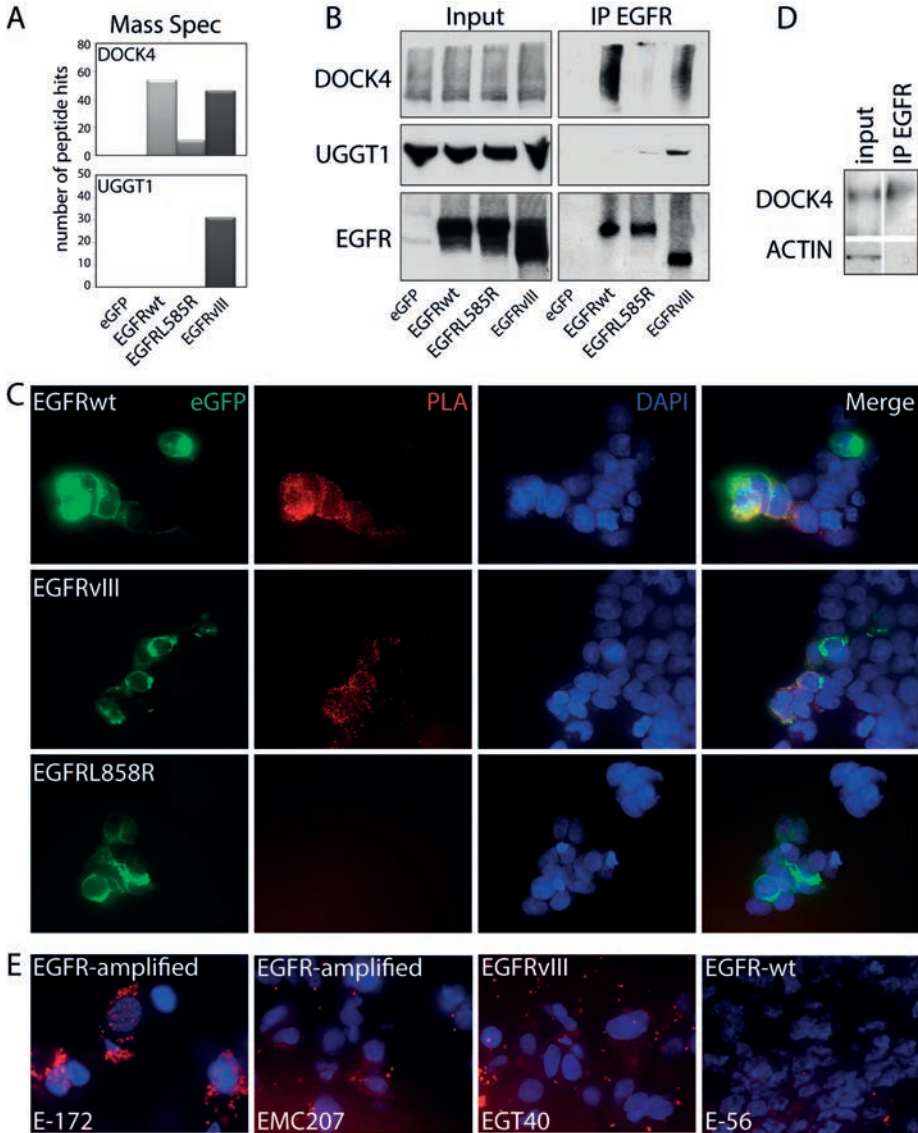
Figure 1. EGFRwt-BG, EGFRvIII-BG or EGFRL858R-BG associate with specific proteins. A) mass spectrometry results for DOCK4 and UGGT1 showing differential binding to EGFR mutations. B) Confirmation of the mass spectrometry results by Western Blot on an independent pulldown. C) A proximity ligation assay confirms that DOCK4 colocalizes with EGFRwt-BG and EGFRvIII-BG but not with EGFRL858R-BG or Bio-GFP control (not shown). All images taken at 63x magnification. D) Native EGFR also associates with DOCK4 as determined by immunoprecipitation of EGFR. E) A proximity ligation assay shows that DOCK4 and EGFR also colocalize in tumors.

EGFR also under native conditions as demonstrated by a co-immunoprecipitation using anti-EGFR antibodies in non-transfected HEK cells (Fig. 1d). Furthermore, PLA confirmed that DOCK4 and EGFR are also colocalised in EGFR amplified GBMs (Fig.

1e). DOCK4 remains associated with EGFR-wt in cells that were serum starved over-night followed by EGF stimulation (Supplementary Fig. 1). These data demonstrate that DOCK4 associates with EGFRwt-BG and EGFRvIII-BG and not (or to a lesser extent) with EGFRL858R-BG.

Because DOCK4 has been implicated in wnt pathway activation [18] we screened for differential ctivation of this pathway activation by the different EGFR constructs. However, both under basal and under wnt activated conditions, no differences in wnt pathway activation were identified (n = 3 independent experiments, data not shown).

Mass spectrometry also highlighted that UGGT1 and MYCBP2 preferentially associate with EGFRvIIIBG and that SMTN preferentially associates with EGFRL858R-BG. PLA assays confirmed the association for all three proteins (Fig. 2), Western blot (WB) further confirmed the association of UGGT1 with EGFRvIII-BG (Fig. 1b). It should be noted that some (minor) association of UGGT1, MYCBP1 and SMTN to other EGFR constructs were found by PLA and/or WB.

We hypothesised that the selective association of different EGFR mutations ultimately would result in the induction of a unique set of genes. We have therefore performed gene expression profiling of cells expressing EGFRwt-BG, EGFRvIII-BG, EGFRL858R-BG or BIOeGFP constructs (n = 3 per construct). Statistical analysis of microarrays (SAM) identified 74, 109 and 187 probesets that were differentially expressed in EGFRwt- BG, EGFRvIII-BG and EGFRL858R-BG expressing cell lines compared to BIO-eGFP control (with differential expression > 2 and at a false discovery rate (fdr) < 0.05, Supplementary Table 2). These probesets correspond to 61, 89 and 156 genes respectively. Many of these genes are found in all three comparisons and are involved in the transcription of DNA and are significantly enriched for the gene-ontology (GO) terms 'sequence-specific DNA binding', 'transcription factor activity', 'transcription regulator activity', 'DNA binding' and 'protein dimerization activity' (all P < 0.001). Top networks identified by Ingenuity pathway analysis include 'Cellular compromise, cellular function and maintenance, gene expression', 'developmental disorder, heredi-tary disorder, neurological disease' and 'neurological disease, cell-mediated immune response, cellular development'.

To determine whether specific mutations have specific gene-expression signatures, we performed SAM analysis comparing gene expression between the different EGFR mutations. A total of 17, 12 and 35 probesets were identified that were differen-tially expressed between EGFRwt-BG versus EGFRvIII-BG, EGFRwt-BG versus EG-FRL858R-BG and EGFRvIII-BG versus EGFRL858RBG respectively (with differential

UGGT1
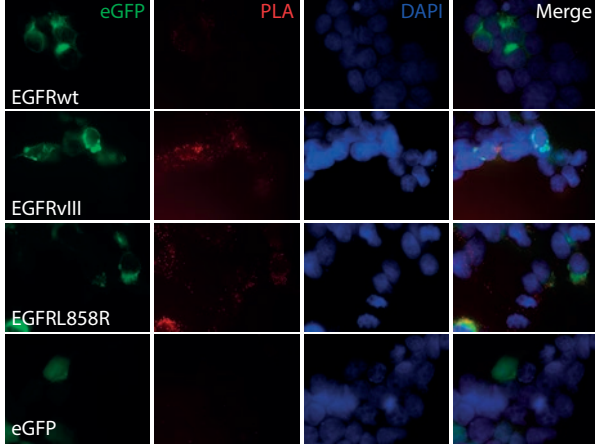
MYCBP2
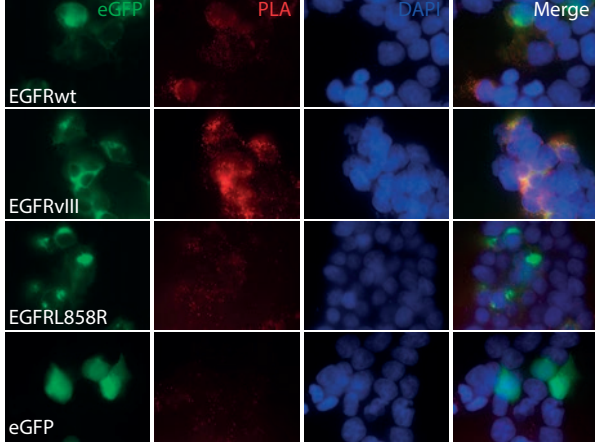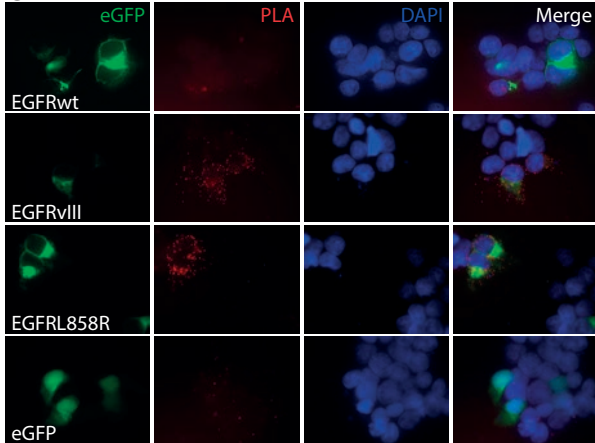
Figure 2. EGFRwt-BG, EGFR-vIII-BG or EGFRL858R-BG associate with specific proteins. A proximity ligation assay shows that UGGT1 colocalizes with EG-FRwt-BG and EGFRvIII-BG but not with EGFRL858R-BG or Bio-GFP control (see also figure 1B). Similarly, MYCBP2 colocalizes predominantly with EGFRvIII-BG wheras SMTN predominantly colocalizes with EGFRL858R-BG. All images taken at 63x magnification.

SMTN

5

Table 2. Probesets that are differentially expressed between EGFR$^{wt\text{-}BG}$ v. EGFR$^{vIII\text{-}BG}$, EGFR$^{wt\text{-}BG}$ v. EGFR$^{L858R\text{-}BG}$, and EGFR$^{vIII\text{-}BG}$ v. EGFR$^{L858R\text{-}BG}$ as identified by SAM analysis

Gene_Symbol	Probeset_ID	eGFP	EGFRwt	EGFRvIII	EGFR-p. L858R	wt v vIII	wt v L858R	vIII v L858R
SOCS3	227697_at	4.5	4.9	9.1	5.6	X		X
RAP1A	1555339_at	13.4	4.9	7.0	4.7	X		X
C10orf10	209183_s_at	6.6	6.8	8.9	6.8	X		X
Hs.527973	206359_at	4.3	4.6	6.6	4.9	X		X
RAP1A	1555340_x_at	14.3	5.5	7.3	5.1	X		X
XR_132893	1565830_at	6.0	4.6	6.0	5.0	X		
SOCS2	203372_s_at	6.8	6.9	7.9	7.4	X		
WDR78	1554140_at	6.5	5.1	6.5	5.7	X		
DTX3L	225415_at	6.6	6.5	7.4	6.6	X		
BC042589	235456_at	7.8	6.4	7.4	6.9	X		
KIAA1267	224489_at	6.8	6.0	6.9	6.4	X		
RAB30	229072_at	6.1	4.9	6.0	5.1	X		
AK022645	232257_s_at	5.2	4.1	5.2	4.5	X		
HSPA6	213418_at	4.8	8.2	6.7	9.3	X		X
EGR1	201693_s_at	6.0	8.9	7.7	10.9	X		X
EGR1	201694_s_at	8.2	11.2	10.2	12.6	X		X
EGFR	210984_x_at	5.6	10.0	9.0	10.8	X		
AKIRIN2	223143_s_at	5.1	5.0	5.8	6.1		X	
ARC	210090_at	5.8	6.8	6.3	9.3		X	
ARL5B	242727_at	5.9	6.1	6.0	7.3		X	X
CCNA1	205899_at	3.9	4.5	3.9	5.9		X	X
EGR3	206115_at	5.6	7.1	6.1	9.3		X	X
FOS	209189_at	5.2	7.1	7.2	9.1		X	
IL12A	207160_at	5.4	5.7	5.8	6.9		X	
PHLDA1	217997_at	4.6	4.6	4.6	5.9		X	
SGMS2	242963_at	5.1	5.1	5.1	6.5		X	
TAC1	206552_s_at	4.8	6.7	6.0	8.2		X	X
TFPI2	209277_at	3.6	4.1	3.6	6.3		X	X
TFPI2	209278_s_at	5.4	6.6	5.6	8.7		X	X
HSPA1L	210189_at	7.5	8.2	7.4	8.7			X
HSPH1	208744_x_at	9.4	9.7	9.2	10.3			X
DNAJB1	200666_s_at	9.4	10.8	9.9	11.8			X
LOC100652898	227404_s_at	6.5	9.5	8.4	10.7			X
INSIG1	201627_s_at	11.0	11.5	10.6	11.7			X
DUSP6	208891_at	6.0	8.1	7.6	8.6			X
DNAJB1	200664_s_at	8.2	9.6	8.7	10.7			X
ANXA1	201012_at	6.1	6.8	6.6	7.8			X

Table 2. Probesets that are differentially expressed between EGFR[wt-BG] *v.* EGFR[vIII-BG], EGFR[wt-BG] *v.* EGFR[L858R-BG], and EGFR[vIII-BG] *v.* EGFR[L858R-BG] as identified by SAM analysis (continued)

Gene_Symbol	Probeset_ID	eGFP	EGFRwt	EGFRvIII	EGFR-p. L858R	wt v vIII	wt v L858R	vIII v L858R
KCTD12	212188_at	8.9	9.7	8.9	10.7			X
HSPA6	117_at	5.4	7.0	6.0	7.9			X
DUSP6	208892_s_at	5.1	7.3	6.8	7.9			X
KCTD12	212192_at	9.8	10.2	9.7	10.8			X
ZCCHC12	228715_at	9.0	10.0	9.0	10.9			X
ETV5	203349_s_at	5.5	8.6	8.0	9.3			X
EGR2	205249_at	6.1	7.6	6.8	9.4			X
C11orf96	227099_s_at	8.5	10.3	9.5	12.0			X
GPR50	208311_at	7.2	8.0	7.2	9.1			X
DOK5	214844_s_at	4.4	5.1	4.5	6.0			X
INSIG1	201625_s_at	9.2	9.8	9.0	10.2			X

Differentially expressed genes (>2 fold change in expression level, fdr <0.2) between mutations are marked with X in one of the last three columns.

5

expression > 2 and fdr < 0.2, Table 2, Fig. 3). These probesets correspond to 15, 11 and 26 different genes respectively. Genes specifically induced by EGFRvIII-BG expression include SOCS3, C10ORF10 and DTX3L (_10, 4, and 2-fold induction respectively). EGFRL858R-BG specifically induces the expression of ARC, TFPI2, SGMS2, ARLB5 and CCNA1 (~ 8, 8, 3, 2 and 4-fold respectively). Gene expression analysis therefore indicates that different mutations in EGFR induce the expression of a unique set of genes.

We next analysed phosphoprotein levels by RPPA arrays on HOG cells stably expressing EGFRwt-BG, EGFRvIII-BG, EGFRL858R-BG or Bio-eGFP control. Three conditions were examined: normal (serum supplemented cell culture), serum free and serum free, EGF stimulated. All data are listed in Supplementary Table 3. Analysis of EGFR on these arrays demonstrates that all stably transfected cell lines, apart from the Bio-eGFP control, have increased levels of EGFR and show increased EGFR phosphorylation on pY1068 and pY1173. Serum deprivation does not result in a loss of EGFR phosphorylation (pY1068 and pY1173) which suggests that EGFR signalling remains active under these conditions. Finally, EGF stimulation results in a strong increase in EGFR_pY1068 (and to a lesser extent in pY1173), predominantly in EGFRwt-BG and EGFRL858R-BG expressing cells but also in BIOeGFP and expressing cells. EGF stimulation does not activate EGFRvIII-BG which is in-line with the fact that this mutation affects the EGF binding domain.
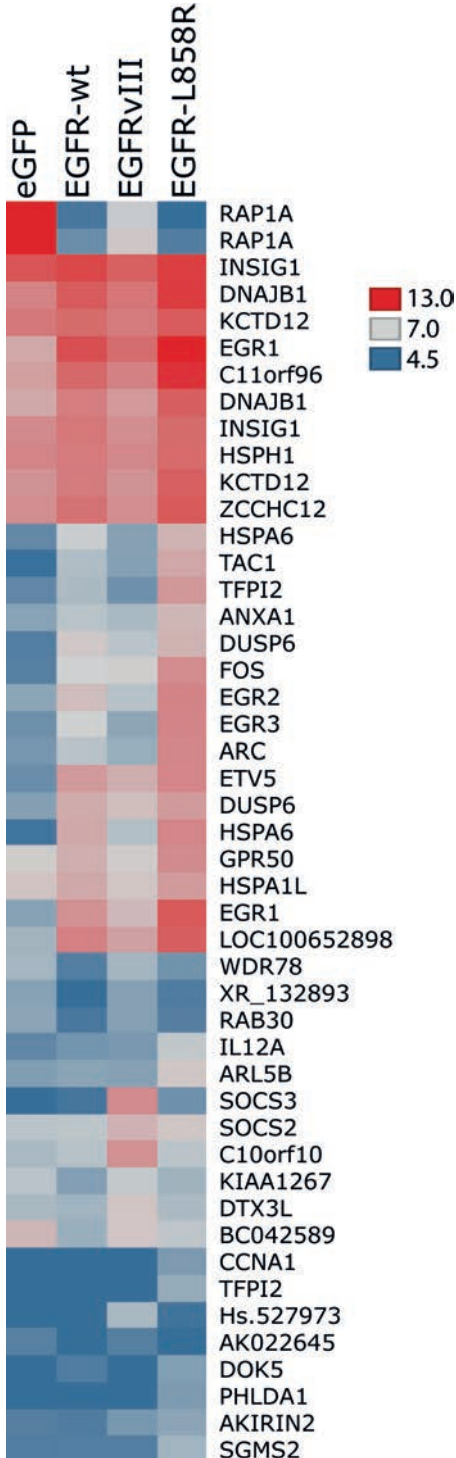
Figure 3. Genes that are differentially expressed between EGFRwt-BG *v.* EGFRvIII-BG, EGFRwt-BG *v.* EGFRL858R-BG, and EGFRvIII-BG *v.* EGFRL858R-BG as identified by SAM analysis. Bio-eGFP control is included for reference. Scales are color coded from 13.0 (red), 7.0 (grey) to 4.5 (blue) as RMA expression values.
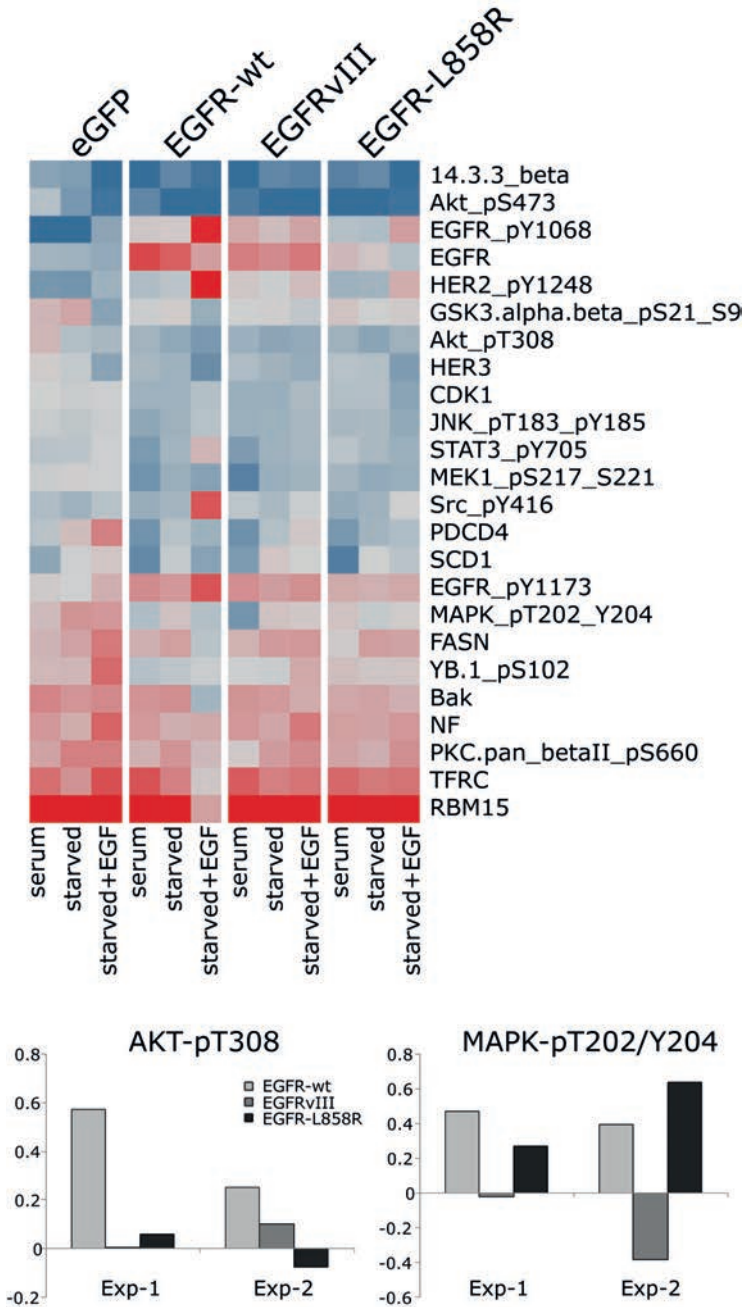
Figure 4. Proteins with >2 fold change in levels between different constructs as determined by RPPA analysis. Shown are RPPA results of these proteins in cells expressing EGFRwt-BG, EGFRvIII-BG, EGFRL858R-BG or Bio-eGFP control under normal cell culture conditions (serum supplemented) and serum free cultures ± EGF. Colors are scaled from the minimum value (blue, -1.26), average (grey, 0.41) to max RPPA vaule (red, 3.42). B) Confirmation by an independent RPPA experiment of AKT-pT308 (left) and MAPK_pT202 (right). Results of the original (exp-1) and confirmation (exp-2) are shown.

To determine whether specific mutations induce differences in their downstream pathway activation, we screened all proteins that showed a > 2-fold change in levels between different constructs (Fig. 4). Examples of differences identified include, under serum conditions (i) lower levels of AKT-pT308 (and AKT_pS473) in EGFRL858R-BG expressing HOG cells compared to EGFRwt-BG, EGFRvIII-BG or BIO-eGFP expressing cells; (ii) lower levels of MAPK_pT202 phosphorylation in EGFRvIII-BG expressing cells compared to those expressing EGFRwt-BG and EGFRL858R-BG. Virtually identical data were obtained in an independent RPPA experiment (Fig. 4, and Supplementary Fig. 2). Western blot experiments (independently performed) further confirmed the differences in AKT-pT308 and MAPK_pT202 phosphorylation (Fig. 4). These data therefore indicate that different mutations in EGFR can induce a differential downstream pathway phosphorylation.

Because our results indicate that each mutation has unique molecular properties, we determined whether the various forms of EGFR also differentially affect cell physiology. HOG cells stably expressing EGFRvIII-BG and EGFRL858R-BG showed a decreased proliferation compared to bio-eGFP or EGFRwt-BG expressing cells (Fig. 5). The differences between constructs were consistently observed over multiple experiments (n = 4 experiments, six wells/experiment and four locations/well). In a wound healing
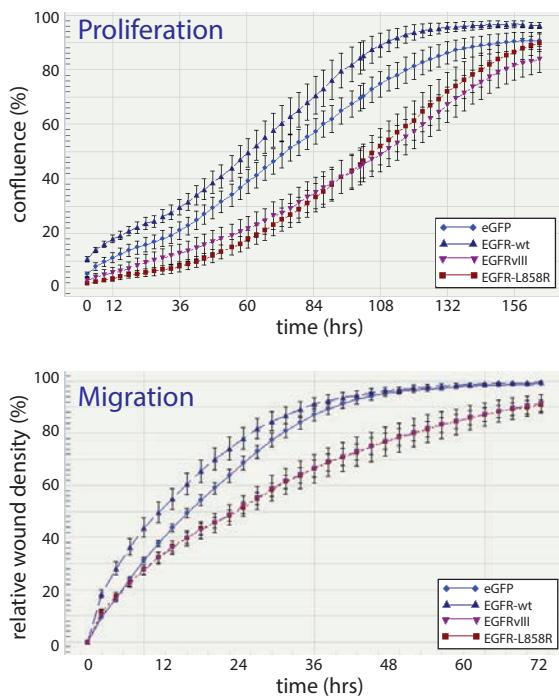
Figure 5. Mutations in EGFR differentially affect proliferation (top) and migration (bottom) in HOG cells stably transfected with EGFRwt-BG, EGFRvIII-BG, EGFRL858R-BG or Bio-eGFP control. EGFRvIII-BG and EGFRL858R-BG have virtually identical migration.

assay, the EGFRvIII-BG and EGFRL858R-BG expressing HOG cells also had a significantly slower migration compared to bio-eGFP or EGFRwt-BG expressing cells (P < 0.001, for all comparisons Fig. 5). The difference between constructs was consistently observed in two independent experiments (n = 2 experiments, six wells/experiment and three locations/well). These data therefore indicate that different mutations differentially affect cell physiology.

DISCUSSION

In this study, we demonstrate different mutations in EGFR associate with different proteins, activate unique downstream signalling pathways (as shown by the induction of a unique set of genes and protein phosphorylation) and that cell lines expressing different EGFR mutation constructs display differences in physiology (proliferation and migration). Our data therefore demonstrate that different mutations have different functional consequences, which may provide an explanation for a tumour type specific mutation spectrum.

Our data are in line with other studies that highlighted differences between wildtype EGFR, EGFRvIII and/or EGFR p.L858R. For example, wildtype EGFR and EGFRvIII induce phosphorylation of different substrates, have differential activation of the JNK, STAT and MAPK signalling pathways, induce the expression of a unique set of genes and have differences in nuclear localisation [9–13,19]. Our data are also in line with a study showing that both wtEGFR and EGFRvIII interact with DNA–Protein Kinase (PRKDC) whereas EGFR p.L858R does not [19]: our biotin pulldown showed a ~two fold reduction in association with PRKDC of EGFRL858R-BG compared to both EGFRwt-BG and GFRvIII-BG (Supplementary Table 1). We did not observe differential association of EGFRwt-BG, EGFRvIII-BG and EGFRL858R-BG with CBL proteins, see [20]. However, binding to Cbl proteins occurs only after stimulation with EGF, whereas our cells were not EGF stimulated.

Apart from EGFR, a few proteins also show mutation specific binding partners and differential activation of downstream signalling pathways. Examples include TP53 (R273H and R267P) and PIK3CA [21–24].

Because tumours often remain dependent on their acquired genetic changes for growth, these changes are direct targets for treatment. However, when each mutation activates a unique set of downstream pathways, it is possible each mutation will require specific inhibition. Indeed, different mutations in EGFR show differential sensitivity towards

inhibitors: activating mutation in the kinase domain are associated with response to erlotinib and gefitinib whereas the EGFR p.A289D mutation is more sensitive to inhibition by lapatinib [7,25,26]. Moreover, kinase domain mutations do not occur in GBMs and inhibitors that act on these mutations (erlotinib and gefitinib) do not show clinical benefit in GBM patients eventhough EGFR is a driver in GBMs [27,28].

Our experiments demonstrate that a number of proteins differentially associate with EGFR constructs. It is interesting to note that mutations in DOCK4, UGGT1, MYCBP2 and SMTN have been found both in GBMs (2/283, 4/283, 1/283 and 1/283 respectively) and pulmonary adenocarcinomas (16/220, 7/220, 17/220 and 4/220). The first of these proteins that was further examined, DOCK4, associates with EGFRvIII-BG and, to a lesser extent, with EGFRwt-BG (but not with EGFRL858R-BG). DOCK4 is mutated in various tumors including bladder ($\sim 10\%$), colorectal ($\sim 10\%$) and lung ($\sim 7\%$). Two mutations in DOCK4 have thus far been identified in GBMs. DOCK4 is involved in cell migration through the activation of RAC1 [29,30]. Whether the difference in cell migration between EGFRwt-BG and EGFRvIII-BG is due to differential association with DOCK4 remains to be determined. DOCK4 also functions as a scaffold protein within the Wnt signaling pathway and is essential for activation of this pathway in vivo [18]. However, we did not find a mutation specific activation of the WNT pathway. A second differential binding protein, UGGT1, was found to predominantly associate with EGFRvIII-BG. UGGT1 plays a central role in the quality control of protein folding in the endoplasmic reticulum (glycosylated proteins) where it promotes substrate solubility [31]. It was recently demonstrated that the L858R mutation in EGFR reduces the disorganised conformation of the protein [32]. Because UGGT1 is involved in the quality control of protein folding, it is possible that the lack of association between UGGT1 and EGFRL858R-BG identified in our study may be a result of an altered (i.e. less disorganised) conformation.

Similar to UGGT1, MYCBP2 also showed preferential association with EGFRL858R-BG. MYCBP2 encodes an E3 ubiquitin ligase which mediates the ubiquitinylation and subsequent degradation of target proteins. The protein is involved in the regulation of the mTOR pathway: knockdown of MYCBP2 inhibits the mTOR pathway [33]. Finally, SMTN showed preferential association with EGFRL858R-BG. SMTN co-localised with a-actin and is involved in the contraction of smooth muscle cells [34]. Whether the differential association with specific EGFR mutations affects the mTOR pathway or actin dynamics in tumour cells remains to be determined.

EGFR is a member of the ERBB protein family, a family of proteins that plays a role in several cancer types [35]. The various ERBB family members can heterodimerise with

each other, and each heterodimer can activate different signal transduction pathways [35,36]. Although we demonstrate in this manuscript that different EGFR mutations activate unique molecular pathways, it remains to be determined whether the different mutations in EGFR also result in different heterodimerisation induced pathway activation. Of note, the various ERBB family members do not overtly show a tumor type specific mutation pattern [4,37].

Our results show that expression of EGFRvIII-BG or EGFRL858R-BG in HOG cells results in a decreased proliferation and migration, which may be counterintuitive for an oncogene. However, such reduced proliferation has been observed before in mutant melanoma cells where expression of EGFR confers a growth disadvantage that is further strengthened by the addition of EGF [38]. Perhaps this is caused when an oncogene (such as EGFR) is expressed in cells that have never been dependent on the oncogene (or the various mutations therein). A similar growth disadvantage (and altered migration pattern) was observed when expressing mutant (R132H) IDH1 into cell lines [39,40]. Interestingly, IDH1 also has a tumor-type specific mutation pattern [41,42].

In summary, our results indicate that there are distinct differences between different mutations in EGFR. Whether these different mutations also have different oncogenic properties remains to be determined. However, these functional differences can lead to the identification of mutation-specific EGFR inhibitors.

Conflict of interest statement

None declared.

Support

Appendix A. Supplementary data

Supplementary data associated with this article can be found, in the online version, at http://dx.doi.org/10.1016/j.ejca.2015.02.006.

5

REFERENCES

[1]   Weinberg RA. The Biology of Cancer: Garland Science; 2007.

[2]   Citri A, Yarden Y. EGF-ERBB signalling: towards the systems level. Nat Rev Mol Cell Biol 2006;7(7):505–16.

[3]   Brennan CW, Verhaak RG, McKenna A, Campos B, Noushmehr H, Salama SR, et al. The somatic genomic landscape of glioblastoma. Cell 2013;155(2):462–77.

[4]   Forbes SA, Bindal N, Bamford S, Cole C, Kok CY, Beare D, et al. COSMIC: mining complete cancer genomes in the Catalogue of Somatic Mutations in Cancer. Nucleic Acids Res 2011;39(Database issue):D945–50.

[5]   Zandi R, Larsen AB, Andersen P, Stockhausen MT, Poulsen HS. Mechanisms for oncogenic activation of the epidermal growth factor receptor. Cell Signal 2007;19(10):2013–23.

[6]   Fan QW, Cheng CK, Gustafson WC, Charron E, Zipper P, Wong RA, et al. EGFR phosphorylates tumor-derived EGFRvIII driving STAT3/5 and progression in glioblastoma. Cancer Cell 2013;24(4):438–49.

[7]   Vivanco I, Robins HI, Rohle D, Campos C, Grommes C, Nghiemphu PL, et al. Differential sensitivity of glioma- versus lung cancer-specific EGFR mutations to EGFR kinase inhibitors. Cancer Discov 2012;2(5):458–71.

[8]   Holland EC, Hively WP, DePinho RA, Varmus HE. A constitutively active epidermal growth factor receptor cooperates with disruption of G1 cell-cycle arrest pathways to induce glioma-like lesions in mice. Genes Dev 1998;12(23):3675–85.

[9]   Chu CT, Everiss KD, Wikstrand CJ, Batra SK, Kung HJ, Bigner DD. Receptor dimerization is not a factor in the signaling activity of a transforming variant epidermal growth factor receptor (EGFRvIII). Biochem J 1997;324(Pt. 3):855–61.

[10] Antonyak MA, Moscatello DK, Wong AJ. Constitutive activation of c-Jun N-terminal kinase by a mutant epidermal growth factor receptor. J Biol Chem 1998;273(5):2817–22.

[11] Pedersen MW, Pedersen N, Damstrup L, Villingshoj M, Sonder SU, Rieneck K, et al. Analysis of the epidermal growth factor receptor specific transcriptome: effect of receptor expression level and an activating mutation. J Cell Biochem 2005;96(2):412–27.

[12] Chumbalkar V, Latha K, Hwang Y, Maywald R, Hawley L, Sawaya R, et al. Analysis of phosphotyrosine signaling in glioblastoma identifies STAT5 as a novel downstream target of DEGFR. J Proteome Res 2011;10(3):1343–52.

[13] Latha K, Li M, Chumbalkar V, Gururaj A, Hwang Y, Dakeng S, et al. Nuclear EGFRvIII-STAT5b complex contributes to glioblastoma cell survival by direct activation of the Bcl-XL promoter. Int J Cancer 2012;132:509–20.

[14] Mellacheruvu D, Wright Z, Couzens AL, Lambert JP, St-Denis NA, Li T, et al. The CRAPome: a contaminant repository for affinity purification-mass spectrometry data. Nat Methods 2013;10(8):730–6.

[15] Chatr-Aryamontri A, Breitkreutz BJ, Heinicke S, Boucher L, Winter A, Stark C, et al. The BioGRID interaction database: 2013 update. Nucleic Acids Res 2013;41(Database issue):D816–23.

[16] Foerster S, Kacprowski T, Dhople VM, Hammer E, Herzog S, Saafan H, et al. Characterization of the EGFR interactome reveals associated protein complex networks and intracellular receptor dynamics. Proteomics 2013;13(21):3131–44.

[17] Kandasamy K, Mohan SS, Raju R, Keerthikumar S, Kumar GS, Venugopal AK, et al. NetPath: a public resource of curated signal transduction pathways. Genome Biol 2010;11(1):R3.

[18] Upadhyay G, Goessling W, North TE, Xavier R, Zon LI, Yajnik V. Molecular association between beta-catenin degradation complex and Rac guanine exchange factor DOCK4 is essential for Wnt/beta-catenin signaling. Oncogene 2008;27(44):5845–55.

[19] Liccardi G, Hartley JA, Hochhauser D. EGFR nuclear translocation modulates DNA repair following cisplatin and ionizing radiation treatment. Cancer Res 2011;71(3):1103–14.

[20] Schmidt MH, Furnari FB, Cavenee WK, Bogler O. Epidermal growth factor receptor signaling intensity determines intracellular protein interactions, ubiquitination, and internalization. Proc Natl Acad Sci U S A 2003;100(11):6505–10.

[21] Coffill CR, Muller PA, Oh HK, Neo SP, Hogue KA, Cheok CF, et al. Mutant p53 interactome identifies nardilysin as a p53R273H-specific binding partner that promotes invasion. EMBO Rep 2012;13(7):638–44.

[22] Vaughan CA, Frum R, Pearsall I, Singh S, Windle B, Yeudall A, et al. Allele specific gain-of-function activity of p53 mutants in lung cancer cells. Biochem Biophys Res Commun 2012;428(1):6–10.

[23] Ross RL, Askham JM, Knowles MA. PIK3CA mutation spectrum in urothelial carcinoma reflects cell context-dependent signaling and phenotypic outputs. Oncogene 2013;32(6):768–76.

5
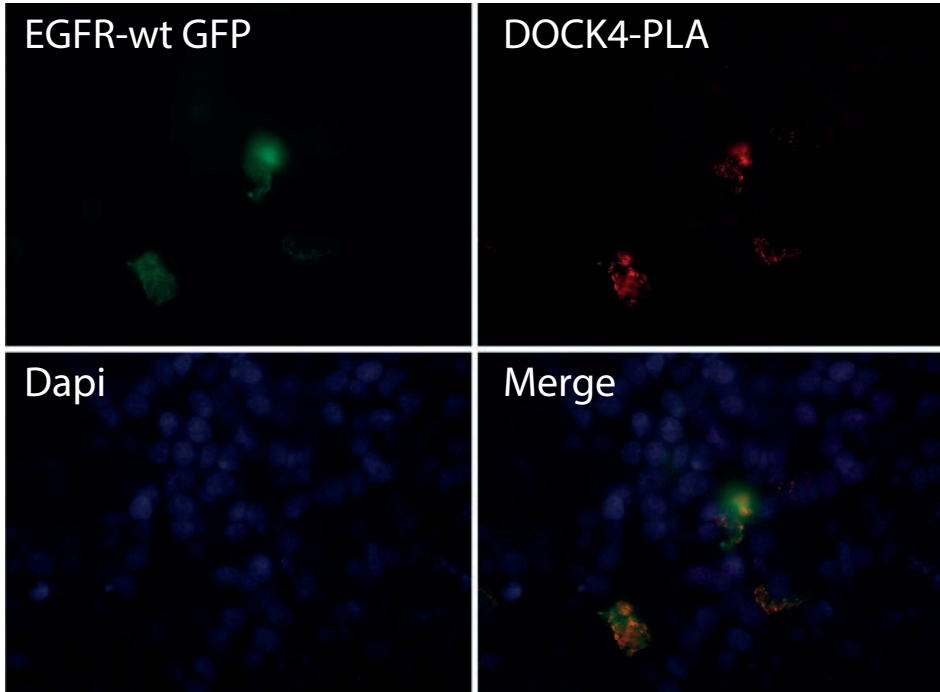
Supplementary Figure 1. A proximity ligation assay confirms that DOCK4 associated with EGFRwt-BG in **cells that** were serum starved overnight followed by EGF stimulation.
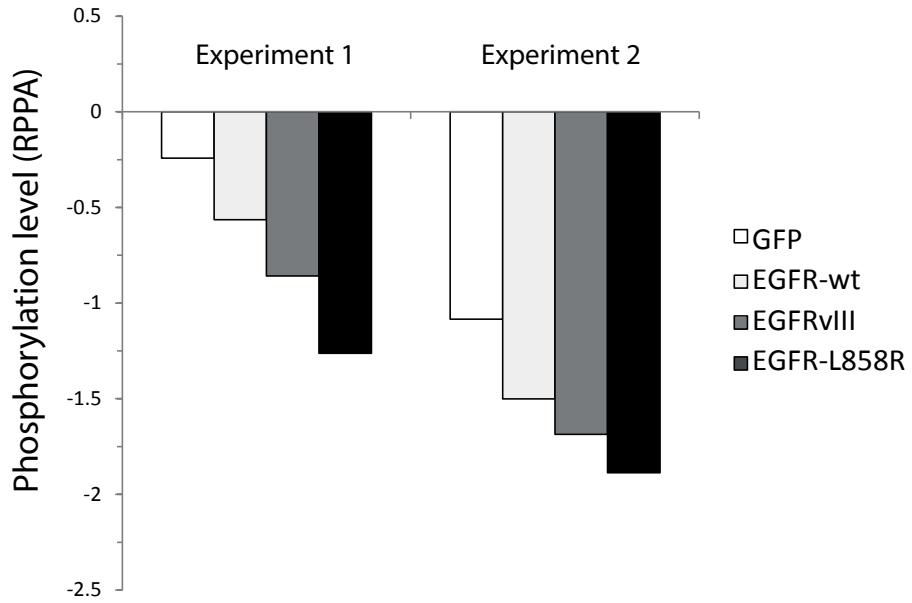
Supplementary Figure 2. Two independent RPPA experiments of Akt-pS473.

Chapter 6

Changes in the *EGFR* amplification and *EGFRvIII* expression between paired primary and recurrent glioblastomas

Martin J. van den Bent[1], Ya Gao[1], Melissa Kerkhof[2], Johan M Kros[3], Thierry Gorlia[4], Kitty van Zwieten[1], Jory Prince[1], Sjoerd van Duinen[5], Peter A. Sillevis Smitt[1], Martin Taphoorn[2], Pim J. French[1]

Depts of [1]Neurology and [3]Pathology, Erasmus MC, PO Box 2040, 3000 CA Rotterdam, the Netherlands
[2]Dept Neurology, Haaglanden MC, The Hague, The Netherlands
[4]EORTC headquarters, Av Mournier 83, 1200 Brussels, Belgium
[5]Pathology dept, Leiden University Medical Center, Leiden, the Netherlands

ABSTRACT

Background

The efficacy of novel targeted therapies is often tested at the time of tumor recurrence. However, for glioblastoma patients, surgical resections at recurrence are performed only in a minority of patients and therefore molecular data are predominantly derived from the initial tumor. Molecular data of the initial tumor for patient selection into personalized medicine trials can therefore only be used when the specific genetic change is retained in the recurrent tumor.

Methods

In this study we determined whether *EGFR* amplification and expression of the most common mutation in GBMs (*EGFRvIII*) is retained at tumor recurrence. Because retention of genetic changes may be dependent on the initial treatment, we only used a cohort GBM samples that were uniformly treated according to the current standard of care, chemo-irradiation with temozolomide.

Results

Our data show that, in spite of some quantitative differences, the *EGFR* amplification status remains stable in the majority (84 %) of tumors evaluated. *EGFRvIII* expression remained similar in 79 % of GBMs. However, within the tumors expressing *EGFRvIII*- at initial diagnosis, approximately half lose their *EGFRvIII* expression at tumor recurrence.

Conclusions

The relative stability of *EGFR* amplification indicates that molecular data obtained in the primary tumor can be used to predict the *EGFR* status of the recurrent tumor but that care should be taken in extrapolating *EGFRvIII* expression from the primary tumor, particularly when expressed at first diagnosis.

INTRODUCTION

Gliomas are the most common type of primary brain tumor of which 60-70 % are diagnosed as glioblastoma multiforme (GBM), the most aggressive variant[1]. The current standard of care for GBM patients includes surgical resection followed by chemo-irradiation[2]. However, tumors invariably relapse and when this occurs, treatment options are limited. In fact, no standard of care exists for recurrent GBM patients. Nitrosoureas, retreatment with (dose-intense) temozolomide, and re-irradiation are often employed but have limited activity. Progression-free survival of recurrent GBM is 2-4 months and post-progression survival is 6-8 months with conventional chemotherapy [3].

Current efforts to improve treatment of GBMs are often based on a personalized medicine approach. In this approach, the efficacy of novel agents are tested on those tumors that harbor specific mutations. Personalized medicine trials will generally be performed after the standard of care treatment, at the time of tumor recurrence. However, surgical resections at recurrence are performed on a minority of glioma patients. Since marker testing based on circulating tumour DNA is not feasible (< 10 % detection rate) for glioma patients [4], molecular data can only be derived from analysis of the tumor itself. Therefore, using molecular data of the initial tumor for inclusion into personalized medicine trials requires the specific genetic change to be retained in the recurrent tumor. A recent study on a limited set of low grade gliomas indicated that only ~ 50 % of all mutations present in the primary tumor are also present in the recurrent tumor [5]. Although this percentage was higher for the known causal cancer genes, this demonstrates the need to obtain more insight into the correlation between molecular changes of the primary and recurrent tumor, especially if this molecular change is the target for treatment at progression. A substantial difference between newly diagnosed and recurrent tumors will indicate that patients require re-surgery for inclusion into a personalized medicine trial.

The epidermal growth factor receptor (EGFR) is a receptor tyrosine kinase that is frequently amplified and mutated in GBMs [6,7]. The most common mutation found in GBM patients, the *EGFRvIII* mutation, is an in-frame deletion of exons 2-7 which results in the receptor being constitutively active. Because *EGFR* amplification and *EGFRvIII* expression contribute to tumor formation, EGFR is a potential target for treatment in GBM patients [8-12]. In this study we therefore screened for differences in *EGFR* status and *EGFRvIII* expression between tumors at initial diagnosis and at recurrence.

6

METHODS

Samples

Glioblastoma samples were collected from two hospitals in the Netherlands (Erasmus MC, Rotterdam and MC Haaglanden, the Hague) from patients operated from 1999-2013, who had resurgery at first recurrence. Use of patient material was approved by the Institutional Review Board of the respective hospitals. Patients were uniformly treated with chemoradiation with temozolomide[2]. All samples were evaluated for tumor content by a central review pathologist (J.M. Kros), samples with insufficient tumor content ($< 30\%$) were omitted from the analysis.

RT-qPCR

DNA and RNA were isolated using the Allprep DNA/RNA FFPE kit (Qiagen, Venlo, the Netherlands) according to the manufacturers' instructions except for an extension of the prot K incubation step from 15' to overnight. *EGFR* amplification status and *EGFRvIII* expression was determined by (RT-) qPCR, using assays from Life Technologies (Bleiswijk, the Netherlands). The assay for *EGFR* DNA (assay number Hs02501405_cn) was designed ~ 1100 bp downstream of exon 1 as few genomic changes occur in this region; genomic breakpoints giving rise to *EGFRvIII* occur further downstream in this intron[13]. Control probes for DNA were *RNase P* (TaqMan copy number reference assay) and *BRAF* (HS04949885). *EGFR* status was determined as the average of the Ct values of control probes – the average *EGFR* Ct values. The qPCR assay used correlated with *EGFR* amplification status as determined by copy number arrays (n = 5 Oncoscan DX, Affymetrix, Santa Clara Ca), examples are shown in supplementary figure 1.

EGFRvIII expression was determined using RT-Q-PCR using a custom made primers/probe set designed over the exon 1-8 transition. Control RT-Q-PCR primers were targeted against *EGFR* wt (HS01076078_m1), RPL30 (Hs00265497_m1) and POP4 (Hs00198357_m1). Samples in which *EGFRvIII* expression > 35 Ct values were scored as negative. *EGFRvIII* expression was scored as percentage of all *EGFR* transcripts (*EGFRvIII* + *EGFR* wildtype (wt)). In this case, 30% expression of *EGFRvIII* indicates *EGFRvIII* expression is 1 Ct value lower than that of *EGFR* wt.

All primers showed linear amplification over a wide range of Ct values (DNA content or RNA expression). This was observed in five independent samples. Slope of the dilution curve was also similar between the three primers used, which allows direct comparison between primers used. All (RT-) Q-PCR experiments were run in duplicate. The concordance correlation coefficient (LIN, equivalent to intraclass correlation coefficient ICC), was used to assess similarities between *EGFR* measurements[14].

RESULTS AND DISCUSSION

EGFR amplification

A total of 89 patients were identified, of which tissue of 76 patients was available from both resections. *EGFR* amplification status could be determined in 55 primary-recurrent tumor pairs (table 1); in remaining patients we were unable to determine *EGFR* status in at least one of the two samples due to low tissue amounts (n = 7), too low tumor content (n = 1), insufficient DNA quality (n = 10) or the block did not contain tumor tissue (n = 3). Of these, *EGFR* amplification, as defined by a ΔCt > 3 between controls and *EGFR*, (which corresponds to an approximately 8 fold (2^3) increase) was present in 40/55 (73 %) samples at first diagnosis. High copy *EGFR* amplification, i.e. those tumors having a ΔCt > 5, (∼ 32 fold, 2^5) was observed in 23/55 (41 %) samples. The patient cohort examined in this study therefore has a higher percentage of tumors with *EGFR* amplification than reported in other studies [6,15]. This higher percentage of *EGFR*-amplified tumors may reflect sample bias or may be caused by differences in sensitivity of the different techniques used. Alternatively, a higher percentage of *EGFR*-amplified tumors may also be a result of selective enrichment for second surgeries (and re-treatment) of *EGFR* amplified tumors.

To test whether *EGFR* amplified tumors are more frequently eligible for resurgery, we have tested for such a selective enrichment on GBM samples treated within the Erasmus MC (between 1989 and 2005) as reported by us[16]. For this analysis, we used molecular subtyping based on gene expression data as a surrogate marker for *EGFR* amplification: *EGFR* amplification occurs predominantly in one molecular subtype (IGS-18, a subtype similar to 'classical' GBMs as defined by the TCGA)[16,17]. Of the tumors diagnosed as GBM at initial presentation, 32 were assigned to IGS-18 of which 7 (22 %) patients received resurgery. This frequency is ∼ 2-3 fold lower in tumours assigned to other subtypes (where *EGFR* amplification is infrequent) including IGS-22 (1/12, 8.3 %) or IGS-23 (6/47, 12.8 % this subtype shows overlap with the TCGA 'mesenchymal' GBMs). Although this difference is not statistically significant, it does provides some support for the bias towards resurgery of *EGFR* amplified tumors found in current. Of note, this potential bias was not observed in the TCGA dataset where 20/39, 2/5 and 11/18 patients received resurgery (tumors assigned to IGS-18, IGS-22 and IGS-23 respectively).

We have also compared clinical data from this study with data from GBMs in a historical cohort (n = 259) to screen for potential sample bias[16]. As may be expected, patients in the recurrent GBM cohort had a better performance score compared to the historical cohort (90.1 ± 8.7 v. 81.6 ± 17.0, P < 0.0001, Ttest), and were of younger

Table 1. Patient characteristics and molecular data

Pat ID	Age (y)	G	extent of resection		Loc	RT	TMZ	Tumor (%)		PD (days)	OS (days)	ev	EGFR (dCt)		EGFRvIII (%)	
			pr	rec				pr	rec				Pr	rec	pr	rec
AAA	54.2	M	PR	CR	P	60			40%	222	396	1		0.43		
AAB	68.3	M	PR	PR	P	60		80%	80%	434	584	1		2.93	86.5	93.7
AAC	68.3	F	PR	PR	T	60		90%	60%	67	304	1	6.28	4.08	85.1	
AAD	64.3	M	PR	PR	T	60				250	451	1	5.82	1.75	0.0	0.0
AAF	43.6	F	PR	PR	F	60		70%	50%	139	590	1	3.43	0.55	0.0	0.0
AAG	43.6	F	PR	PR	T	60	2	70%	70%	108	379	1	0.85	3.51	0.0	0.0
AAI	57.7	M	PR	PR	T	5		70%	60%	26	445	1	3.64	0.61	0.0	
AAJ	60.9	F	PR	PR	T	60	2	70%	50%	143	282	1	0.92	3.55	0.0	
AAK	58.0	F	PR	PR	P	60	4	70%	60%	182	605	1	3.29	2.88	0.0	0.0
AAL	60.1	M	PR	PR	O	60	3	70%	60%	187	373	1	2.54	6.32	0.0	0.0
AAM	63.0	F	PR	PR	T	60	6	70%	60%	271	410	1	5.82	2.59	85.2	79.7
AAN	50.3	F	PR	PR	P	60		70%	70%	455	527	1	6.00	4.41	36.1	0.0
AAS	37.3	M	PR	PR	F	60	6	80%	70%	264	508	1		4.38	0.0	0.0
AAT	62.5	F	PR	PR	F	60	6	80%	50%	833	1277	1	6.62	3.84	68.9	0.0
AAU	52.5	F	PR	PR	FP	60	6	70%	80%	647	1279	1			0.0	0.0
AAV	60.9	M	PR	PR	T	60	12	70%	60%	532	1412	1	5.39	6.49	0.0	0.0
AAW	40.7	F	PR	CR	F	60	1	70%	60%	104	448	1	0.54	0.51	0.0	0.0
AAX	43.0	F	PR	PR	O	60	1			61	754	1	11.29	9.41		0.2
AAY	69.6	F	PR	PR	F	60		80%	80%	257	315	1	0.36	0.84	0.0	0.0
ABA	52.9	F	PR	PR	T	60	6	70%	80%	241	470	1	3.52	5.97	0.0	0.0
ACA	65.3	M	PR	PR	F	60	6	90%	70%	147	247	1	8.74	3.87	0.0	0.0
ADA	55.7	M	PR	PR	F	60	6			363	602	1	6.71	4.48		0.0

Table 1. Patient characteristics and molecular data (continued)

Pat ID	Age (y)	G	extent of resection		Loc	RT	TMZ	Tumor (%)		PD (days)	OS (days)	ev	EGFR (dCt)		EGFRvIII (%)	
			pr	rec				pr	rec				Pr	rec	pr	rec
AFA		M	PR	PR	F	60	6	80%	80%	496	850	1	0.26	0.20	0.0	0.0
AGA	50.5	M	CR	PR	T	70	6	90%	70%	305	535	1	5.04	4.70	0.0	0.0
AHA	50.8	M	PR	PR	F	60	4	70%	80%	195	332	1	4.43	7.01		0.0
AIA	65.2	M	PR	PR	T	60	6			280	437	1	2.28	4.05		0.0
AlA	50.5	M	CR	PR	T	60	6	90%	70%	274		0	6.97	8.86	7.5	0.0
AMA	61.9	M	PR	CR	P	60	6	70%	70%	1707	1740	1	4.08	3.72		91.5
AOA	64.5	F	CR	CR	P	60	12	80%	80%	434		0	6.30	0.78	0.7	0.0
AQA	75.1	F	CR	PR	T	40	9	60%	70%	352		0	3.67	1.10	0.0	0.0
ARA	68.9	M	PR	CR	F	60	6			258		0	3.06	0.38		0.0
CAB	55.8	M	PR	PR	O	60	4	50%	60%	214	479	1	-0.23	3.93		
CAC	44.6	M	PR	CR	T	60	5	70%	30%	270	576	1	8.45	1.93	71.5	6.5
CAD	51.6	M	PR	PR	T	60	5	60%	70%	252	348	1	-0.30	3.33		0.0
CAF	28.4	M	PR	CR	T	60	6	70%	70%	276	694	1	4.65	6.68	54.1	27.4
CAK	45.7	F	PR	PR	P	60	2	40%	30%	229	395	1	1.43	3.43	0.0	
CAM	47.2	M	B	PR	T	60		60%	60%	388	520	1	7.48	8.70		0.0
CAN	66.0	M	PR	B	T	60	6	80%	50%	270	494	1	4.08	6.58		0.0
CAO	50.4	M	PR	PR	T	60	6	70%	70%	605	940	1	8.10	10.75	9.9	0.0
CAS	53.8	M	CR	B	F	60		80%	30%	198	560	1	6.65	3.10	1.9	
CAV	31.4	F	PR	PR	T	60	6	70%	70%	451	673	1		3.10	0.0	0.0
CAX	39.8	M	PR	PR	P	60	2	70%	20%	162	1079	1	4.18	3.40		0.0
CAZ	43.0	F	PR	B	T	60	6	80%	50%	905	1240	1	2.83	2.15	0.0	0.0
CBA	56.6	M	PR	PR	F	60	6	60%	40%	109	190	1	2.33	0.80	0.0	0.0

6

Table 1. Patient characteristics and molecular data (continued)

Pat ID	Age (y)	G	extent of resection		Loc	RT	TMZ	Tumor (%)		PD (days)	OS (days)	ev	EGFR (dCt)		EGFRvIII (%)	
			pr	rec				pr	rec				Pr	rec	pr	rec
CBE	53.9	F	PR	PR	T	59	6	80%	70%	297	523	1	4.45	6.15	0.0	0.0
CBF	59.7	F	PR	PR	F	60		80%	70%	232	513	1	5.98	4.33	87.3	95.9
CBG	31.7	M	PR	PR	F	648		90%	80%	389	702	1	1.40		0.0	
CBH	72.8	M	PR	PR	O	40		70%	60%	120	333	1	1.03			0.0
CBI	41.6	F	PR	PR	O	60	6	80%	90%	290	633	1	5.35	5.55	61.2	47.0
CBM	55.3	M	PR	PR		60	6	60%	60%	271	353	1	3.03	3.58	0.0	0.0
CBP	61.0	F	PR	PR	P	60	2	70%	80%	181	546	1	-0.05	0.10	0.0	0.0
CBQ	61.3	M	PR	PR	P	60	6	80%	70%	698	1283	1	5.40	4.65	0.0	0.0
CBR	60.1	M	PR		T	60	2	70%	90%	1291	343	1	1.45		0.0	0.0
CBS	52.7	F	PR	PR	T	60	2	70%	70%	170	260	1	4.73	2.25	0.0	0.0
CBT	52.5	M	PR	CR	F	60	6	60%	70%	289	681	1	6.55	6.90	51.0	20.6
CBV	50.0	M	PR	PR	F	60	6	30%		308	1383	1	3.75			
CBW	49.3	M	PR	PR	T	60	8	70%	60%	1261	1903	1	0.52	3.30	0.0	0.0
CCA	45.4	F	CR	PR	P	60	6	70%	70%	885	1488	1	7.58	8.08	0.0	0.5
CCB	52.1	M	PR	B	T	60	5	60%	60%	202	511	1	4.30	3.90	12.4	
CCD	52.5	F	PR	PR		60		80%	70%	283	327	1	4.65	4.60	0.0	0.0
CCP	43.2	F	PR	PR	F	59				203	279	1	2.10	-0.95	0.0	
CCV	49.2	M	PR		T	60	3	80%		411	413	1	8.10		0.0	
CCW	48.0	F	PR	PR	T	60		70%	30%	191	529	1	7.25	6.60	52.3	0.0
CCX	49.9	M	PR	PR	P	65		30%	70%	2069	2743	1	3.48	3.50	22.7	0.0
CCZ	51.2	F	PR	PR	O	60	3	80%	70%	247	277	1	8.43	8.88	76.9	51.4
CDA	65.6	M	PR	PR	T	60	6	80%	50%	628	890	1	5.88	4.10	0.0	

Table 1. Patient characteristics and molecular data (continued)

Pat ID	Age (y)	G	extent of resection		Loc	RT	TMZ	Tumor (%)		PD (days)	OS (days)	ev	EGFR (dCt)		EGFRvIII (%)	
			pr	rec				pr	rec				Pr	rec	pr	rec
CDB	36.5	M	PR	PR	T	60		80%	30%	109	223	1		3.75	0.0	83.9
CAY	48.8	F	PR	PR	O	60	6			282	336	1		8.50		7.0
CBO	63.6	M	PR	B	T	60	5			262	512	1	2.20		0.0	
AEA	45.0	F	CR	CR	T	60	6			281	402	1		4.08		0.0
AAE	53.0	F	PR	PR	F	60	6			1026	1357	1		4.60		0.0
AAH	46.8	M	PR	PR	P	60				335	545	1	8.52		1.4	
ANA	65.6	M	CR	PR	T	60	6			430		0		8.95		0.0
AAP	47.9	F	PR	PR	T	60	4			534	1802	1	10.34		63.7	
AAR	52.8	M	CR	PR	P	60	3			186	393	1				2.6
AKA	61.4	F	CR	PR	F	60	3	90%	70%	211	364	1		0.94		0.0

G: gender, M: Male, F: Female. Pr: primary tumor, rec: recurrent tumor. TMZ: number of cycles. RT dose (Gy). Loc: tumor location: P= Parietal, F= Frontal, O= Occipital, T= Temporal, FP: fossa posterior

6

115

age $(51.2 \pm 12.7$ v. 55.7 ± 13.6, P < 0.0001, Ttest). Our cohort also had a significantly lower male/female ration compared to our historic cohort (48/42 v. 175/84, P = 0.006, Fischers' exact test). There were also some differences in tumor location (n = 27, 15, 7 and 36 *v.* n = 40, 33, 12 and 29 for frontal, parietal, occipital and temporal location respectively), though this difference did not reach statistical significance (P = 0.06, Chi-square test). However, re-resection of GBMs will only be performed on tumors that are relatively accessible for surgery, which inevitably results in a location bias.
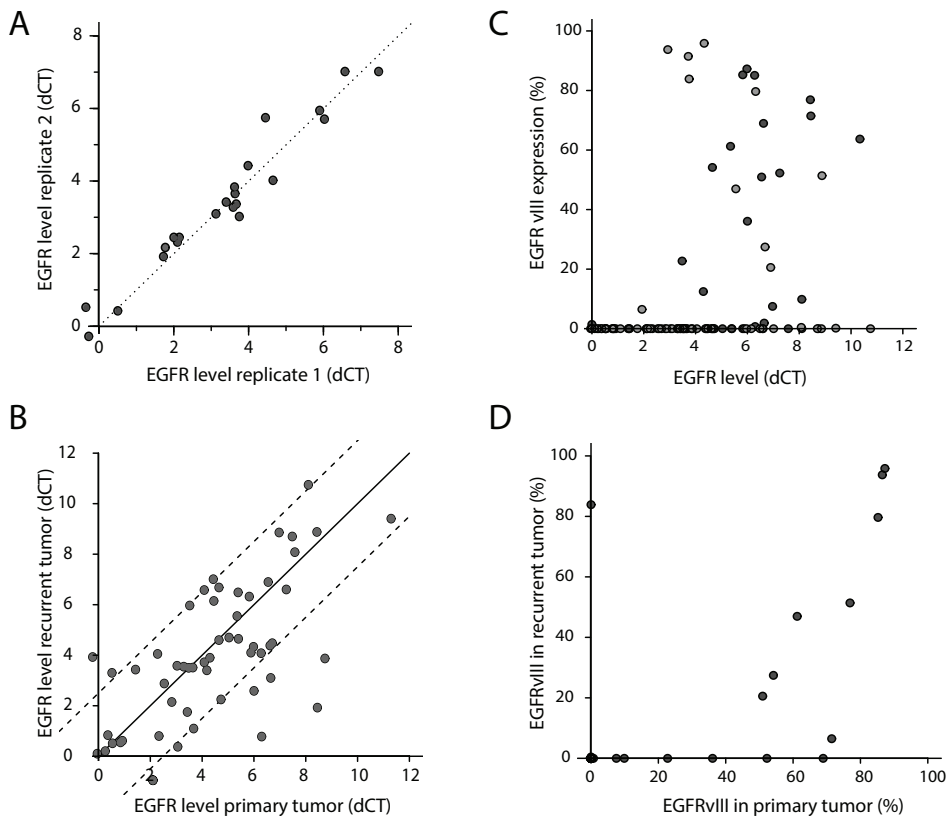

Figure 1. (A) Variability of EGFR amplification within biological replicates. As can be seen, the EGFR status between replicates was relatively constant in our samples. (B) EGFR amplification of primary versus recurrent glioblastomas. Although EGFR amplification varied between the primary and recurrent tumor, the difference was generally within 2.5 DCt values (dotted lines) of each other. (C) EGFRvIII expression, plotted as a percentage of all EGFR transcripts, is predominantly observed in samples with EGFR amplification (ie, those with dCt .3). Points in dark grey are from initial diagnoses, and light grey is from the recurrent tumor. (D) EGFRvIII expression in primary versus recurrent tumors. As can be seen, the relative expression of EGFRvIII was often lower in recurrent tumors than in primary tumors, with 7 samples showing EGFRvIII expression only in the primary tumor.

EGFRvIII expression

Of the 76 patients with tissue available from the primary and recurrent tumor, *EGFR-vIII* expression could be evaluated in 111 samples from 69 patients (table 1). Data from both primary and recurrent samples was generated for 42 patients; data from either the primary or recurrent tumor was of insufficient quality in the remaining 27 patients (in most cases, RT-QPCR could detect transcripts but the Ct values were too high to reliably allow quantification of *EGFRvIII* expression). *EGFRvIII* expression was detected in 34 samples and, apart from one (recurrent) sample, only occurred in samples with a genomic amplification of the *EGFR* locus (figure 1B). For the one sample with *EGFRvIII* expression without *EGFR* amplification (patient CAC) it should be noted that high copy *EGFR* amplification and *EGFRvIII* expression was detected in the primary tumor *but* the recurrent tumor had a much lower tumor content (30%). *EGFRvIII* expression was detected in 17/35 (49%) of primary tumors with *EGFR* amplification (ΔCt > 3), which is a similar frequency as previously reported[6].

Similar to reported [15], our data show that *EGFR* amplification status was highly variable between tumors: while some tumors show only modest amplification levels (3-4 ΔCt values), other tumors showed a much stronger amplification (up to 10 ΔCt value difference between *EGFR* and controls). Although the *EGFR* amplification status is variable between tumors, within biological replicates the *EGFR* status was relatively constant (n = 22, figure 1A). *EGFRvIII* expression was also highly variable between different tumors and ranged from < 1% up to > 90% of all *EGFR* transcripts being *EGFRvIII*. *EGFR* amplification and *EGFR* gene expression levels were correlated (figure 2).

Most GBMs retain their EGFR amplification status at tumor recurrence

EGFR amplification of the recurrent tumor did differ from the primary tumor but the difference was generally within 2-2.5 ΔCt values of each other (figure 1C). The overall concordance correlation coefficient between primary and recurrent tumors was 0.65. Cases where the difference between primary and recurrent tumors was < 2.5 ΔCt values (n = 42 tumor pairs) were considered to have retained their *EGFR* amplification status. In 13 tumors the difference in *EGFR* amplification between primary and recurrent tumors was > 2.5 ΔCt values; only four tumors showed a marked (≥ 4 ΔCt values) difference between the initial tumor at recurrence. More detailed analysis failed to detect any specific characteristics for these tumors with respect to extent of resection, use of steroids, *MGMT* promoter methylation and tumor location. Also, whilst we do observe a slightly higher tumor content in the primary tumor (71% ± 14% v. 63% ± 17%, P < 0.001, paired T-test) this change is unlikely to explain discrepancies in *EGFR* amplification status between the tumor at initial diagnosis and at recurrency:
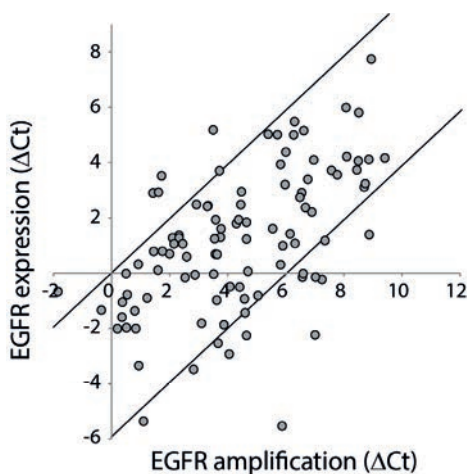
6

Figure 2. Correlation between *EGFR* amplification status (x-axis) and *EGFR* gene expression levels (y-axis) as determined by (RT-)QPCR on tumor DNA or RNA.

a two-fold decrease in tumor content would result in a maximal decrease in Ct value of one (i.e. one PCR cycle). The *EGFR* amplification status would change in eight/ thirteen samples showing a change > 2.5 ΔCt values between primary and recurrent: Five from amplified to non-amplified (of which three from high copy amplification i.e. ΔCt values > 5 to not-amplified) and three from *EGFR* not amplified to amplified (all of which resulting in moderate levels of *EGFR* amplification i.e. ΔCt values > 3 but < 5). Overall, the *EGFR* amplification status (dichotomized to either non-amplified or amplified) remained identical in most tumor pairs (46/55; 84 %, table 2).

Table 2. summary of *EGFR* and *EGFRvIII* data

		EGFR in recurrent tumour		
		Non-amp	Amp	n
EGFR in primary tumour	Non-amp	10	5*	15
	Amp	7*	33	40
	n	17	38	55

		EGFRvIII in recurrent tumour		
		Absent	Present	n
EGFRvIII in primary tumour	Absent	25	2	27
	Present	7	8	15
	n	32	10	42

Cutoff value for *EGFR* amplification is ΔCt>3 between *EGFR* and control probes. * Of the samples that change *EGFR* status from wt > amplified or from amplified > wt, 9 shown a difference in ΔCt value > 2.5 between the primary and recurrent tumor. When considering a change in EGFR amplification status also requires > 2.5 ΔCt values difference between primary and recurrent tumors, 46/55 (84%) tumors retain their EGFR status. Only 5 show a difference in ΔCt value > 3 between the primary and recurrent tumor.

GBMs can lose EGFRvIII expression at tumor recurrence

The relative expression of *EGFRvIII* often was lower in recurrent tumors than that in the primary tumor. Of the 15 tumors with detectable *EGFRvIII* expression in the primary tumor, 8 showed a > 20 % decrease in relative abundance of *EGFRvIII* transcripts (figure 1D). In fact, in seven out of fifteen *EGFRvIII* positive tumors at first surgery, the *EGFRvIII* variant was lost at the time of progression. These data are in line with data reported in a different study using an unselected patient cohort[18], although intratumoral heterogeneity may also explain part of this variability[19,20].

Of the 15 tumors with *EGFRvIII* expression, corresponding *EGFR* amplification status was available for 14. The majority of these (9/14) showed a relative increase in *EGFR* amplification (ΔCt between the tumor at initial diagnosis and at recurrence between 0 and 3), eventhough *EGFRvIII* expression decreased (n = 8) or stayed the same (n = 1). In fact only 3/14 showed concordant decrease in *EGFR* amplification status(> 2.0 ΔCt values between initial recurrent tumors) and decrease in *EGFRvIII* expression.

Qualitatively *EGFRvIII* status (present or absent) remained similar between the primary and recurrent tumor in 33/42 (79 %) samples: in 25 samples *EGFRvIII* was absent from the primary and recurrent tumor, in 8 samples it was expressed in both (table 2). The loss of *EGFRvIII* expression may be explained by the hypothesis that *EGFRvIII* deletions occur after *EGFR* amplification and that individual cells harbor varying levels of *EGFRvIII*[5]. Loss of *EGFRvIII* expression at tumor recurrent then represents clonal selection of the tumor. Indeed, gliomas are heterogeneous tumors in which distinct subpopulations of cells, each with different genetic makeup, exist[5,21]. However, recent evidence also suggests the genomic *EGFRvIII* deletion is an early event and that *EGFRvIII* expression is regulated by the tumor[19]. In fact, mice experiments demonstrated that at regrowth, the ratio of *EGFRwt/EGFRvIII* expression is similar to the primary tumor even when sorting for *EGFRvIII* high or low expressing tumor cells[22] (see also [23]). Loss of *EGFRvIII* expression then is a result of epigenetic regulation.

In summary, our data show that, in spite of some quantitative differences, the *EGFR* amplification status remains stable in the majority (~ 84 %) of tumors evaluated. *EGFRvIII* status also remained similar in 79 % of GBMs; however when focusing on *EGFRvIII* expressing tumors, only 50 % retain *EGFRvIII* expression at recurrence. The relative stability of *EGFR* amplification expression therefore indicates that molecular data obtained in the primary tumor can be used to predict the *EGFR* status of the recurrent tumor. Care should be taken in extrapolating *EGFRvIII* expression, in trials on recurrent glioblastoma that target EGFRvIII mutations a rebiopsy should be considered.

6

REFERENCES

1. Louis DN, Ohgaki H, Wiestler OD,Cavenee WK. (2007) *WHO Classification of Tumours of the Central Nervous System*, 4th Ed., Lyon

2. Stupp R, Mason WP, van den Bent MJ, et al.Radiotherapy plus concomitant and adjuvant temozolomide for glioblastoma. *N Engl J Med.* 2005; 352(10): 987-996

3. Gorlia T, Stupp R, Brandes AA, et al.New prognostic factors and calculators for outcome prediction in patients with recurrent glioblastoma: a pooled analysis of EORTC Brain Tumour Group phase I and II clinical trials. *Eur J Cancer.* 2012; 48(8): 1176-1184

4. Bettegowda C, Sausen M, Leary RJ, et al.Detection of circulating tumor DNA in early- and late-stage human malignancies. *Sci Transl Med.* 2014; 6(224): 224ra224

5. Johnson BE, Mazor T, Hong C, et al.Mutational analysis reveals the origin and therapy-driven evolution of recurrent glioma. *Science.* 2014; 343(6167): 189-193

6. Brennan CW, Verhaak RG, McKenna A, et al.The somatic genomic landscape of glioblastoma. *Cell.* 2013; 155(2): 462-477

7. Parsons DW, Jones S, Zhang X, et al.An integrated genomic analysis of human glioblastoma multiforme. *Science.* 2008; 321(5897): 1807-1812

8. Rich JN, Reardon DA, Peery T, et al.Phase II trial of gefitinib in recurrent glioblastoma. *J Clin Oncol.* 2004; 22(1): 133-142

9. van den Bent MJ, Brandes AA, Rampling R, et al.Randomized phase II trial of erlotinib versus temozolomide or carmustine in recurrent glioblastoma: EORTC brain tumor group study 26034. *J Clin Oncol.* 2009; 27(8): 1268-1274

10. Vivanco I, Robins HI, Rohle D, et al.Differential sensitivity of glioma- versus lung cancer-specific EGFR mutations to EGFR kinase inhibitors. *Cancer discovery.* 2012; 2(5): 458-471

11. Gan HK, Fichtel L, Lassman AB, et al.A phase 1 study evaluating ABT-414 in combination with temozolomide (TMZ) for subjects with recurrent or unresectable glioblastoma (GBM). *J Clin Oncol.* 2014; 32(5S): 2021

12. Sampson JH, Heimberger AB, Archer GE, et al.Immunologic escape after prolonged progression-free survival with epidermal growth factor receptor variant III peptide vaccination in patients with newly diagnosed glioblastoma. *J Clin Oncol.* 2010; 28(31): 4722-4729

13. Frederick L, Eley G, Wang XY,James CD.Analysis of genomic rearrangements associated with EGRFvIII expression suggests involvement of Alu repeat elements. *Neuro-oncol.* 2000; 2(3): 159-163

14. Lin LI.A concordance correlation coefficient to evaluate reproducibility. *Biometrics.* 1989; 45(1): 255-268

15. Hobbs J, Nikiforova MN, Fardo DW, et al.Paradoxical relationship between the degree of EGFR amplification and outcome in glioblastomas. *Am J Surg Pathol.* 2012; 36(8): 1186-1193

16. Gravendeel LA, Kouwenhoven MC, Gevaert O, et al.Intrinsic gene expression profiles of gliomas are a better predictor of survival than histology. *Cancer Res.* 2009; 69(23): 9065-9072

17. Erdem-Eraslan L, Gravendeel LA, de Rooi J, et al.Intrinsic molecular subtypes of glioma are prognostic and predict benefit from adjuvant procarbazine, lomustine, and vincristine chemotherapy in combination with other prognostic factors in anaplastic oligodendroglial brain tumors: a report from EORTC study 26951. *J Clin Oncol.* 2013; 31(3): 328-336

18. Montano N, Cenci T, Martini M, et al.Expression of EGFRvIII in glioblastoma: prognostic significance revisited. *Neoplasia.* 2011; 13(12): 1113-1121

19. Del Vecchio CA, Giacomini CP, Vogel H, et al.EGFRvIII gene rearrangement is an early event in glioblastoma tumorigenesis and expression defines a hierarchy modulated by epigenetic mechanisms. *Oncogene.* 2013; 32(21): 2670-2681

20. Francis JM, Zhang CZ, Maire CL, et al.EGFR variant heterogeneity in glioblastoma resolved through single-nucleus sequencing. *Cancer discovery.* 2014; 4(8): 956-971

21. Snuderl M, Fazlollahi L, Le LP, et al.Mosaic amplification of multiple receptor tyrosine kinase genes in glioblastoma. *Cancer Cell.* 2011; 20(6): 810-817

22. Nathanson DA, Gini B, Mottahedeh J, et al.Targeted therapy resistance mediated by dynamic regulation of extrachromosomal mutant EGFR DNA. *Science.* 2014; 343(6166): 72-76

23. Szerlip NJ, Pedraza A, Chakravarty D, et al.Intratumoral heterogeneity of receptor tyrosine kinases EGFR and PDGFRA amplification in glioblastoma defines subpopulations with distinct growth factor response. *Proc Natl Acad Sci U S A.* 2012; 109(8): 3041-3046

6
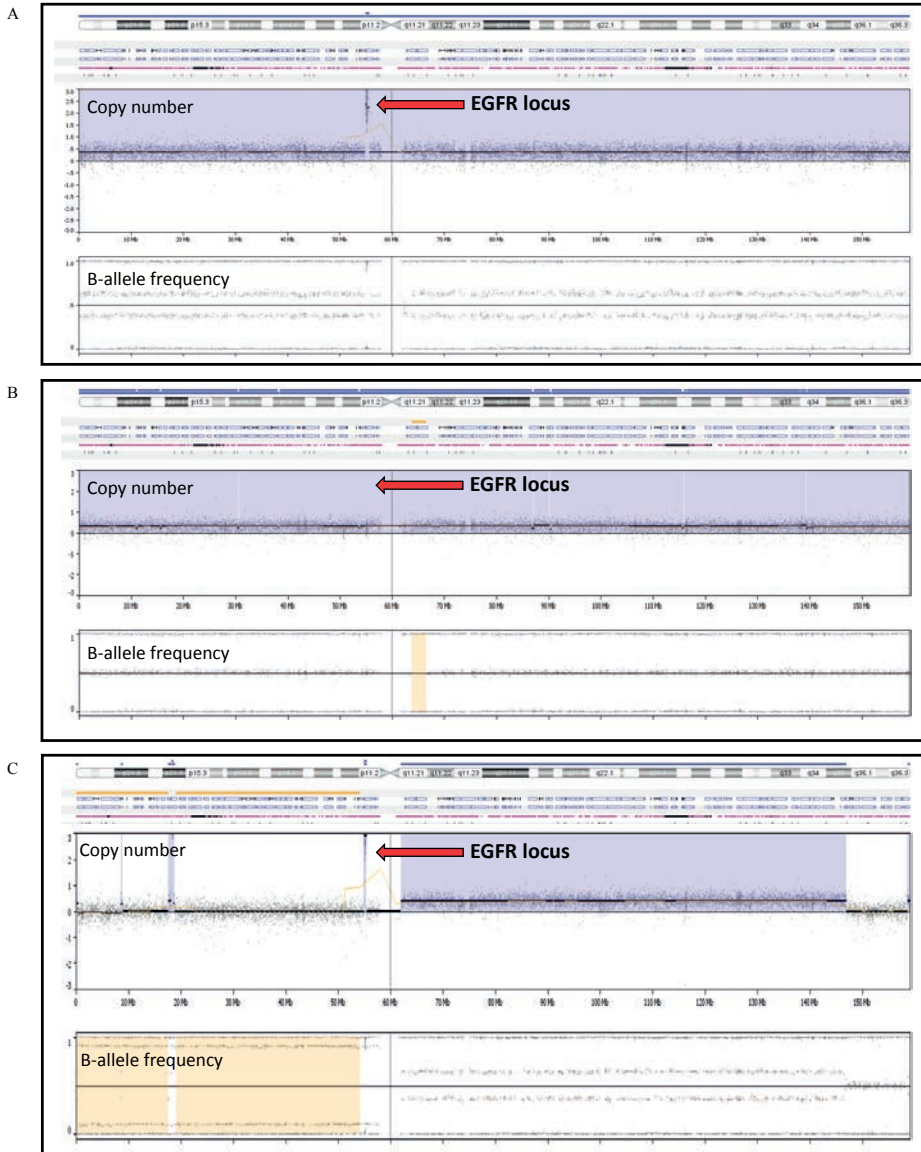
Supplementary Figure 1. Correlation Q-PCR with CNV by Oncoscan DX arrays. Three examples showing Q-PCR results (DCt) and copy number and B-allele frequency of chromosome 7. A: Example 1: EGFR amplified. Patient CCZ, sample at first diagnosis. EGFR amplficiation is visualized by the focal increase in copy number. QPCR DCt results for this sample was 8.4. On top of the high copy EGFR ampification, trisomy of chromosome 7 is seen. B: Example 2: EGFR wt. Patient CBH, sample at first diagnosis. QPCR DCt = 1.0. C: Example 3: EGFR amplified. Patient CCV, sample at first diagnosis. QPCR DCt = 8.1.

Chapter 7

Expression based Intrinsic Glioma Subtypes are prognostic in low grade gliomas of the EORTC22033-26033 clinical trial.

Y Gao[1], B Weenink[1], MJ van den Bent[2], L Erdem-Eraslan[1], JM Kros[3], PAE Sillevis Smitt[1], K Hoang-Xuan[4], A A Brandes[5], M. Vos[6], F Dhermain[7], R Enting[8], GF Ryan[9], O Chinot[10], M Ben Hassel[11], ME van Linde[12], W P Mason[13], JMM Gijtenbeek[14], C. Balana[15], A. von Deimling[16], Th Gorlia[17], R Stupp[18], ME Hegi[19], BG Baumert[20,21] and PJ French[1].

[1] De`partment of Neurology, Erasmus University Medical Center, 3000CA Rotterdam

[2] Department of Neurology, Daniel Den Hoed Cancer Center, 3075 EA Rotterdam, the Netherlands

[3] Department of Pathology, Erasmus University Medical Center, 3000CA Rotterdam

[4] APHP Pitié-Salpêtrière, Sorbonne Universités, UPMC, ICM, UMR S 1127, Paris, France

[5] Ospedale Bellaria, Bologna, Italy

[6] Med Ctr Haaglanden, The Netherlands

[7] I. Gustave Roussy, Villejuif, France

[8] UMCG and University of Groningen, Groningen, The Netherlands

[9] Peter MacCallum Cancer Center, Melbourne, Australia

[10] Aix Marseille, Université, APHM La Timone, Marseille, France

[11] Centre Eugène Marquis, Rennes, France

[12] VU University Medical Center and Academic Medical Center, Amsterdam, Netherlands

[13] Princess Margaret Hospital, University of Toronto, Toronto, ON, Canada

[14] Radboud University Medical Center Nijmegen, The Netherlands

[15] ICO Badalona Hospital, Germans Trias I Pujol, Barcelona, Spain

[16] German Cancer Consortium (DKTK) and CCU Neuropathology German Cancer Research Center (DKFZ) and Department Neuropathology, Institute of Pathology, University of Heidelberg, Heidelberg, Germany

[17] European Organisation for Research and Treatment of Cancer Headquarters, Brussels,Belgium

[18] Neuroscience Research Centre, CHUV, Lausanne, Switzerland

[19] Department of clinical Neurosciences, Lausanne University Hospital, Lausanne, Switzerland

[20] Depts. of Radiation-Oncology Paracelsus Clinic Osnabrueck and University of Muenster, Germany

[21] Maastricht University MedicalCentre and GROW (School for Oncology), Maastricht, The Netherlands

ABSTRACT

Introduction

The EORTC22033-26033 clinical trial (NCT00182819) investigated whether initial temozolomide (TMZ) chemotherapy confers survival advantage compared to radiotherapy (RT) in low grade glioma patients (LGG). In this study we performed gene expression profiling on tissues from this trial in order to identify markers associated with progression free survival and treatment response.

Methods

Gene expression profiling, performed on 195 samples, was used to assign tumors to one of six intrinsic glioma subtypes (IGS; molecularly similar tumors as previously defined using unsupervised expression analysis) and to determine the composition of immune-infiltrate. DNA copy number changes were determined using OncoScan arrays.

Results

We confirm that IGS-subtypes are prognostic in the EORTC22033-26033 clinical trial. Specific genetic changes segregate in distinct IGS subtypes: most samples assigned to IGS-9 have *IDH*-mutations and 1p19q codeletion, samples assigned to IGS-17 have *IDH*-mutations without 1p19q codeletion and samples assigned to other intrinsic subtypes often are *IDH*-wildtype. A trend towards benefit from RT was observed for samples assigned to IGS-9 (HR for TMZ is 1.90, P = 0.065), but not for samples assigned to IGS-17 (HR 0.87, P = 0.62). We did not identify genes significantly associated with progression free survival (PFS) within intrinsic subtypes, though follow-up time is limited. We also show that LGGs and GBMs differ in their immune-infiltrate which suggests that LGGs are less amenable to checkpoint inhibitor type immune therapies. Gene-expression analysis also allows identification of relatively rare subtypes. Indeed, one patient with a pilocytic astrocytoma (PA) was identified.

Conclusion

Intrinsic glioma subtypes are prognostic for PFS in EORTC22033-26033 clinical trial samples.

INTRODUCTION

Low grade or grade II gliomas (LGGs) are a heterogeneous set of primary brain tumors that mainly occur in the 4th and 5th decade of life [1,2]. The incidence is relatively low (< 1 per 100.000 persons/year) and, as they are slow growing tumors, patients have a relatively favorable prognosis, especially compared to gliomas of higher grade. Nevertheless, LGGs have the tendency to evolve into gliomas of higher grade, and most patients will ultimately die from the disease [3,4]. Based on their histological appearance, three subtypes of LGG can be distinguished: oligodendrogliomas, astrocytomas and mixed oligoastrocytomas. The current WHO classification has incorporated molecular markers (1p19q codeletion, and mutations in the *IDH1/2* and *ATRX* genes) to delineate astrocytoma and oligodendroglioma, but no longer considers oligoastrocytomas as a separate entity as they cannot molecularly be distinguished from other entities. [2,5]

Treatment options for LGG patients include surgery, radiotherapy (RT) and chemotherapy (or combinations thereof), or a watchful waiting strategy can be adopted [4,6]. Nevertheless, the optimal management of patients with a LGG has remained controversial and only relatively few randomized phase III clinical trials have been performed. Earlier trials focusing on the effect of RT showed no effect of RT dosing on overall survival and, in a separate trial, there was no effect of early vs delayed RT after surgery on overall survival [7-9]. Data from two large randomized clinical trials recently reported on the efficacy of chemotherapy in LGGs. Firstly, the RTOG9802 clinical trial, examining the role of the addition of procarbazine, lomustine and vincristine (PCV) chemotherapy after RT, showed improved survival of this regimen when compared to RT only [10]. Second, the EORTC22033-26033 clinical trial examined the role of RT vs temozolomide (TMZ) chemotherapy and found no difference between the two on progression free survival (PFS) or in quality of life [11,12]. Because of the limited follow-up time, data on overall survival is not available.

Interestingly, correlative molecular marker analysis in the EORCT22033-26033 study identified a subpopulation of patients that benefit from RT: Within the group of patients harboring tumors with an IDH mutation and in which the 1p and 19q chromosomal arms were not codeleted ('*Molecular Astrocytomas*'), an improved PFS was noted when they were treated with RT. No such benefit was observed within the group of IDH-mutated, 1p19q-codeleted tumors ('*Molecular Oligodendrogliomas*') [11]. We have previously shown that gene-expression profiling and subsequent molecular subtyping based on the gene-expression profile (intrinsic glioma subtypes) can identify prognostic subgroups and identify genes and subtypes that are associated with response to treatment [13-15]. In this study we have therefore performed gene expression

7

profiling, and associated immunophenotyping, of 195/477 samples included in the EORTC22033-26033 clinical trial to identify markers associated with survival and to aid in the identification of patients that benefit most from RT or TMZ treatment.

METHODS

Patient samples

Patients were considered eligible in the EORTC22033-26033 trial (clinical trial identifier NCT00182819), if they had been diagnosed with a histologically confirmed supratentorial, diffusely infiltrating grade II glioma (either astrocytoma, oligoastrocytoma or oligodendroglioma) according to the WHO 2006 classification [16]. Patients should present with at least one high-risk feature (age ≥40 years, progressive tumor disease, tumor size > 5 cm, tumor crossing the midline, neurological symptoms). Details of the eligibility criteria and the consolidated standards on reporting trials (Consort) flow diagram have been described previously [11]. Patients were registered for the trial at any time after initial diagnosis (allowing for tissue collection and molecular analysis) and randomized at a time-point when treatment was required. A total of 707 patients were registered in the EORTC22033-26066 study of which 477 were randomized to receive either RT or TMZ. For this analysis a clinical cut-off date of 17th of January 2013 was used and the database was locked on 7th of August 2013. *IDH* mutation status and 1p/19q codeletion status were obtained as described in Baumert et al [11]. *MGMT* methylation status was determined using the MGMT-STP27 algorithm based on genome wide methylation array data [17] (Bady et al, submitted). All patients gave written informed consent for correlative molecular analysis.

RNA isolation and array hybridization

Sufficient material for expression analysis was available for 203/477 randomized patients. Eight samples failed QC so that expression profiles from a total of 195 samples are presented here. Of these, RNA was isolated from FFPE tissue blocks (n = 166) or from snap frozen tissue samples (n = 29). RNA extraction, purification and quantification from FFPE and FF material was reported previously [18,19]. Purified RNA (250 ng) was used for labeling and hybridization on DASL beadchips (Illumina, San Diego, CA) that were run by Service XS, Leiden, the Netherlands. Expression data were quantile normalized and corrected for batch effects using preprocessCore (Bioconductor) and ber (R) packages respectively. RNA expression profiles were then assigned to one of six intrinsic molecular subtypes of glioma as previously defined [18], using the ClusterRepro R package [20]. These intrinsic subtypes can be recapitulated on FFPE material with high concordance and using various expression profiling platforms [13,14,19]. SAM analysis was performed on FFPE samples using SAMR, an R package [21]. The SAM approach to identify genes

associated with treatment response is similar to previously reported [14,22]. Expression data are available via NCBI GEO datasets, GSE107850. Analysis of the immune infiltrate was assessed using the immunophenoscore R script (https://github.com/MayerC-imed/Immunophenogram) [23]. Glioblastoma samples of patients treated in the BELOB trial were used for immunophenotype comparison between low and high-grade gliomas[14].

DNA isolation and Genotyping

DNA was extracted for genotyping on a subset of samples using a QIAamp DNA FFPE tissue kit (Qiagen). Genotyping was performed using the OncoScan FFPE assays Kit (Affymetrix, Santa Clara, CA), a platform that allows determing copynumber changes and loss of heterozygosity (LOH) in FFPE samples using molecular inversion probes [24,25]. Copynumber changes were analyzed using Nexus Express for Oncoscan (Affymetrix).

Statistical analysis

Distribution of frequencies were compared between subtypes using the Chi-squared test. A Fishers' exact test was used in case the assumptions for chi-square distribution were violated as indicated in the respective tables. Kaplan–Meier survival curves were compared using the log-rank test using the survival package in R[26]. PFS was calculated from the time of initial diagnosis/surgery to the date of clinical or radiological progression or death (whichever occurred first). The significance of prognostic factors was determined with a multivariate analysis using Cox regression.

RESULTS

Expression data was generated successfully for 195/477 samples and most parameters were balanced between the 'included' (i.e. those with gene expression data) and the 'not included' cohort. However, the 'included' subset contained fewer biopsies, which may be expected due to the limited amounts of tissue available from this type of material (table 1). The included cohort also contained a higher proportion of astrocytomas and *IDH*-wt tumors. Interestingly, both variables are correlated with type of surgery: biopsies are more frequently performed in WHO2006 astrocytomas compared to non-astrocytomas (91/189 [48 %] *v.* 75/287 [26 %], P < 0.0001) and biopsies are more often performed on IDH-wt tumors (41/65 [74 %] *v.* 107/326 [33 %], P < 0.0001). Despite these differences, progression free survival of included vs not included patients was similar (39.8 vs 43.8 months respectively, supplementary figure 1). Progression free survival of included vs not included was also similar within the molecularly defined subgroups 'IDH-mutated, 1p19q codeleted (molecular olidogendrogliomas)', 'IDH-mutated, 1p19q non-codeleted (molecular astrocytomas)' and 'IDH-wt' (supplementary table 1).

Table 1. Comparison between included vs not included samples

variable		All	Included	Not inc	P
Treatment	RT	240	96	144	0.760
	TMZ	237	99	138	
Type of surgery	Biopsy	189	38	151	<0.001*
	Partial resection	206	116	90	
	Total resection	81	41	40	
	n/a	1	0	1	
Histology	Astrocytoma	167	51	116	0.002
	Oligoastrocytoma	118	51	67	
	Oligodendroglioma	192	93	99	
Performance	0	294	122	172	0.86
	1	165	65	100	
	2	18	8	10	
Gender	Female	202	85	117	0.71
	Male	275	110	165	
IDH mutation status	Mutated	327	166	161	<0.001
	Normal	65	14	51	
	n/a	85	15	70	
1p19q status	Codeleted	117	63	54	0.25*
	Intact	240	112	128	
	n/a	120	20	100	
MGMT methylation	Methylated	113	102	11	1 **
	Unmethylated	7	7	0	
Age	Age (years) mean ± SD	44.6 ± 11.7	43.9 ± 11.1	45.1 ± 12.2	0.31
	< Median	238	101	137	0.55
	> Median	239	94	145	

Abbreviations: RT: radiotherapy; TMZ: temozolomide. Performance: ECOG performance score. Chi squared test comparison between included vs not included samples only; Note on performance score, Chi-square test without performance score 2 also has P<0.001. *: Chi-squared test performed without n/a samples, **: Fishers' exact test.

Intrinsic glioma subtypes are prognostic in EORTC22033-26033 trial samples

Expression data from clinical trial samples were assigned to one of six 'Intrinsic Glioma Subtypes' (IGS-9, IGS-16, IGS-17, IGS-18, IGS-22 or IGS-23) as previously defined [17]. As can be expected in LGGs, the majority of samples were assigned to the prognostically favorable subtypes IGS-9 and IGS-17 (n = 74 and 115 respectively, figure 1 and table 2). In concordance with previously published data, samples assigned to IGS-9 predominantly had an *IDH* mutation (68/69), had 1p19q codeletion (45/68) and were diagnosed as oligodendroglioma (52/74, supplementary table 2) [13,18]. Samples assigned to IGS-17 predominantly contained tumors with an *IDH*-mutation (97/108), but 1p19q codeletion was rarely observed (17/102) and tumors were more frequently diagnosed,
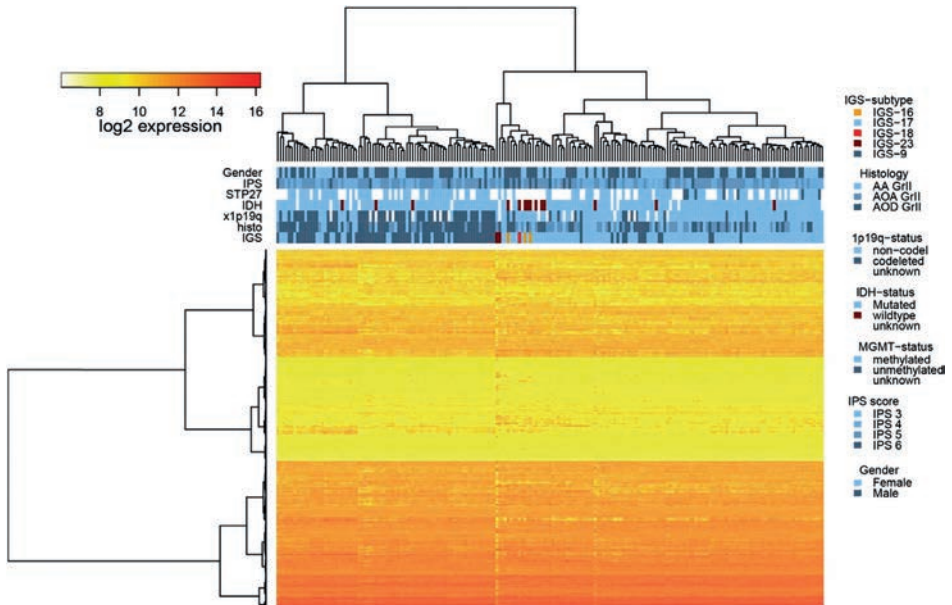
Figure 1. Heatmap showing association of gene-expression with clinical, pathological and other molecular data (*IDH*-mutation status, *MGMT*-promoter methylation status, 1p19q codeletion, intrinsic glioma subtype and immunophenoscore). As can be seen, most patients assigned to IGS-9 have 1p19q codeletion and are diagnosed as oligodendrogliomas.

based on local diagnosis, as astrocytoma or oligoastrocytoma (76/115). In the samples assigned to other molecular subtypes (n = 6), IDH-mutations were infrequent (1/5) as was 1p19q codeletion (1/5).

Patients with most favorable prognosis were those with tumors assigned to IGS-9 (PFS 53 months) or IGS-17 (PFS 40 months), and patients with worst prognosis were those assigned to other molecular subtypes (11.8 months, figure 2). Differences between all groups were significant (logrank P < 0.0001), differences between the two most favorable subtypes, IGS-9 and IGS-17, were however, not significant (P = 0.17, HR 0.74, 95 % CI [0.49-1.13], though this could be related to limited follow-up time in which relatively few events have occurred. The IGS-'other' subtype remained significant in a multivariate analysis that included other known prognostic factors such as age, type of surgery, histological diagnosis, treatment and performance score (table 3).

Treatment response per IGS-subtype

A trend towards benefit from RT compared to TMZ was observed for samples assigned to IGS-9 (HR for TMZ is 1.90, 95 % CI [0.95, 3.80], P = 0.065, figure 3). No such difference was observed for samples assigned to IGS-17 (HR for TMZ vs RT is 0.87, 95 % CI[0.50, 1.51], P = 0.62). Too few patients were assigned to other molecular

Table 2. Association between specific genetic changes, histology and IGS-subtype

variable		IGS-9	IGS-17	IGS other	not inc	P
All samples		74	115	6	282	
Treatment	RT	38	54	4	144	0.66
	TMZ	36	61	2	138	
Type of surgery	Biopsy	13	22	3	151	0.87
	Partial resection	46	67	3	90	
	Total resection	15	26	0	40	
	n/a	0	0	0	1	
Histology	Astrocytoma	11	38	2	116	p<0.001
	Oligoastrocytoma	11	38	2	67	
	Oligodendroglioma	52	39	2	99	
Performance	0	58	61	3	172	<0.001
	1	16	46	3	100	
	2	0	8	0	10	
Gender	Female	35	48	2	117	0.55
	Male	39	67	4	165	
IDH status	Mutated	68	97	1	161	0.09
	Normal	1	9	4	51	
	n/a	5	9	1	70	
1p19q status	Codeleted	45	17	1	54	< 0.001
	Intact	23	85	4	128	
	n/a	6	13	1	100	
MGMT	Methylated	45	56	1	11	0.04
	Unmethylated	0	7	0	02	
Age	Age (years) mean ± SD	47.2 ± 10.7	42.1 ± 11.0	38.8 ± 7.5	45.1 ± 12.2	0.013*
	< 44.6 years	25	72	4	137	<0.001
	> 44.6 years	49	43	2	145	

Chi squared test comparison between IGS-9 and IGS-17 only; Note on performance score, Chi-square test without performance score 2 also has P<0.001. IDH-mutation status was done using a Fishers' exact test. *: Anova based on all categories, anova on only IGS-9 and IGS-17: P= 0.002; anova of IGS-9, IGS-17 and IGS-other: P=0.004.

subtypes to assess response to treatment. Our gene expression data therefore provides preliminary evidence that patients with tumors assigned to IGS-9 can benefit from RT whereas no such benefit is observed in tumors assigned to IGS-17. It should be stressed however, that this is a post-hoc analysis performed on a subset of samples included in the EORTC22033-26033 clinical trial.

No genes were found to be significantly associated with progression free survival within molecular subgroups by SAM analysis, also not when subgroups were stratified by treatment. Identification of such genes may require a more mature dataset.

Table 3. Multivariate analysis for PFS

		HR	SE	p	95% CI
Age		0.97	0.01	0.014	0.95-0.99
Type of Surgery	Partial resection vs. Biopsy	0.80	0.27	0.424	0.47-1.37
	Total resection vs .Biopsy	0.76	0.33	0.409	0.40-1.45
Histology	Oligoastrocytoma vs. Astrocytoma	0.87	0.29	0.620	0.49-1.52
	Oligodendroglioma vs. Astrocytoma	0.89	0.24	0.650	0.55-1.45
Treatment	TMZ vs RT	1.41	0.22	0.113	0.92-2.14
Gender	Male vs. Female	1.21	0.21	0.375	0.80-1.82
Performance	ECOG 1 vs. ECOG 0	0.77	0.23	0.267	0.49-1.22
	ECOG 2 vs. ECOG 0	4.49	0.45	0.001	1.87-10.73
IGS-subtype	IGS-9 vs. IGS-17	0.96	0.24	0.864	0.60-1.54
	IGS-other vs. IGS-17	7.40	0.50	0.000	2.75-19.89

n= 195, number of events= 101

7

Immunophenotyping

Transcriptomic analysis has recently proved a valuable tool in the prediction of response to checkpoint inhibitors in various tumor types. This response prediction is done by a deconvolution of the gene expression data and subsequent cataloguing of the immune infiltrate of the tumor [23]. 'Immunophenotyping' has thus far only been performed on historical and archival samples which makes it difficult to estimate the relevance of potential confounding clinical and patient parameters. We therefore analysed the immune infiltrate of samples included in the EORTC22033-26033 clinical trial. We also included data from the BELOB trial, a randomized phase II trial on recurrent glioblastomas (GBM, n = 110, expression data from the initial tumor) to allow comparisons between LGG and GBM [14]. Such comparison is possible as the GBM samples were run on the same platform, and processed in batches alongside the EORTC22033-26033 samples. Any analysis involving clinical parameters were analyzed within the individual clinical trials to avoid potential patient bias.

In general, LGGs have a slightly lower overall immunophenoscore (IPS, a score derived from immunophenotyping that is associated with response to checkpoint inhibitors in melanomas) than GBMs (P = 0.004). Specifically, LGGs score higher on checkpoint (CP) and suppressor cell (SC) populations, but score lower on the effector cell (EC) and antigen processing (MHC) populations. This difference was apparent per IPS score (supplementary figure 2). For example, LGGs and GBMs with IPS score of 4 have an MHC score of respectively 0.86 ± 0.16 and 1.21 ± 0.24 (P < 0.0001, n = 77 and n = 25). Similarly, LGGs with an IPS score of 5 have an SC score of 0.005 ± 0.13 whereas GBMs have a score of -0.29 ± 0.18 (P < 0.001).
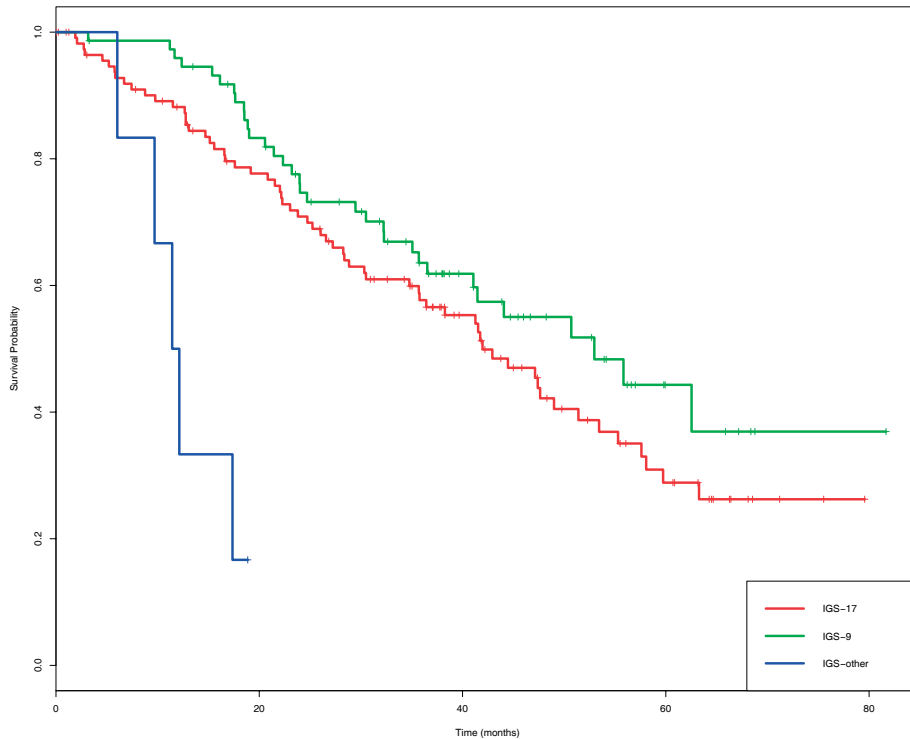
Figure 2. Intrinsic glioma subtypes are prognostic for progression free survival in patients treated within the EORTC22033-26033 clinical trial. Patients with most favorable prognosis were those with tumors assigned to IGS-9 (grey) or IGS-17 (dotted), and patients with worst prognosis were those assigned to other molecular subtypes (black), P<0.0001.

Within the EORTC22033-26033 samples, the Immunophenoscore was significantly correlated to histological subtype of the tumor (P < 0.001), presence or absence of IDH mutations (P = 0.03), but not to gender, age, MGMT-promoter methylation status, 1p19q codeletion or IGS-subtype (Chi squared test). Within the BELOB trial, correlation between immunophenoscore and IDH-mutations could not be confirmed, though the number of IDH-mutated tumors in that cohort was low (n = 5). In fact, the immunophenoscore was not associated with any clinical or molecular parameter in this trial (age, gender, IGS-subtype, treatment, MGMT-promoter or IDH-mutation status). In neither trial, IPS score was associated with outcome (supplementary figure 3). In summary, IPS score appears to be independent of known clinical and prognostic molecular markers. Moreover, the higher IPS score in GBMs suggests that LGGs are less amenable to checkpoint inhibitor type immune therapies.
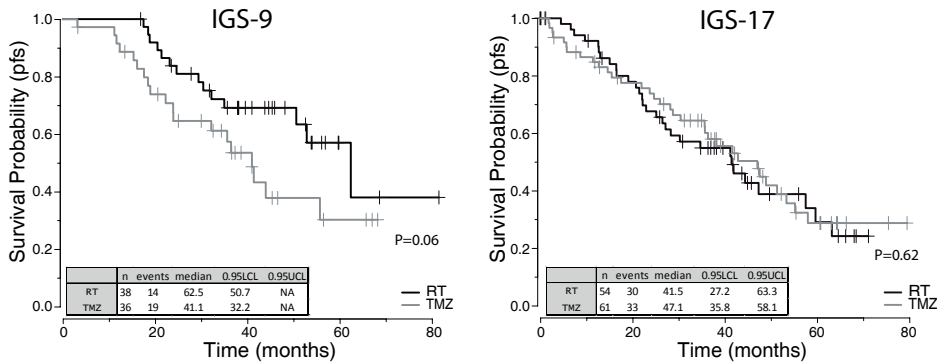
Figure 3. Progression free survival stratified by IGS-subtype and treatment: Samples assigned to IGS-9 show a trend towards benefit from RT compared TMZ (left panel, HR for TMZ is 1.90, P=0.065). No such difference was observed for samples assigned to IGS-17 (right panel, HR for TMZ vs RT is 0.87, P=0.62. Too few patients were assigned to other molecular subtypes to assess response to treatment (not shown).

Identification of pilocytic astrocytoma in 22033 clinical trial samples

Three out of the 195 samples were assigned to IGS-16 in the EORTC-22033 dataset. A hallmark of IGS-16 is that pilocytic astrocytomas (PAs, gliomas with favorable prognosis) are almost always assigned to this specific subtype [18]. However, this expression based intrinsic subtype does not only contain PAs; other histological subtypes of gliomas (including GBMs) may also be assigned to IGS-16. As it is sometimes difficult to distinguish between pilocytic and grade II astrocytomas by histology, it is therefore possible that one or more of the three EORTC 22033 samples assigned to IGS-16 are actually PAs [27]. Additional genetic testing to determine diagnosis is therefore required.

We therefore screened for typical genetic hallmarks of PAs (i.e. tandem duplication of 7q34 involving the BRAF locus [28] [29]) in samples assigned to IGS-16. Genotyping arrays were used to determine the genetic changes in these samples. One of the three samples assigned to IGS-16 indeed showed the characteristic tandem duplication on 7q34, and a lack of other genetic changes (figure 4). The centromeric breakpoint lies within the BRAF locus. Of note, 12 samples from the TCGA dataset (combined LGG and GBM) are also assigned to IGS-16 [30-32], and analysis of the genotype confirms that one of these samples (TCGA-HT-7691) harbors a BRAF-KIAA1549 gene-fusion (and no other notable mutations and/or copy number aberrations). Genotyping analysis therefore indicates that at least one sample of the EORTC22033 clinical trial (and one TCGA sample in other datasets) can molecularly be classified as a pilocytic astrocytoma.
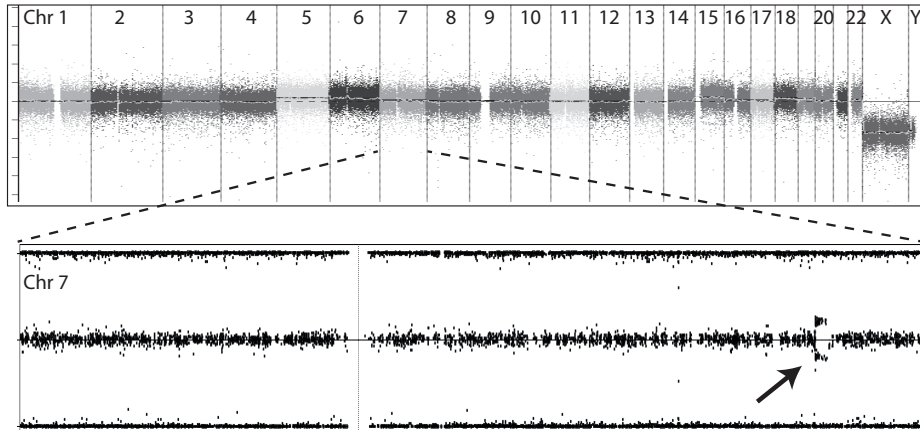
Figure 4. Identification of a pilocytic astrocytoma in a sample of the EORTC22033-26033 clinical trial. Three out of the 195 samples were assigned to IGS-16, a subtype to which pilocytic astrocytomas are assigned. In one of these samples we identified classical hallmark genetic changes of PAs: a tandem duplication on 7q34 (lower panel) and a marked absence of other genetic changes (upper panel). The centromeric breakpoint lies within the *BRAF* gene between 140.5 and 140.57 Mb, the Q-terminal breakpoint lies between 142.65 and 143.03 Mb.

DISCUSSION

In this study we have performed gene-expression profiling on samples of patients that were treated within the EORTC22033-26033 clinical trial. We show that intrinsic glioma subtypes show overlap with histological and molecular subtypes of glioma and that the IGS- subtypes are prognostic for PFS. Our data are in line with other studies that demonstrated the prognostic significance of gene-expression-based molecular subtypes in gliomas, but is only the second to be performed on randomized phase III clinical trial material [13,18,31,33,34]. We confirm earlier observations that specific genetic changes segregate in defined IGS-subtypes [13,14,18].

The randomized phase III clinical trial EORTC22033-26033 was initiated to optimize treatment for LGG patients. The overall trial result demonstrated equal efficacy of RT *v.* TMZ monotherapy in LGG patients both on PFS and quality of life [11,12]. Interestingly, correlative molecular marker analysis provided evidence for reduced benefit from TMZ in patients with *IDH*-mutated, 1p19q intact tumors. Our gene expression data did not support this observation: we show that samples assigned to IGS-17, of which most are *IDH*- mutated and 1p19q intact, have equal benefit from RT and TMZ.

The difference in the predictive effect between IGS-subtype and *IDH*-mutant, 1p19q codeleted tumors (despite a large degree of overlap in samples), may be explained by the fact that IGS subtyping probes a different type of tumor characteristic and thus

is not identical to molecular marker analysis of 1p19q and *IDH*-status. Analysis of DNA markers such as 1p19q and *IDH*-status do not take epi-genetic or phenotypic variability (such as those associated with tumor grade) into account. Alternatively, our gene-expression analysis only examined a subset of tumors, and those contained fewer biopsies and fewer astrocytomas compared to the entire dataset. The difference in the predictive effect between IGS-subtype and 1p19q (intact or codeleted) in *IDH*-mutant tumors may however, at least in part, also be explained by an incorrect determination of molecular markers. For example, IGS-subtyping has a degree of error due to e.g. intratumoral heterogeneity or effects of RNA-quality on tumor classification [35,36]. Alternatively, the various methods to determine 1p19q codeletion also do not always give concordant results [37,38].

Several older trials have also analyzed the efficacy of alkylating chemotherapy in 1p19q intact low grade gliomas. One trial demonstrated efficacy of procarbazine, CCNU and vincristine (PCV) monotherapy in LGG, and the efficacy was not associated with 1p/19q codeletion (though numbers for correlative marker analysis were small) [39]. A separate trial that examined the efficacy of the addition of chemotherapy to RT also showed that both LGG tumors with and without 1p19q codeletion responded to TMZ, though tumors with 1p19q codeletion showed a higher response rate [40]. Since 1p19q codeletion is associated with histological subtype, data from the recently published RTOG9802 trial also confirm the efficacy of combined RT + PCV treatment: efficacy was observed in all histological subtypes. Similar data, but on grade III gliomas, confirm the efficacy of PCV chemotherapy in both 1p19q codeleted and non codeleted tumors [41-43] [44]. Data from these trials and data obtained in the current study therefore suggest that alkylating chemotherapy is effective in IDH-mutated, 1p19q intact gliomas, though it is possible that the response duration is shorter than in 1p19q codeleted gliomas.

Checkpoint inhibitors have recently gained attention as novel therapeutic agents in various cancer types including GBMs [45-48]. Since only a subset of patients benefit from these treatments, identification of (bio-) markers associated with response is of clinical relevance. The mutational load, i.e. the number of mutations that lead to a neo-epitope of the tumor, has been coined as predictive response marker. However, analysis of the tumors' immune infiltrate, which can be done by a deconvolution of the gene expression data, also can identify tumors likely to respond [23]. Such 'Immunophenotyping' has thus far only been performed on historical and archival samples which makes it difficult to estimate the relevance of potential confounding clinical and patient parameters. Our gene expression data from the EORTC22033-26033 and BELOB clinical trials therefore can help determine the relevance of immunophenotyping in glioma samples. Our data show that in neither trial, IPS score was associated with outcome and that the IPS

score appears to be independent of known clinical and prognostic molecular markers. Nevertheless, GBMs in general have a higher IPS score and score higher on the effector cell and antigen processing populations than LGGs (even within defined IPS scores). These data suggest that LGGs are less amenable than GBMs to checkpoint inhibitor type immune therapies, which is in concordance with findings from other groups [49].

Our gene expression analysis has also identified one patient treated within EORTC22033-26033 with the hallmark genetic change of PAs: tandem duplication of 7q34. It is important to identify such patients as they have better prognosis and require a different treatment than diffuse low grade gliomas[50]. We identified this patient based on the assignment of the tumor to IGS-16. However, IGS-16 does not only contain PAs: a few samples (of other histological subtypes with associated poorer prognosis) are also assigned to IGS-16, which necessitates additional molecular testing. The PA identified in the EORTC22033-26033 clinical trial also highlights difficulties to distinguish this tumor type by histology[27]. In addition to the EORTC22033-26033 trial sample, we also identify a PA sample in the TCGA dataset. Additional genomic testing of samples assigned to IGS-16 therefore may be warranted.

To summarize, gene-expression profiling of samples included in the EORTC22033-26033 clinical trial confirmed the prognostic relevance of IGS subtyping. We failed to find evidence for differential treatment benefit in one or more specific molecular subgroups. IGS-subtyping has also identified one PA in the EORTC22033-26033 clinical trial and one in the TCGA database.

REFERENCES

1. Ostrom QT, Gittleman H, Fulop J, et al. CBTRUS Statistical Report: Primary Brain and Central Nervous System Tumors Diagnosed in the United States in 2008-2012. *Neuro-oncology.* 2015;17 Suppl 4:iv1-iv62.

2. Louis DN, Perry A, Reifenberger G, et al. The 2016 World Health Organization Classification of Tumors of the Central Nervous System: a summary. *Acta Neuropathol.* 2016;131(6):803-820.

3. Sanai N, Chang S, Berger MS. Low-grade gliomas in adults. *J Neurosurg.* 2011;115(5):948-965.

4. Soffietti R, Baumert BG, Bello L, et al. Guidelines on management of low-grade gliomas: report of an EFNS-EANO Task Force. *Eur J Neurol.* 2010;17(9):1124-1133.

5. Sahm F, Reuss D, Koelsche C, et al. Farewell to oligoastrocytoma: in situ molecular genetics favor classification as either oligodendroglioma or astrocytoma. *Acta Neuropathol.* 2014;128(4):551-559.

6. Ryken TC, Parney I, Buatti J, Kalkanis SN, Olson JJ. The role of radiotherapy in the management of patients with diffuse low grade glioma : A systematic review and evidence-based clinical practice guideline. *J Neurooncol.* 2015;125(3):551-583.

7. Karim AB, Maat B, Hatlevoll R, et al. A randomized trial on dose-response in radiation therapy of low-grade cerebral glioma: European Organization for Research and Treatment of Cancer (EORTC) Study 22844. *International journal of radiation oncology, biology, physics.* 1996;36(3):549-556.

8. van den Bent MJ, Afra D, de Witte O, et al. Long-term efficacy of early versus delayed radiotherapy for low-grade astrocytoma and oligodendroglioma in adults: the EORTC 22845 randomised trial. *Lancet.* 2005;366(9490):985-990.

9. Shaw E, Arusell R, Scheithauer B, et al. Prospective randomized trial of low- versus high-dose radiation therapy in adults with supratentorial low-grade glioma: initial report of a North Central Cancer Treatment Group/Radiation Therapy Oncology Group/Eastern Cooperative Oncology Group study. *J Clin Oncol.* 2002;20(9):2267-2276.

10. Buckner JC, Shaw EG, Pugh SL, et al. Radiation plus Procarbazine, CCNU, and Vincristine in Low-Grade Glioma. *N Engl J Med.* 2016;374(14):1344-1355.

11. Baumert BG, Hegi ME, van den Bent MJ, et al. Temozolomide chemotherapy versus radiotherapy in high-risk low-grade glioma (EORTC 22033-26033): a randomised, open-label, phase 3 intergroup study. *Lancet Oncol.* 2016;17(11):1521-1532.

12. Reijneveld JC, Taphoorn MJ, Coens C, et al. Health-related quality of life in patients with high-risk low-grade glioma (EORTC 22033-26033): a randomised, open-label, phase 3 intergroup study. *Lancet Oncol.* 2016;17(11):1533-1542.

13. Erdem-Eraslan L, Gravendeel LA, de Rooi J, et al. Intrinsic molecular subtypes of glioma are prognostic and predict benefit from adjuvant procarbazine, lomustine, and vincristine chemotherapy in combination with other prognostic factors in anaplastic oligodendroglial brain tumors: a report from EORTC study 26951. *J Clin Oncol.* 2013;31(3):328-336.

14. Erdem-Eraslan L, van den Bent MJ, Hoogstrate Y, et al. Identification of patients with recurrent glioblastoma who may benefit from combined bevacizumab and CCNU therapy, a report from the BELOB trial. *Cancer Res.* 2016;76(3):525-534.

15. French PJ, Swagemakers SMA, Nagel JHA, et al. Gene expression profiles associated with treatment response in oligodendrogliomas. *Cancer Res.* 2005;65(24):11335-11344.

16. Louis DN. Molecular pathology of malignant gliomas. *Annual review of pathology.* 2006;1:97-117.

17. Bady P, Sciuscio D, Diserens AC, et al. MGMT methylation analysis of glioblastoma on the Infinium methylation BeadChip identifies two distinct CpG regions associated with gene silencing and outcome, yielding a prediction model for comparisons across datasets, tumor grades, and CIMP-status. *Acta Neuropathol.* 2012;124(4):547-560.

18. Gravendeel LA, Kouwenhoven MC, Gevaert O, et al. Intrinsic gene expression profiles of gliomas are a better predictor of survival than histology. *Cancer Res.* 2009;69(23):9065-9072.

19. Gravendeel LA, de Rooi JJ, Eilers PH, van den Bent MJ, Sillevis Smitt PA, French PJ. Gene expression profiles of gliomas in formalin-fixed paraffin-embedded material. *Br J Cancer.* 2012;106(3):538-545.

20. Kapp AV, Tibshirani R. Are clusters found in one dataset present in another dataset? *Biostatistics (Oxford, England).* 2007;8(1):9-31.

21. Tusher VG, Tibshirani R, Chu G. Significance analysis of microarrays applied to the ionizing radiation response. *Proc Natl Acad Sci U S A.* 2001;98(9):5116-5121.

22. van den Bent MJ, Gravendeel LA, Gorlia T, et al. A hypermethylated phenotype is a better predictor of survival than MGMT methylation in anaplastic oligodendroglial brain tumors: a report from EORTC study 26951. *Clin Cancer Res.* 2011;17(22):7148-7155.

23. Charoentong P, Finotello F, Angelova M, et al. Pan-cancer Immunogenomic Analyses Reveal Genotype-Immunophenotype Relationships and Predictors of Response to Checkpoint Blockade. *Cell Rep.* 2017;18(1):248-262.

24. Foster JM, Oumie A, Togneri FS, et al. Cross-laboratory validation of the OncoScan(R) FFPE Assay, a multiplex tool for whole genome tumour profiling. *BMC medical genomics.* 2015;8:5.

25. Hardenbol P, Baner J, Jain M, et al. Multiplexed genotyping with sequence-tagged molecular inversion probes. *Nat Biotechnol.* 2003;21(6):673-678.

26. *A Package for Survival Analysis in S* [computer program]. Version 2.382015.

27. Korshunov A, Meyer J, Capper D, et al. Combined molecular analysis of BRAF and IDH1 distinguishes pilocytic astrocytoma from diffuse astrocytoma. *Acta Neuropathol.* 2009;118(3):401-405.

28. Jones DT, Kocialkowski S, Liu L, et al. Tandem duplication producing a novel oncogenic BRAF fusion gene defines the majority of pilocytic astrocytomas. *Cancer Res.* 2008;68(21):8673-8677.

29. Hasselblatt M, Riesmeier B, Lechtape B, et al. BRAF-KIAA1549 fusion transcripts are less frequent in pilocytic astrocytomas diagnosed in adults. *Neuropathol Appl Neurobiol.* 2011;37(7):803-806.

30. Cancer Genome Atlas Research N, Brat DJ, Verhaak RG, et al. Comprehensive, Integrative Genomic Analysis of Diffuse Lower-Grade Gliomas. *N Engl J Med.* 2015;372(26):2481-2498.

31. Ceccarelli M, Barthel FP, Malta TM, et al. Molecular Profiling Reveals Biologically Discrete Subsets and Pathways of Progression in Diffuse Glioma. *Cell.* 2016;164(3):550-563.

32. Brennan CW, Verhaak RG, McKenna A, et al. The somatic genomic landscape of glioblastoma. *Cell.* 2013;155(2):462-477.

33. Li A, Walling J, Ahn S, et al. Unsupervised analysis of transcriptomic profiles reveals six glioma subtypes. *Cancer Res.* 2009;69(5):2091-2099.

34. Phillips HS, Kharbanda S, Chen R, et al. Molecular subclasses of high-grade glioma predict prognosis, delineate a pattern of disease progression, and resemble stages in neurogenesis. *Cancer Cell.* 2006;9(3):157-173.

35. Sottoriva A, Spiteri I, Piccirillo SG, et al. Intratumor heterogeneity in human glioblastoma reflects cancer evolutionary dynamics. *Proc Natl Acad Sci U S A.* 2013;110(10):4009-4014.

36. Parker NR, Hudson AL, Khong P, et al. Intratumoral heterogeneity identified at the epigenetic, genetic and transcriptional level in glioblastoma. *Sci Rep.* 2016;6:22477.

37. Horbinski C, Nikiforova MN, Hobbs J, et al. The importance of 10q status in an outcomes-based comparison between 1p/19q fluorescence in situ hybridization and polymerase chain reaction-based microsatellite loss of heterozygosity analysis of oligodendrogliomas. *J Neuropathol Exp Neurol.* 2012;71(1):73-82.

38. Jha P, Sarkar C, Pathak P, et al. Detection of allelic status of 1p and 19q by microsatellite-based PCR versus FISH: limitations and advantages in application to patient management. *Diagn Mol Pathol.* 2011;20(1):40-47.

39. Buckner JC, Gesme D, Jr., O'Fallon JR, et al. Phase II trial of procarbazine, lomustine, and vincristine as initial therapy for patients with low-grade oligodendroglioma or oligoastrocytoma: efficacy and associations with chromosomal abnormalities. *J Clin Oncol.* 2003;21(2):251-255.

40. Kaloshi G, Benouaich-Amiel A, Diakite F, et al. Temozolomide for low-grade gliomas: predictive impact of 1p/19q loss on response and outcome. *Neurology.* 2007;68(21):1831-1836.

41. Cairncross G, Wang M, Shaw E, et al. Phase III trial of chemoradiotherapy for anaplastic oligodendroglioma: long-term results of RTOG 9402. *J Clin Oncol.* 2013;31(3):337-343.

42. Cairncross JG, Wang M, Jenkins RB, et al. Benefit from procarbazine, lomustine, and vincristine in oligodendroglial tumors is associated with mutation of IDH. *J Clin Oncol.* 2014;32(8):783-790.

43. van den Bent MJ, Brandes AA, Taphoorn MJ, et al. Adjuvant procarbazine, lomustine, and vincristine chemotherapy in newly diagnosed anaplastic oligodendroglioma: long-term follow-up of EORTC brain tumor group study 26951. *J Clin Oncol.* 2013;31(3):344-350.

44. Dubbink HJ, Atmodimedjo PN, Kros JM, et al. Molecular classification of anaplastic oligodendroglioma using next-generation sequencing: a report of the prospective randomized EORTC Brain Tumor Group 26951 phase III trial. *Neuro-oncology.* 2016;18(3):388-400.

45. Bouffet E, Larouche V, Campbell BB, et al. Immune Checkpoint Inhibition for Hypermutant Glioblastoma Multiforme Resulting From Germline Biallelic Mismatch Repair Deficiency. *J Clin Oncol.* 2016.

46. Larkin J, Chiarion-Sileni V, Gonzalez R, et al. Combined Nivolumab and Ipilimumab or Monotherapy in Untreated Melanoma. *N Engl J Med.* 2015;373(1):23-34.

47. Sundar R, Cho BC, Brahmer JR, Soo RA. Nivolumab in NSCLC: latest evidence and clinical potential. *Therapeutic advances in medical oncology.* 2015;7(2):85-96.

48. Eggermont AM, Chiarion-Sileni V, Grob JJ, et al. Prolonged Survival in Stage III Melanoma with Ipilimumab Adjuvant Therapy. *N Engl J Med.* 2016;375(19):1845-1855.

49. Berghoff AS, Kiesel B, Widhalm G, et al. Correlation of immune phenotype with IDH mutation in diffuse glioma. *Neuro-oncology.* 2017.

50. Collins VP, Jones DT, Giannini C. Pilocytic astrocytoma: pathology, molecular mechanisms and markers. *Acta Neuropathol.* 2015;129(6):775-788.

7

Supplementary Table 1. Survival per molecular subtype included vs not included

Molecular subset	inc/not inc	n	events	median	0.95LCL	0.95UCL
all patients	included	195	101	43.5	37.7	52.7
	not included	282	161	39.8	35.3	47.7
IDH-mutated, 1p19q codeleted	included	60	26	55.1	35.3	NR
	not included	44	15	NR	41.2	NR
IDH-mutated, 1p19q intact	included	92	47	46.5	40.5	56.8
	not included	73	37	48.2	34.7	NR
IDH-wt	included	14	10	16.6	9.6	NR
	not included	51	42	20.6	15.1	27.3

NR: not reached

Supplementary Table 2. correlation of molecular markers with IGS-subtype

IDH status	1p19q status	IGS-9	IGS-17	IGS-other	not included
IDH mutated	1p19q	43	17	0	44
	no codel	20	71	1	73
	undetermined	5	9	0	44
IDH wt	1p19q	0	0	1	6
	no codel	0	7	3	32
	undetermined	1	2	0	13
IDH undetermined	1p19q	2	0	0	4
	no codel	3	7	0	23
	undetermined	0	2	1	43
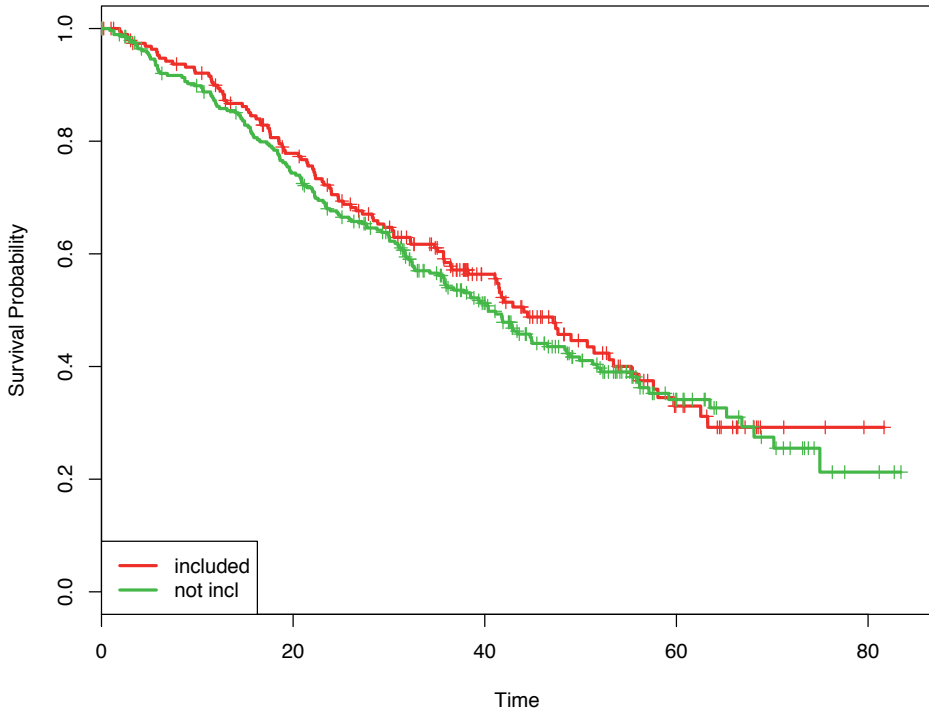
Supplementary Figure 1. Survival between 'included' and 'not-included' (i.e. those in which gene expression analysis was performed or not). No differences between included and not included were identified, also not when stratified by molecular subgroup (IDH-mutation and 1p19q codeletion, not shown).
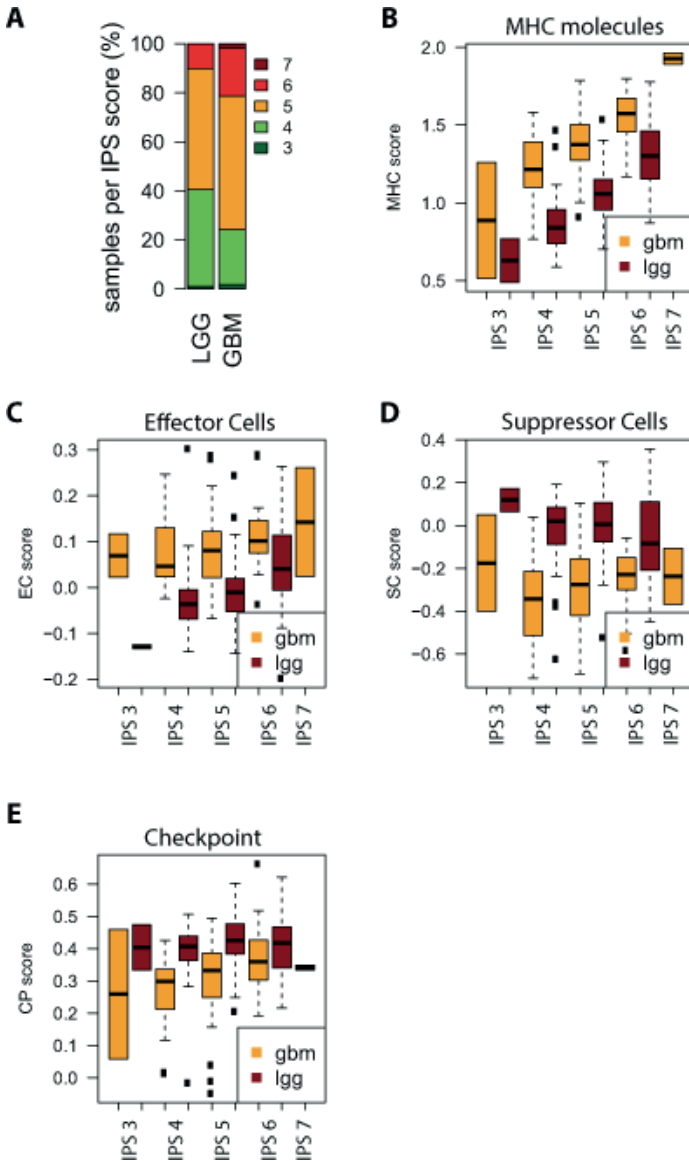
Supplementary Figure 2. Immunophenotypes in 22033 and BELOB clinical trials. A: distribution of IPS scores in the EORTC22033-26033 (LGG) and BELOB (GBM) clinical trials. As can be seen, GBMs tend to have higher IPS scores than LGGs. Other figures represent the immune infiltrate per IPS score stratified by the EORTC22033-26033 (LGG) and BELOB (GBM) trials. As can be seen, GBMs have more MHC expression (B) and higher effector cell population (C) per IPS score. In contrast LGGs have higher suppressor and immunemodulator (D and E).
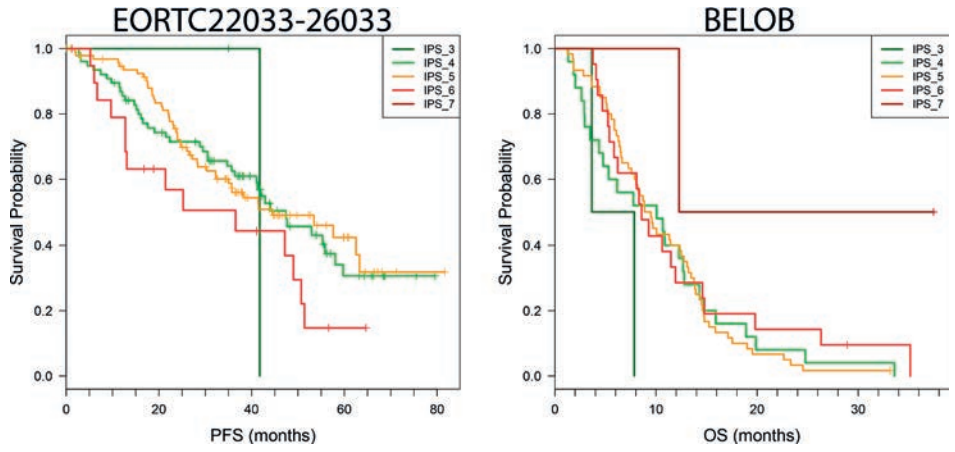
Supplementary Figure 3. Survival per IPS score in the EORTC22033-26033 and BELOB clinical trials. IPS score is not associated with improved outcome in either trial.

Chapter 8

General discussion and future perspective

Diffuse gliomas are the most common type of malignant primary brain tumors. New treatment options are urgently needed as the prognosis for the majority of glioma patients remains dismal. Novel therapies may be developed if we have a better understanding on the oncogenic pathways involved. In this thesis, we focused on the molecular function and clinical implication of mutations in *IDH1* and *EGFR*, which are involved in the oncogenesis of two distinct subtypes of diffuse gliomas.

ONCOGENIC BIOLOGY OF *IDH* MUTATIONS

Tumors depend on their acquired genetic changes for growth and therefore these changes are good targets for treatment. Several large-scale sequencing studies on diffuse gliomas have identified common genetic events that drive oncogenesis in the various glioma subtypes. One of the most common genetic changes in diffuse low grade gliomas (LGG) involves the *IDH1* gene. Mutations in *IDH1* (or similar mutations in *IDH2*) belong to the earliest genetic changes in LGGs and they are almost always clonal (i.e. present in all tumor cells). Mutations in *IDH1* or *IDH2* alter the normal function of these proteins and result in an enzyme with a novel activity whereby D2HG is produced. Patients with *IDH*-mutated gliomas have a better prognosis and benefit more from chemotherapy/radiation therapy than patients with *IDH* wildtype gliomas [1, 2].

Since mutations in *IDH* genes are amongst the most common identified in LGGs, and because of their clonality and mutation-specific enzymatic activity, they are considered a good target for therapy. Indeed, inhibitors targeting the mutant-specific activity have been developed and these are currently being tested for clinical activity. Although promising clinical responses have been reported in acute myeloid leukemia (AML) patients, the clinical benefit for glioma patients has thus-far been limited [3-5], though the field is still awaiting reports on the clinical trials. The response to IDH inhibitors in AML patients is also remarkable considering the fact that mutations in AML are most-often subclonal, indicating that the tumor was not dependent on the mutation for initial growth. Additional research into the molecular mechanisms affected by mutant IDH1 and IDH2 therefore is required. However, this research is hampered because there are only few preclinical model systems of *IDH*-mutated gliomas.

In this thesis, we have described the generation of two model systems for *IDH*-mutated gliomas. In **Chapter 2** we report on an *in vivo* transgenic zebrafish model system for *IDH1* mutations with CNS-specific expression at the early stage of the embryonic development. Although the D2HG level was significantly increased, our zebrafish remained healthy and no tumors were formed in our models, also not in a *Tp53* mutant

8

background. Although other transgenic model systems for *Idh* mutations (mice and drosophila) developed phenotypes (brain hemorrhage or wing expansion defects), thusfar no gliomas were identified in any of the *in vivo* animal model systems [6, 7]. This absence suggests that *IDH* mutations alone are insufficient to initiate glioma formation. However, expression of mutant IDH1 in the subventricular zone did result in precancerous subventricular nodules, which suggests involvement of mutant IDH at the early stages of tumor development [8]. The absence of full blown tumors is in contrast to AML where hematopoietic expression of *IDH* mutations alone is sufficient to initiate leukemia in several mouse models and mutant IDH is involved in maintaining the malignancies [9-12].

There are several possibilities as to why no gliomas are formed in the *in-vivo* model systems. Perhaps additional genetic changes should be incorporated including (a combination of) mutations in *TP53*, *ATRX* and/or other, less-common, mutations. Alternatively, the model systems created to-date did not target the correct cell of origin for gliomas. In this case, alternative promoters should be used to drive expression of mutant IDH.

In **Chapter 3** we report on establishing short term cultures of LGGs and show that these cultures retain mutant tumor cells and other driver mutations (albeit at a lower VAF compared to the VAF in the original tumor) and therefore may offer an *in vitro* assay to study downstream pathway alterations and to determine the efficacy of (new) therapeutics. As only very few *IDH*-mutated primary tumor lines have been established to date, and those that have contain many more genetic changes and may even no longer be dependent on the mutation for growth, our assay is a welcome addition to study LGGs. Apart from primary patient-derived lines [13], other options to create *in vitro* model systems include the creation of tumor models using human-induced pluripotent stem cells (HiPSCs) by transforming neuro progenitor cells (NPCs) [14].

The importance of further examining the molecular pathways affected by *IDH1* mutations is shown in **Chapter 4** where we identify a novel pathway that is inhibited by mutant IDH1. Our results demonstrate that MUL1 is a novel binding partner of IDH1 and its function in activating NF-kB is inhibited in *IDH1*-mutated cells, ultimately leading to less sensitivity to TNFα-induced apoptosis. The data described in this chapter can help understand gliomagenesis and identify novel targets for treatment in IDH mutant gliomas.

Generation of proper model systems is important as it will help understand clinical responses to IDH inhibitors. For example, IDH inhibitors initially showed prominent

efficacy in inhibiting tumorigenic properties of different cancer cell lines with *IDH* mutations [15-17] *in vitro* and *in vivo*, though some of the more recent studies failed to confirm this observation [16, 18]. Other therapies for *IDH*-mutated tumors can also be further explored in these model systems. For example, *Sulkowski et al*. showed that the *IDH* mutation-induced D2HG-dependent deficiency in DNA homologous recombination, results in sensitivity to PARP inhibitor treatment [19]. Alternatively, IDH-mutant cells are highly dependent on the level of NAD + and inhibiting the NAD + salvage pathway resulted in cytotoxicity of IDH-mutant cells [18].

It should also be noted that inhibiting D2HG production of *IDH* mutation may pose a risk to patients. For example, *IDH*-mutated gliomas are more sensitive to chemotherapy and radiotherapy due to impaired DNA repair system[17, 20]. As such, inhibiting mutant IDH activity may actually antagonize chemotherapy efficacy. These data demonstrate that further research to better understand the biology of *IDH* mutations in gliomas is required.

8

The overall results of the randomized phase III European Organization for Research and Treatment (EORTC) 22033-26033 clinical trial did not show differences in clinical efficacy between radiotherapy (RT) vs temozolomide (TMZ) [21]. In **Chapter 7**, we sub-grouped LGGs from the EORTC22033-26033 clinical trial into previously defined intrinsic glioma subtypes (IGS) using gene expression profiling. We have confirmed the prognostic value of IGS. LGG assigned to IGS-9 (most were *IDH*-mutated with 1p19q codeletion) benefited more from RT than from TMZ whereas this benefit was not observed in IGS-17 (most were *IDH*-mutated with intact 1p19q). However, we did not identify predictive markers for response to treatment and it is of note that the follow-up time was limited.

ONCOGENIC BIOLOGY OF MUTATIONS IN *EGFR*

Activating mutations in *EGFR* have been identified in various cancer types. Interestingly, different mutations in this gene are found in different types of cancer. For example, *EGFRvIII* is frequently identified in GBMs whereas over 40 % of non-small cell lung cancer (NSCLC) patients with EGFR mutations carry the *EGFR L858R* mutation. Both *EGFRvIII* and *EGFR L858R* result in a constitutively active form of EGFR, which activates signaling pathways involved in cell proliferation, differentiation and survival. It should be noted that common *EGFR* mutations in NSCLC are mainly within the tyrosine kinase domain, whereas common *EGFR* mutations in GBMs are mainly in the extracellular domain of the receptor. Importantly, EGFR has been considered as a

good therapeutic target for *EGFR*-mutated GBMs as preclinical models demonstrated sustained dependency on the mutation [22, 23]. However, and in marked contrast to *EGFR*-mutated pulmonary adenocarcinoma, inhibiting EGFR phosphorylation by tyrosine kinase inhibitors (TKIs) did not decrease tumor growth nor improve survival, despite the fact the EGFR phosphorylation was effectively inhibited, also in patients (at least for gefitinib) [24-28]. This suggests that an additional oncogenic function of EGFR is required for tumor growth in gliomas. In this thesis, we first examined whether EGFR remains a target for therapy in recurrent GBMs. In **Chapter 6**, we show that *EGFR* amplification in the majority (85 %) of the primary GBMs is retained at recurrence. However, only about 50 % of *EGFRvIII*-positive primary GBMs retained *EGFRvIII* expression at recurrence. Therefore, care should be taken in using EGFRvIII as target as its status may change [29]. In **Chapter 5**, we have also further examined EGFR and its signaling pathway to understand the differences in treatment response between gliomas and pulmonary adenocarcinomas. We have identified mutant-specific binding partners for different *EGFR* mutations (*EGFRvIII* and *EGFR L858R*), which each activated distinct downstream pathways.

In the future, further research into the molecular pathways affected by EGFR is required to understand the lack of treatment response to EGFR TKIs of glioma patients. The proteins and pathways identified in **Chapter 5** may serve as a starting point to provide new insights for treatment development. Apart from the role of EGFR in signal transduction, several studies have reported a role of EGFR in the nucleus, where it directly binds to DNA and induces transcription of various genes [30-32]. Indeed, several of the mutation-specific EGFR-binding partners have a presumed role in the nucleus. This role may be mutation specific as EGFRvIII reportedly has a higher presence in the nucleus than EGFR L858R [33]. Therefore, future research should also include nuclear EGFR as potential treatment target in gliomas.

REFERENCES

1   Houillier C, Wang X, Kaloshi G, Mokhtari K, Guillevin R, Laffaire J, Paris S, Boisselier B, Idbaih A, Laigle-Donadey F, Hoang-Xuan K, Sanson M, Delattre JY: Idh1 or idh2 mutations predict longer survival and response to temozolomide in low-grade gliomas. Neurology 2010;75:1560-1566.

2   van den Bent MJ, Brandes AA, Taphoorn MJ, Kros JM, Kouwenhoven MC, Delattre JY, Bernsen HJ, Frenay M, Tijssen CC, Grisold W, Sipos L, Enting RH, French PJ, Dinjens WN, Vecht CJ, Allgeier A, Lacombe D, Gorlia T, Hoang-Xuan K: Adjuvant procarbazine, lomustine, and vincristine chemotherapy in newly diagnosed anaplastic oligodendroglioma: Long-term follow-up of eortc brain tumor group study 26951. J Clin Oncol 2013;31:344-350.

3   Fathi AT, DiNardo CD, Kline I, Kenvin L, Gupta I, Attar EC, Stein EM, de Botton S, Investigators ACS: Differentiation syndrome associated with enasidenib, a selective inhibitor of mutant isocitrate dehydrogenase 2: Analysis of a phase 1/2 study. JAMA Oncol 2018

4   Birendra KC, DiNardo CD: Evidence for clinical differentiation and differentiation syndrome in patients with acute myeloid leukemia and idh1 mutations treated with the targeted mutant idh1 inhibitor, ag-120. Clin Lymphoma Myeloma Leuk 2016;16:460-465.

5   DiNardo CD, Stein EM, de Botton S, Roboz GJ, Altman JK, Mims AS, Swords R, Collins RH, Mannis GN, Pollyea DA, Donnellan W, Fathi AT, Pigneux A, Erba HP, Prince GT, Stein AS, Uy GL, Foran JM, Traer E, Stuart RK, Arellano ML, Slack JL, Sekeres MA, Willekens C, Choe S, Wang H, Zhang V, Yen KE, Kapsalis SM, Yang H, Dai D, Fan B, Goldwasser M, Liu H, Agresta S, Wu B, Attar EC, Tallman MS, Stone RM, Kantarjian HM: Durable remissions with ivosidenib in idh1-mutated relapsed or refractory aml. N Engl J Med 2018;378:2386-2398.

6   Sasaki M, Knobbe CB, Itsumi M, Elia AJ, Harris IS, Chio, II, Cairns RA, McCracken S, Wakeham A, Haight J, Ten AY, Snow B, Ueda T, Inoue S, Yamamoto K, Ko M, Rao A, Yen KE, Su SM, Mak TW: D-2-hydroxyglutarate produced by mutant idh1 perturbs collagen maturation and basement membrane function. Genes Dev 2012;26:2038-2049.

7   Reitman ZJ, Sinenko SA, Spana EP, Yan H: Genetic dissection of leukemia-associated idh1 and idh2 mutants and d-2-hydroxyglutarate in drosophila. Blood 2015;125:336-345.

8   Bardella C, Al-Dalahmah O, Krell D, Brazauskas P, Al-Qahtani K, Tomkova M, Adam J, Serres S, Lockstone H, Freeman-Mills L, Pfeffer I, Sibson N, Goldin R, Schuster-Boeckler B, Pollard PJ, Soga T, McCullagh JS, Schofield CJ, Mulholland P, Ansorge O, Kriaucionis S, Ratcliffe PJ, Szele FG, Tomlinson I: Expression of idh1r132h in the murine subventricular zone stem cell niche recapitulates features of early gliomagenesis. Cancer Cell 2016;30:578-594.

9   Sasaki M, Knobbe CB, Munger JC, Lind EF, Brenner D, Brustle A, Harris IS, Holmes R, Wakeham A, Haight J, You-Ten A, Li WY, Schalm S, Su SM, Virtanen C, Reifenberger G, Ohashi PS, Barber DL, Figueroa ME, Melnick A, Zuniga-Pflucker JC, Mak TW: Idh1(r132h) mutation increases murine haematopoietic progenitors and alters epigenetics. Nature 2012;488:656-659.

10 Chen C, Liu Y, Lu C, Cross JR, Morris JP, Shroff AS, Ward PS, Bradner JE, Thompson C, Lowe SW: Cancer-associated idh2 mutants drive an acute myeloid leukemia that is susceptible to brd4 inhibition. Gene Dev 2013;27:1974-1985.

11 Kats LM, Reschke M, Taulli R, Pozdnyakova O, Burgess K, Bhargava P, Straley K, Karnik R, Meissner A, Small D, Su SM, Yen K, Zhang JW, Pandolfi PP: Proto-oncogenic role of mutant idh2 in leukemia initiation and maintenance. Cell Stem Cell 2014;14:329-341.

12 Chaturvedi A, Cruz MMA, Jyotsana N, Sharma A, Yun HY, Gorlich K, Wichmann M, Schwarzer A, Preller M, Thol F, Meyer J, Haemmerle R, Struys EA, Jansen EE, Modlich U, Li ZX, Sly LM, Geffers R, Lindner R, Manstein DJ, Lehmann U, Krauter J, Ganser A, Heuser M: Mutant

8

idh1 promotes leukemogenesis in vivo and can be specifically targeted in human aml. Blood 2013;122:2877-2887.

13   Luchman HA, Stechishin OD, Dang NH, Blough MD, Chesnelong C, Kelly JJ, Nguyen SA, Chan JA, Weljie AM, Cairncross JG, Weiss S: An in vivo patient-derived model of endogenous idh1-mutant glioma. Neuro Oncol 2012;14:184-191.

14   Sancho-Martinez I, Nivet E, Xia Y, Hishida T, Aguirre A, Ocampo A, Ma L, Morey R, Krause MN, Zembrzycki A, Ansorge O, Vazquez-Ferrer E, Dubova I, Reddy P, Lam D, Hishida Y, Wu MZ, Esteban CR, O'Leary D, Wahl GM, Verma IM, Laurent LC, Izpisua Belmonte JC: Establishment of human ipsc-based models for the study and targeting of glioma initiating cells. Nat Commun 2016;7:10743.

15   Popovici-Muller J, Saunders JO, Salituro FG, Travins JM, Yan S, Zhao F, Gross S, Dang L, Yen KE, Yang H, Straley KS, Jin S, Kunii K, Fantin VR, Zhang S, Pan Q, Shi D, Biller SA, Su SM: Discovery of the first potent inhibitors of mutant idh1 that lower tumor 2-hg in vivo. ACS Med Chem Lett 2012;3:850-855.

16   Rohle D, Popovici-Muller J, Palaskas N, Turcan S, Grommes C, Campos C, Tsoi J, Clark O, Oldrini B, Komisopoulou E, Kunii K, Pedraza A, Schalm S, Silverman L, Miller A, Wang F, Yang H, Chen Y, Kernytsky A, Rosenblum MK, Liu W, Biller SA, Su SM, Brennan CW, Chan TA, Graeber TG, Yen KE, Mellinghoff IK: An inhibitor of mutant idh1 delays growth and promotes differentiation of glioma cells. Science 2013;340:626-630.

17   Li L, Paz AC, Wilky BA, Johnson B, Galoian K, Rosenberg A, Hu G, Tinoco G, Bodamer O, Trent JC: Treatment with a small molecule mutant idh1 inhibitor suppresses tumorigenic activity and decreases production of the oncometabolite 2-hydroxyglutarate in human chondrosarcoma cells. PLoS One 2015;10:e0133813.

18   Tateishi K, Wakimoto H, Iafrate AJ, Tanaka S, Loebel F, Lelic N, Wiederschain D, Bedel O, Deng G, Zhang B, He T, Shi X, Gerszten RE, Zhang Y, Yeh JJ, Curry WT, Zhao D, Sundaram S, Nigim F, Koerner MVA, Ho Q, Fisher DE, Roider EM, Kemeny LV, Samuels Y, Flaherty KT, Batchelor TT, Chi AS, Cahill DP: Extreme vulnerability of idh1 mutant cancers to nad+ depletion. Cancer Cell 2015;28:773-784.

19   Sulkowski PL, Corso CD, Robinson ND, Scanlon SE, Purshouse KR, Bai H, Liu Y, Sundaram RK, Hegan DC, Fons NR, Breuer GA, Song Y, Mishra-Gorur K, De Feyter HM, de Graaf RA, Surovtseva YV, Kachman M, Halene S, Gunel M, Glazer PM, Bindra RS: 2-hydroxyglutarate produced by neomorphic idh mutations suppresses homologous recombination and induces parp inhibitor sensitivity. Sci Transl Med 2017;9

20   Molenaar RJ, Verbaan D, Lamba S, Zanon C, Jeuken JW, Boots-Sprenger SH, Wesseling P, Hulsebos TJ, Troost D, van Tilborg AA, Leenstra S, Vandertop WP, Bardelli A, van Noorden CJ, Bleeker FE: The combination of idh1 mutations and mgmt methylation status predicts survival in glioblastoma better than either idh1 or mgmt alone. Neuro Oncol 2014;16:1263-1273.

21   Baumert BG, Hegi ME, van den Bent MJ, von Deimling A, Gorlia T, Hoang-Xuan K, Brandes AA, Kantor G, Taphoorn MJ, Hassel MB, Hartmann C, Ryan G, Capper D, Kros JM, Kurscheid S, Wick W, Enting R, Reni M, Thiessen B, Dhermain F, Bromberg JE, Feuvret L, Reijneveld JC, Chinot O, Gijtenbeek JM, Rossiter JP, Dif N, Balana C, Bravo-Marques J, Clement PM, Marosi C, Tzuk-Shina T, Nordal RA, Rees J, Lacombe D, Mason WP, Stupp R: Temozolomide chemotherapy versus radiotherapy in high-risk low-grade glioma (eortc 22033-26033): A randomised, open-label, phase 3 intergroup study. Lancet Oncol 2016;17:1521-1532.

22   Klingler S, Guo BF, Yao J, Yan HY, Zhang L, Vaseva AV, Chen SD, Canoll P, Horner J, Wang YA, Paik JH, Ying HQ, Zheng HW: Development of resistance to egfr-targeted therapy in malignant

glioma can occur through egfr-dependent and -independent mechanisms. Cancer Research 2015;75:2109-2119.

23 Vivanco I, Robins HI, Rohle D, Campos C, Grommes C, Nghiemphu PL, Kubek S, Oldrini B, Chheda MG, Yannuzzi N, Tao H, Zhu S, Iwanami A, Kuga D, Dang J, Pedraza A, Brennan CW, Heguy A, Liau LM, Lieberman F, Yung WK, Gilbert MR, Reardon DA, Drappatz J, Wen PY, Lamborn KR, Chang SM, Prados MD, Fine HA, Horvath S, Wu N, Lassman AB, DeAngelis LM, Yong WH, Kuhn JG, Mischel PS, Mehta MP, Cloughesy TF, Mellinghoff IK: Differential sensitivity of glioma- versus lung cancer-specific egfr mutations to egfr kinase inhibitors. Cancer Discov 2012;2:458-471.

24 Uhm JH, Ballman KV, Wu WT, Giannini C, Krauss JC, Buckner JC, James CD, Scheithauer BW, Behrens RJ, Flynn PJ, Schaefer PL, Dakhill SR, Jaeckle KA: Phase ii evaluation of gefitinib in patients with newly diagnosed grade 4 astrocytoma: Mayo/north central cancer treatment group study n0074. Int J Radiat Oncol 2011;80:347-353.

25 van den Bent MJ, Brandes AA, Rampling R, Kouwenhoven MCM, Kros JM, Carpentier AF, Clement PM, Frenay M, Campone M, Baurain JF, Armand JP, Taphoorn MJB, Tosoni A, Kletzl H, Klughammer B, Lacombe D, Gorlia T: Randomized phase ii trial of erlotinib versus temozolomide or carmustine in recurrent glioblastoma: Eortc brain tumor group study 26034. Journal of Clinical Oncology 2009;27:1268-1274.

26 Maemondo M, Inoue A, Kobayashi K, Sugawara S, Oizumi S, Isobe H, Gemma A, Harada M, Yoshizawa H, Kinoshita I, Fujita Y, Okinaga S, Hirano H, Yoshimori K, Harada T, Ogura T, Ando M, Miyazawa H, Tanaka T, Saijo Y, Hagiwara K, Morita S, Nukiwa T, Grp NJS: Gefitinib or chemotherapy for non-small-cell lung cancer with mutated egfr. New Engl J Med 2010;362:2380-2388.

27 Hegi ME, Diserens AC, Bady P, Kamoshima Y, Kouwenhoven MC, Delorenzi M, Lambiv WL, Hamou MF, Matter MS, Koch A, Heppner FL, Yonekawa Y, Merlo A, Frei K, Mariani L, Hofer S: Pathway analysis of glioblastoma tissue after preoperative treatment with the egfr tyrosine kinase inhibitor gefitinib--a phase ii trial. Mol Cancer Ther 2011;10:1102-1112.

28 Raizer JJ, Abrey LE, Lassman AB, Chang SM, Lamborn KR, Kuhn JG, Yung WK, Gilbert MR, Aldape KA, Wen PY, Fine HA, Mehta M, Deangelis LM, Lieberman F, Cloughesy TF, Robins HI, Dancey J, Prados MD, North American Brain Tumor C: A phase ii trial of erlotinib in patients with recurrent malignant gliomas and nonprogressive glioblastoma multiforme postradiation therapy. Neuro Oncol 2010;12:95-103.

29 Clark PA, Iida M, Treisman DM, Kalluri H, Ezhilan S, Zorniak M, Wheeler DL, Kuo JS: Activation of multiple erbb family receptors mediates glioblastoma cancer stem-like cell resistance to egfr-targeted inhibition. Neoplasia 2012;14:420-428.

30 Erdem-Eraslan L, Gao Y, Kloosterhof NK, Atlasi Y, Demmers J, Sacchetti A, Kros JM, Sillevis Smitt P, Aerts J, French PJ: Mutation specific functions of egfr result in a mutation-specific downstream pathway activation. Eur J Cancer 2015;51:893-903.

31 Lin SY, Makino K, Xia W, Matin A, Wen Y, Kwong KY, Bourguignon L, Hung MC: Nuclear localization of egf receptor and its potential new role as a transcription factor. Nat Cell Biol 2001;3:802-808.

32 Huo LF, Wang YN, Xia WY, Hsu SC, Lai CC, Li LY, Chang WC, Wang Y, Hsu MC, Yu YL, Huang TH, Ding QQ, Chen CH, Tsai CH, Hung MC: Rna helicase a is a DNA-binding partner for egfr-mediated transcriptional activation in the nucleus. P Natl Acad Sci USA 2010;107:16125-16130.

33 Liccardi G, Hartley JA, Hochhauser D: Egfr nuclear translocation modulates DNA repair following cisplatin and ionizing radiation treatment. Cancer Res 2011;71:1103-1114.

SUMMARY

Diffuse gliomas are the most frequent malignant brain tumors in adults, with an incidence of ~ 5 per 100 000 persons in United States each year. With the WHO 2016 classification, diffuse gliomas are grouped into astrocytomas (WHO grade II and grade III), oligodendrogliomas (grade II and III) and glioblastomas (grade IV) based on presence of specific molecular changes (e.g. isocitrate dehydrogenase 1/2 (IDH1/2) mutations) and histological appearance. Current treatments for diffuse glioma patients include surgical resection followed by radiotherapy alone or in combination with chemotherapy. However, progression almost always occurs and most patients eventually die from the disease. To improve the clinical outcome of glioma patients, there is considerable need for novel treatment options. This requires both development of appropriate model systems and a better understanding of the molecular pathways affected by driver mutations within different glioma subgroups. In this thesis we therefore describe two novel model systems and analyzed in detail the effects of IDH1 and EGFR mutations in glioma.

In Chapter 2, we describe the generation of a zebrafish model system for IDH1-mutated gliomas. We have generated over ten different transgenic zebrafish models that expressed *IDH1* mutants under the control of various CNS-specific promoters. A significant increase in the level of D2HG was observed in all transgenic lines expressing *IDH1^{R132C}* or *IDH1^{R132H}* and the elevated D2HG levels could be lowered by treatment of the transgenic zebrafish with an inhibitor of mutant IDH1 activity. However, despite increased levels of D2HG we did not identify a strong phenotype as previously described in other *in vivo* IDH-mutated model systems (e.g. brain hemorrhage in the mouse model or defect wing expansion in the drosophila model). No tumor was observed in our transgenic zebrafish models nor CNS-specific tumors when backcrossing with *tp53*-mutant fish. Therefore, our study suggested that IDH1 mutation alone is not sufficient to promote tumorigenesis. A different model system for IDH mutated tumors is described in Chapter 3, where we have established short-term cultures of primary *IDH*-mutated gliomas, including those with 1p19q co-deletion. Despite a rapid reduction in the number of viable tumor cells, we were able to show that that inhibiting mutant IDH activity does not affect the number or viability of tumor cells. These data are important as they caution the clinical efficacy of these inhibitors.

Studying the molecular pathways affected by driver genes may lead to the identification of novel treatment targets. In Chapters 4 and 5, we therefore studied in detail the molecular pathways affected by mutant IDH1 or EGFR. In Chapter 4, we demonstrated Mul1 is a novel binding partner of both wildtype and mutant IDH1 and its role in regu-

lating the NF-κB pathway is inhibited in IDH1^{R132H}-cells. This deregulation may explain why *IDH*-mutated glioma remain proliferating and suggest MUL1 may be a target for treatment in *IDH*-mutated gliomas. In Chapter 5, we aimed to understand why targeting EGFR in pulmonary adenocarcinomas provided clinical benefit whilst targeting in GBMs has no effect. We made different, tumor-specific, *EGFR* mutation constructs and identified mutation-specific binding partners. This differential binding between EGFR and other proteins likely results in differential activation of downstream pathways and cell migration. Our observations that each mutation activates unique pathways may help explain the disappointing results from clinical trials in GBM patients and argue for the development of mutation specific inhibitors. In Chapter 6 we studied the stability of specific mutations in EGFR. This is important as specific mutations function as treatment targets. We show ~ half of patients expressing EGFRvIII, an in-frame deletion of exons 2-7, lost the mutation at tumor recurrence. Therefore our results caution the use of treatments targeting EGFRvIII at tumor progression when using molecular data from the primary tumor.

In Chapter 7, we grouped patients from the European Organization for Research and Treatment of Cancer (EORTC) 22033-26033 clinical trial into intrinsic glioma subtypes (IGS), molecular subtypes based on gene expression profile. We showed that IGS are prognostic for progression free survival but did not find additional markers associated with survival or treatment response.

In summary, in this thesis, we describe both *in vitro* and *in vivo* model systems for IDH-mutated gliomas and describe novel mutation-specific functional consequences of both IDH1 and EGFR. Our data will help identify novel treatment options for glioma patients and will allow selection of patients that are responsive to treatment.

SAMENVATTING

Diffuse gliomen zijn de meest voorkomende vorm van kwaadaardige hersentumoren bij volwassenen, met een incidentie van ongeveer 5 per 100 000 personen per jaar. Diffuse gliomen worden, volgens de WHO 2016 classificatie van hersentumoren, onderverdeeld in astrocytomen (graad II en III), oligodendrogliomen (graad II en III) en glioblastomen (graad IV). Deze indeling wordt gemaakt op basis van de aanwezigheid van specifieke moleculaire veranderingen (b.v. mutaties in de isocitraat dehydrogenase 1 of 2 genen [*IDH1/2*]) en histologische kenmerken. De standaardbehandeling van gliomen is een chirurgische resectie gevolgd door radiotherapie, al dan niet gecombineerd met chemotherapie. Echter, na verloop van tijd treedt altijd progressie op en de meeste patiënten overlijden uiteindelijk ook aan de ziekte. Vanwege de ernst van de ziekte is er een grote behoefte aan nieuwe behandelmogelijkheden. Dit vereist zowel ontwikkeling van betere wetenschappelijke modelsystemen als een uitgebreidere kennis van de moleculaire processen in de verschillende glioom subtypen. In dit proefschrift beschrijven we twee nieuwe modelsystemen en analyseren we in detail de effecten van *IDH1* en *EGFR* mutaties in gliomen.

In hoofdstuk 2 beschrijven we een nieuw modelsysteem in zebravissen voor gliomen met een *IDH1* mutatie. Hiervoor zijn in totaal meer dan tien verschillende lijnen gemaakt, allen met een net iets andere variant van het IDH1 gen (of een verschillende promoter). In alle lijnen die *IDH1^{R132C}* of *IDH1^{R132H}* tot expressie brachten vonden we een verhoogde concentratie van het D2HG metaboliet. Deze verhoging wordt ook in patiënten waargenomen en kon effectief verlaagd worden door het behandelen van de zebravissen met een *IDH* remmer. We vonden geen aanwijzingen voor het ontstaan van tumoren in onze transgene zebravissen (of andere fenotypische veranderingen), ook niet na kruising met *TP53* gemuteerde zebravissen. Hiermee toonden we aan dat een *IDH1* mutatie alleen (of in combinatie met *TP53*) niet voldoende is voor het ontstaan van tumoren. In hoofdstuk 3 beschrijven we een ander modelsysteem voor *IDH* gemuteerde gliomen. Bij dit systeem werden tumorcellen direct na de operatie voor enige dagen tot enkele weken in leven gehouden in celkweek. Deze kweken werden geïnitieerd voor zowel astrocytaire als oligodendrogliale tumoren (i.e.inclusief gliomen met een co-deletie van chromosomale armen 1p en 19q). Deze korte-termijn kweken zijn belangrijk omdat er nagenoeg geen IDH-gemuteerde glioom cellijnen beschikbaar zijn en cellijnen waarbij de tumor een codeletie heeft van de 1p en 19q chromosomale armen zijn in het geheel (nog) niet beschreven. In ons modelsysteem konden we aantonen het remmen van de mutant activiteit van *IDH* geen invloed had op de levensvatbaarheid van de tumorcellen. Dit is een belangrijke bevinding, omdat het derhalve onzeker is of *IDH* remmers enig klinisch effect kunnen bewerkstelligen.

Het ontrafelen van het effect van genmutaties is een belangrijk onderdeel in de zoektocht naar nieuwe behandelmogelijkheden. In hoofdstuk 4 en 5 hebben we daarom de invloed van *IDH1* en *EGFR* mutaties op de cellulaire signaaltransductie cascades onderzocht. In hoofdstuk 4 tonen we aan dat Mul1 een bindingspartner is van zowel wildtype als gemuteerd IDH1. Tevens toonden we aan dat de regulerende rol van MUL1 in de NF-κB signaaltransductiecascade wordt geremd in cellen met een $IDH1^{R132H}$ mutatie. Deze deregulering kan verklaart mogelijk waarom *IDH*-gemuteerde gliomen ongeremd prolifereren en dat MUL1 potentieel een aangrijpingspunt zou kunnen vormen voor behandeling.

In hoofdstuk 5 hebben we onderzoek gedaan naar het onderliggende mechanisme waarom remming van *EGFR* in longcarcinomen een goed klinisch effect heeft, terwijl behandeling met dezelfde middelen bij *EGFR* gemuteerde glioblastomen geen effect heeft. Interessant gegeven is dat longtumoren en gliomen verschillende typen mutaties hebben in het *EGFR* gen, en het is mogelijk dat hierdoor verschillen in signaaltransductie cascades ontstaan. Om dit te onderzoeken hebben we verschillende *EGFR* constructen gegenereerd met de frequent voorkomende genmutaties zowel van longcarcinomen als van glioblastomen. Het blijkt dat elke mutatie zijn eigen, mutatie-specifieke, bindingspartners heeft. Vervolgens toonden we aan dat deze verschillende bindingspartners leiden tot differentiële activering van signaaltransductie cascades. Deze bevindingen kunnen de teleurstellende trialresultaten van *EGFR* remmers bij glioblastomen verklaren en zou kunnen betekenen dat elke mutatie zijn eigen specifieke remmer nodig heeft. In hoofdstuk 6 onderzochten we de stabiliteit van specifieke *EGFR* mutaties in glioblastomen. We vonden dat bij ongeveer de helft van de patiënten met expressie van *EGFRvIII* (de meest voorkomende mutatie in *EGFR* in hersentumor patiënten) deze mutatie niet meer aanwezig is in de recidief tumor. Omdat de EGFRvIII status van de tumor kan veranderen is voorzichtigheid geboden bij een gerichte behandeling tegen EGFRvIII.

In hoofdstuk 7 hebben we patiënten uit de European Organization for Research and Treatment of Cancer (EORTC) 22033-26033 klinische trial gekarakteriseerd op basis van RNA expressie. We hebben aangetoond dat deze indeling op basis van genexpressie gecorreleerd is met progressievrije overleving en dus dat deze indeling gebruikt kan worden om de prognose van de patiënt te bepalen.

Samenvattend beschrijven we in dit proefschrift zowel *in vitro* als *in vivo* modelsystemen voor *IDH1*-gemuteerde gliomen en beschrijven mutatie-specifieke, functionele gevolgen van zowel *IDH1* als *EGFR* mutaties. Onze bevindingen helpen bij het identificeren van nieuwe behandelmogelijkheden voor gliomen en geven meer inzicht in de selectie van patiënten voor de juiste behandeling.

概要

弥漫性神经胶质瘤是一种成人中最常见的恶性脑瘤，　　　美国年发病率约5人/10万人口。基于特定的分子变化　　（例如异柠檬酸脱氢酶1或2的基因突变）和病理切片特征，2016年的世界卫生组织（WHO）分类方案将弥漫性神经胶质瘤分为星型细胞瘤（二级和三级），少枝细胞瘤（二级和三级）和胶质母细胞瘤（简称GBM，四级）。

目前弥漫性神经胶质瘤的治疗以手术切除为主，术后配合以放疗或化疗，或放化疗结合。然而，随着病情恶化，患者生存率极低。为了提高神经胶质瘤患者的生存率，我们必须寻找新的治疗方法。这需要为不同亚型的神经胶质瘤研发合适的模型系统，以及更好的了解驱动基因突变影响的分子通路。本论文中描述了两个我们所构建的新的模型系统，以及深入的研究了异柠檬酸脱氢酶1（简称IDH1）和表皮生长因子受体（简称EGFR）基因突变在神经胶质瘤成瘤过程中的功能。

在第二章中，我们描述了为带有IDH1突变的神经胶质瘤所构建的斑马鱼模型系统。我们构建了十余种由各类神经中枢系统特异性转录因子所调控的不同IDH1基因突变的转基因斑马鱼模型。D-2 -羟基类固醇（简称D2HG）在所有表达IDH1R132C 突变的斑马鱼模型中有明显的升高，并且升高的D2HG可被IDH1抑制剂降低。然而，除了D2HG的升高，我们并未发现其他带有IDH突变的活体动物模型中描述过的表型（例如老鼠模型中的脑出血，或者果蝇模型中的翅膀伸展缺陷）。我们的斑马鱼模型中并未发现任何肿瘤，甚至与带有tp53突变的斑鱼杂交后也没有产生中枢神经系统类的肿瘤。因此我们认为单有IDH1基因突变不足以促使神经胶质瘤的形成。

第三章描述了我们为IDH1突变的肿瘤所构建的体外模型，即短期原代体外培养的神经胶质瘤，这当中还包含了带有1p19q co-deletion的胶质瘤。尽管体外培养引起存活的肿瘤细胞数量急剧下降，我们发现IDH1抑制剂能有效抑制IDH1的癌变酶活性，同时并不影响肿瘤细胞的生长。我们的研究结果建议进行IDH1抑制剂的临床测试需谨慎。

研究驱动基因突变影响的分子通路对于寻找新型治疗方法起着重要的作用。IDH1和EGFR突变是两个不同弥漫性胶质瘤亚型的驱动基因。因此，在第四章和第五章，我们深入研究了被IDH1和EGFR基因突变影响的分子通路。在第四章中我们新发现Mul1不仅是IDH1野生型和突变型的结合蛋白，并且，Mul1调控NF-□ B 通路的功能在IDH1R132H突变的细胞中受阻。这个发现可以解释为何神经胶质瘤细胞可以不受控制的生长。我们因此也建议Mul1可以在未来作为治疗IDH1突变的神经胶质瘤的靶点。在第五章中，我们旨在研究为何肺癌中EGFR靶向疗法有很好的临床效果而在胶质母细胞瘤中却没有任何疗效。我们做了不同的肿瘤特异性EGFR突变的质粒，找到了突变特异性的结合蛋白。不同EGFR突变型与不同的蛋白结合反应，最终激活了不

同的下游信号通路引起了细胞增值和迁移。我们的研究结果可以帮助解释EGFR靶向疗法的临床测试在胶质母细胞瘤患者中的失败，同时我们的结果建议研发具有EGFR突变特异性的抑制剂作以为新的靶向疗法。

在第六章中，我们研究了EGFR突变在肿瘤原发和复发时的状态。这一研究对于靶向疗法有着重要意义。我们的数据显示近一半带有EGFRvIII突变的胶质母细胞瘤患者在肿瘤复发时失去了EGFRvIII突变。由于靶向疗法是基于原发肿瘤的分子状态而决定的，因此带有EGFRvIII的患者在肿瘤复发的时候需谨慎选择靶向疗法。

第七章中，我们将欧洲癌症治疗研究组织（EORTC）22033-26033 临床测试中的病人基于基因表达的简况分组到本征胶质瘤亚型（IGS）中。我们发现IGS有评估预后的价值。但是我们并未找到因放化疗提高存活时间的分子标志物。

总的来说，在这篇论文里我们描述了带有神经胶质瘤IDH突变的体内和体外的模型系统，并描述了IDH1和EGFR功能上的突变特异性。我们的发现可以帮助神经胶质瘤患者寻找新的潜在靶向治疗方案，也可以为携带不同基因突变的病人寻找更有效的疗法。

ACKNOWLEDGEMENT

Finally I'm writing my favorite chapter!

Reaching the finishing line of a journey to obtain my PhD would be impossible without the support and help from my colleagues, friends and family. I would like to thank everyone who has helped me during this journey. Because of you, the past five years have become much easier than it could have been.

Dear **Prof. Dr. Peter Sillevis Smitt**, my promoter, thank you for all the remarks and suggestions during our bi-monthly one-on-one work discussion. I really enjoy discussing science with you. I'm also very impressed by your ambition when it comes to sports. When I just finished a 10k-run at the strijd van salland event, you went for a second round of 60k-cycling. You are a very cool big boss!

My greatest thanks and appreciation must go to my supervisor, **Dr. Pim French**. Thank you so much for giving me the opportunity to join your research group. I still remember how we met the first time. It was in Manchester in September 2012. Because of rejected Schengen visa application, I couldn't make it to the interview that we've planned at the Erasmus MC in the Netherlands. You showed understanding and profession for this unexpected situation by offering to fly to Manchester for the interview. Working for/with you in the past five years, I have learned so much about how to be a critical scientist and how to do proper research. I always admire your broad and deep knowledge in both fundamental and clinical research, and of course your R programming skills. You have always been a model for my career and I hope that one day in the future, I could have my own research group just like you do. Moreover, as the only non-Dutch speaking member of the team, I had a definite soft landing in the lab because of you. I truly appreciate everything you did for me, your support, your patience and your jokes. And thanks for inspiring me in sports. Thank you for being not only a supervisor but also a great friend to me.

Dear **Dr. Martine Lamfers**, thank you for giving me the opportunity to join your research group and collaborate on the project for culturing lower grade gliomas. Thanks for all the remarks for my papers and thesis. I have learned a lot from you and I appreciate that you helped me to become a very independent researcher.

I would like to thank the rest members of my small committee: **Prof. Dr. John Martens**, **Prof. Dr. Judith Bovée** and **Prof. Dr. Rob Willemsen**, for reading and assessing my thesis thoroughly.

To my direct colleagues:

Dear **Lale**, getting to know you and working with you was one of the best things happen to me when I re-started my life in the Netherlands. We have so much in common and we have so much to share. Thank you for pushing me to finish up my thesis. Thank you for your career advice. Thank you for helping me with moving. Thank you for finding me a plumber when I had troubles with my bathroom. I was so glad that you stayed at the Erasmus MC for your new job. I enjoy all the coffee time with you and the great Turkish food you made.

Dear **Maarten**, thank you for patiently explaining all the medical terms during our discussion. Thank you for explaining why the proposition page is a very important tradition in a Dutch PhD thesis. Thank you for helping me with translating all my Dutch mails and bills. Thank you for saving me €7k when I bought the kitchen (together with Pim). Thank you for filling up my tax forms. Thank you for bringing me to the emergency room when I sprained my ankle. Thanks for your trust in my driving skills when no one in the lab dares to sit in my car… (due to limited space I'll only mention those above as examples). I am so glad to work with you and become a good friend with you. Thank you for being my paranymph for my defense!

Dear **Azi**, my other lovely paranymph, I'm so glad to become one of your best friends during the last year of our PhD. Thank you for dragging me for running and of course, your favorite workout. I enjoy every moment when we talk, drink, have dinner on no matter how short of a notice. Good luck with your new life in Belgium and a wonderful time with Tjitse. As you said, Belgium isn't far away and we can visit each other, any time!

Dear **Iris**, the lord, thank you for helping me with all the experiments. Thank you for helping me with making plans. Thank you for comforting me when I'm stressed. Thank you for giving me confidence when I'm doubting myself. Thank you for being so positive like sunshine in the lab. I enjoyed working with you and also having drinks, (Korean-) BBQ with you.

Dear **Bas** and **Kaspar**, you two are the funniest guys in the lab. I lost counting on how many times I teared because you guys made me laugh so hard. Besides, thanks for those great times with discovering high-quality food and drinks in the city.

Dear **Zineb**, thank you for our quality time during coffee breaks at the Erasmus and our trips in Madrid, Las Vegas, San Francisco and Yosemite. You are like an older sister

to me. Thank you for being patient with me and always grinning with "oh my god Diya….you are kidding me". Thank you for giving me so many great advises for life and career.

Dear **Maurice**, thank you for helping me with all the experiments during my PhD. You are the first student I guided during my PhD but I think you taught me a lot especially when it comes to cloning. Dear **Bart**, thank you for all the experiments you did for the EGFR project. You are an excellent student and your contribution to the projects has released a lot of stress from me. I'm so glad that you'll stay at the Erasmus MC for a new job. Any lab is lucky to have you.

Dear **Esther**, thank you so much for your patience since I happen to have quite some last-minute orders for reagents before your vacation. Dear **Mariska**, I always enjoy the nice (cup-)cakes you made and thank you for sharing interesting stories about your guinea pigs.

Dear **Mircea**, thanks for creating shade for me with your shirt when I was bothered by the intensive sunshine during our trip in Paris. Thanks for being so sweet and mean to me at the same time. Thanks for sharing snacks and candy in the office so often (you always catch the moment when I'm on a diet).

To the ones in the lab of Neurosurgery, dear **Cassandra**, **Jenneke**, **Marielle**, **Tessa** and **Trisha**, many thanks for your kind help and support whenever I worked on the 22nd floor. Dear **Eric**, thank you so much for fixing my computer and sharing fun stories during lunch. Dear **Sieger** and **Jeroen**, thanks for your questions, remarks and suggestions at the neuro-oncology meetings in the past years.

Lots of thanks to my colleagues at the group of proteomics, **Lona**, **Coşkun**, **Martijn**, **Lennard** and **Theo**. Thanks for generously sharing lab materials in the past few years and joyful time during the retreat of neuro-oncology.

Dear **Tjakko**, you are a great scientist. I enjoy discussing science with you. And many thanks for your suggestions for the zebrafish project. Dear **Herma**, I'm always amazed when we do experiments with zebrafish. You are practically a "walking protocol" when it comes to experiments with zebrafish. Thanks for your guidance with all of the zebrafish work during my PhD.

Dear **Marcel** and **Thierry**, thank you for kindly sharing/giving buffers and antibodies with/to me. Marcel, you even did quite some IHC staining for my project without any hesitate. Your kind help and support means a lot to me.

Dear **Dr. Martin van Royen**, thanks for your kind help with the live-cell imaging and the FRAP experiments. I also enjoy the fun chit-chat with you in the labs or the hallway of JNI.

亲爱的**爸爸妈妈**, 感恩你们一直以来物质上,精神上无私的支持. 你们是我学习, 生活和工作等等一切一切的榜样. 有这样的爸爸妈妈真的很骄傲很满足. 自从2007年出国以来,我们一直聚少离多. 谢谢你们的体谅,也谢谢你们把自己的生活照顾的那么好, 让我跟大文文在外学习少了很多担忧与牵挂. 亲爱的**姥爷姥姥**, 感谢这一路的支持. 谢谢你们总想着了解我的科研动向. 每次回家都能收到姥爷的墨宝尝到姥姥准备的佳肴. 祝福你们身体健康, 福寿绵长.

亲爱的**大文文**, 亲爱的姐姐, 感谢出国至今一直有你陪伴. 终究还是你先做了高博士. 希望你会一直不忘初心,保持对科研的热忱, 也希望这份热忱会带给你美好的未来. 我们家未来第一个教授应该就是你了! 也祝福你跟杨帆早日开花结果. 在瑞士学成尽早回荷兰跟我们团聚.

感谢大济南和北京的亲戚们, 每次回家的时候总会有你们热情的招待和对中国酒文化的深刻指导. 也谢谢你们每逢各类传统佳节总会与我们的父母一起庆祝, 减轻了许多他们的惦念之情.

Dear 若愚,我们的邢总, 第一次见你的时候就觉得怎么会有这么有气质的美女出现在医学院呢. 再后来我们变成了无话不谈的好朋友. 不论是开心的还是压抑的时刻, 我们总会分享,相互见证了彼此的成长. 你的自律一直是我想要学习的目标. 如今事业家庭双丰收, 祝福你和Max幸福甜蜜, 现在只缺一个娃了 (我觉得我就是你麻麻派来的救兵哈哈).

Dear 黄玲, 很庆幸认识你, 聪明独立体贴的你. 你对问题总是有很独到的见解. 当我束手无策的时候你总是可以帮我逻辑的分析再给我一个很理智的建议. 你在我心里就像我的姐姐一样. 谢谢你让我做你的paranymph, 见证了一个新晋妈妈是如何边带孩子边准备答辩然后无缝衔接成功入职深圳的医院的过程. 祝福你和同伟还有路可在深圳生活顺心, 也希望你们可以有空多回荷兰跟我们聚聚.

Dear 莹颖, 经常在晚上离开实验室的时候碰到你去实验室. 每次看到你都觉得你好厉害. 带着恒宇宝宝倒也不耽误你跟大家出来聚餐玩狼人杀. 跟你总有说不完的话. 谢谢你给我的指引, 生活,学习还有工作上的. 也谢谢你对我的认可, 在我迷茫的时候. 你的

肯定对我的意义很大. 好开心你最终选择了在荷兰工作, 未来还有很多很多需要你带着我去探索.

Dear **平臻**, 从内梅亨到鹿特丹, 我们11年的友情从未间断过. 谢谢你们系里有好玩的活动都会带上我, 也因为你, 我熟识了更多的朋友. 说到做实验最拼的就是你. 见你发了那么多大文章为你高兴的同时, 总想告诉你还是要好好休息. 祝福你跟Mirjam幸福快乐, 双双顺利毕业, 未来可以做自己想做的事情.

Dear **温蓓**, 蓓蓓, 谢谢你还有刘老师过去对我的帮助, 当然最重要的是谢谢你带来的欢乐(虽然我们总是吵吵闹闹). 有你在的饭局, 狼人杀和小木屋的旅行总是那么开心. 你的智慧在各类事情上都体现的淋漓尽致. 一直觉得你就是刘老师身边长不大的小女孩, 可自从你生完双胞胎以后, 心理素质和生活能力简直就像是开了外挂. 希望两个宝宝健康快乐的成长, 跟刘老师早日团聚. 期待早日参加你的博士答辩.

Dear **长斌**, 我们的北半球一哥. 读博最早认识你, 像你这样学识渊博做饭又好吃还很贴心的医生真的太少啦. 晚上或者周末在实验室加班的时候总能碰到你. 缺了试剂跑去找你也总是能借到. 很开心课余时间可以找你讨论课题, 也很感谢你传授/分享那些读文章和做实验的经验. 虽然你回国以后并未继续做医生, 但我觉得你这样的人才在哪里都可以为医疗事业做出贡献. 祝愿早日找到女朋友这样就可以用大家给你凑得那份女友基金啦!

Dear **吴斌**, 我们的吴医生. 文艺青年说的就是你, 去撒哈拉拍沙漠, 去北极圈拍极光, 还有你拉着大家去大湖那边拍流星. 正因为这样我们一起出去玩的时候总是你负责给大家拍大片. 你有咱们山东人的仗义还有热情, 感谢你过去的几年对我的照顾和帮助. 看到你和祥瑞那么幸福真心为你高兴. 未来希望你顺利毕业, 早点在荷兰安家.

Dear **陈思**, 思姐, 你积极向上充满活力的性格一直感染着我. 从荷兰的高中一路优秀毕业生到博士, 不到你毕业都不知道你一直都是那么优秀. 那么低调的你, 在跳舞的时候会毫不吝啬的闪光. 每次跟你girls night out都好开心. 有你在的聚会总是充满欢乐. 祝福你的事业继续大展宏图, 跟Bob永远幸福.

Dear **小鲁**, 谢谢过去几年里的无话不谈和倾力相助. 尽管你很宅, 但是常常跟大家一起出来玩. 你的冷幽默真的很好笑. 学术做的那么好,身后一票迷妹追着. 希望你尽快找到理想的妹子, 未来顺利毕业.

Dear **展民**, 谢谢你和莹颖时常叫我去你们家吃饭, 你的厨艺实在是太惊艳了. 谢谢你在我需要的时候总是随叫随到(当然也要谢谢莹颖的指导方针). 希望未来能找到自己喜欢的工作, 顺利毕业, 开心带娃.

Dear **舟桥**, 谢谢你组织打彩蛋 让我认识了那么多MC的小伙伴. 谢谢你开车带我们去南法. 有你在的狼人杀, k歌总是那么尽兴. 因为你常去跑马拉松, 也带动了我对长跑的热情. 不管在哪里你都是那么耀眼. 在国内做医生很辛苦也要注意身体. 祝你和女朋友幸福美满, 有机会常回荷兰看看.

Dear **潇磊**, 有才就是任性. 在国内做医生太累就转行回荷兰做律师可能只有你做得出来. 谢谢你毫无保留的分享各类经验, 谢谢你出乎意料的搞笑, 谢谢你帮我照顾调皮捣蛋的兔兔. 每次跟你吃饭狼人杀都好开心. 祝愿你早日成家, 事业顺心.

Dear **海波**, 对你是相见恨晚. 谢谢你过去的倾力相助. 还有一起计划出游, 挖生蚝钓螃蟹. 最开心就是跟你一起玩狼人杀, 还有你的搞笑和正宗的济宁口音的普通话. 佩服你坚定不移要在学术的路上走下去的决心. 为你在发了那么多大文章而高兴. 未来的周教授, 祝福你早日跟女朋友修成正果, 更多的CNS.

Dear **俊俊**, 好开心认识那么特别的你, 谢谢你对我的认可, 谢谢你组织那么多次活动. 你拿到全荷狼王的桂冠的时候好为你开心. 祝愿在牛津的新工作开心顺利, 早日跟男朋友团聚. 外面世界好大, 年轻的你真的应该继续闯一闯.

Dear **步子文**, 大文姐，谢谢你让我爸妈把你当半个闺女使唤，谢谢你贴心的卡片和礼物。 Dear **于雪**, 眼眼，谢谢你这枚开心果一直以来的陪伴，支持和鼓励。Dear **王祖程**, 海豹， 即使我不在济南, 因为你在, 我妈妈从未错过母亲节和生日的鲜花。Dear **张郑思**, 宝宝，谢谢你不管走多远都不忘用明信片的方式分享当地的喜悦，谢谢你每次回国都带我吃好的玩好的。

茜薇, Henk-Jelle, Jack, 二师兄, 浩波, 秋实, 静静, 笑非, 婉璐, 国颖, 文世, 姚瑶, 文浩, 娜娜姐, 杉哥, 璐璐, 罗南姐, 张凯哥, 涛哥, 武医生, 贺英, 陈忠丽, 超平, 凯音, 世豪, 小岳岳, 孙伟, 每次聚餐, 狼人杀, 出游, 滑雪都好开心. 谢谢你们带来的欢乐和陪伴, 让我在荷兰的生活从不觉得寂寞. 愿我们每个人都能过上自己想要的生活, 不论未来在哪里, 期待我们的友情永不散场.

Dear **David**, my schatje, my fiancé, thank you for taking care of me, our life, our house and Tutu. Thank you for your support, patience and understanding during my PhD. I'm so lucky to have you in my life and I'm looking forward to the future that we are about to build up together.

LIST OF PUBLICATIONS

1. **Gao Y**, de Wit M, Struys EA, van der Linde HCZ, Salomons GS, Lamfers MLM, Willemsen R, Sillevis Smitt PAE, and French PJ. IDH1-mutated transgenic zebrafish lines: An in-vivo model for drug screening and functional analysis. *PLoS One*; 2018, 13(6): e0199737

2. **Gao Y**, Weenink B, van den Bent MJ, Erdem-Eraslan L, Kros JM, Smitt PAES, Hoang-Xuan K, Brandes AA, Vos M, Dhermain F, Enting R, Ryan GF, Chinot O, Ben Hassel M, van Linde ME, Mason WP, Gijtenbeek JMM, Balana C, von Deimling A, Gorlia T, Stupp R, Hegi ME, Baumert BG, and French PJ. Expression-based intrinsic glioma subtypes are prognostic in low-grade gliomas of the EORTC22033-26033 clinical trial. *European Journal of Cancer*; 2018, 94: 168-178

3. **Gao Y**, Wies Vallentgoed and Pim J. French. Finding the right way to target EGFR in glioblastomas; lessons from Lung Adenocarcinomas. *Cancers* **2018**, *10*(12), 489; doi: 10.3390/cancers10120489

4. **Gao Y**, de Wit M, de Heer I, Prince J, Struys EA, Verheul C, Salomons GS, Sillevis Smitt PAE, and French PJ. Oncogenic mutations in IDH1 affect the MUL1-mediated NF-κB pathway activation. *Under revision*.

5. **Gao Y**, Verheul C, de Wit M, de Heer I, Struys EA, Dubbink HJ, Atmondimedjo PN, Pierson TM, Salomons GS, Leenstra S, Sillevis Smitt PAE, Lamfers MLM* and French PJ*. Reducing D2HG by AGI-5198 does not affect the tumor cell population in short-term primary cultures of IDH-mutated gliomas. *Manuscript in preparation. * co-last author*

6. **Gao Y,** de Wit M, Mercieca D, de Heer I, van Royen M, Aerts J, Sillevis Smitt PAE, French PJ. Protein aggregate formation predicts clinical responses to EGFR Tyrosine Kinase Inhibitors. *Manuscript in preparation.*

7. Erdem-Eraslan L, van den Bent MJ, Hoogstrate Y, Naz-Khan H, Stubbs A, van der Spek P, Bottcher R, **Gao Y**, de Wit M, Taal W, Oosterkamp HM, Walenkamp A, Beerepoot LV, Hanse MCJ, Buter J, Honkoop AH, van der Holt B, Vernhout RM, Smitt PAES, Kros JM, and French PJ. Identification of Patients with Recurrent Glioblastoma Who May Benefit from combined Bevacizumab and CCNU Therapy: A Report from the BELOB Trial. *Cancer Research*; 2016, 76(3): 525-534

8. Draaisma K, Wijnenga MMJ, Weenink B, **Gao Y**, Smid M, Robe P, van den Bent MJ, and French PJ. PI3 kinase mutations and mutational load as poor prognostic markers in diffuse glioma patients. *Acta Neuropathologica Communications; 2015, 3:*

9. van den Bent MJ, **Gao Y**, Kerkhof M, Kros JM, Gorlia T, van Zwieten K, Prince J, van Duinen S, Smitt PAS, Taphoorn M, and French PJ. Changes in the EGFR amplification and EGFRvIII expression between paired primary and recurrent glioblastomas. *Neuro-Oncology*; 2015, 17(7): 935-941

10. Erdem-Eraslan L*, **Gao Y***, Kloosterhof NK, Atlasi Y, Demmers J, Sacchetti A, Kros JM, Smitt PS, Aerts J, and French PJ. Mutation specific functions of EGFR result in a mutation-specific downstream pathway activation. *European Journal of Cancer*; 2015, 51(7): 893-903. *co-first author*

11. Karuppiah V, Collins RF, Thistlethwaite A, **Gao Y,** and Derrick JP. Structure and assembly of an inner membrane platform for initiation of type IV pilus biogenesis. *Proc Natl Acad Sci U S A;* 2013, 110(48): E4638-47

PH.D. PORTFOLIO

Name PhD student:	Ya Gao
Erasmus MC Department:	Neurology
Research School:	Molecular Medicine
PhD period:	2013-2017
Promoter	Prof. Peter A.E. Sillevis Smitt
Co-promoters	Dr. Pim J. French
	Dr. Martine L. Lamfers

PhD training

Courses	Year	ECTS
Basic and Translational Oncology	2013	1.8
Ensembl Workshop	2013	0.6
InDesign CS5	2013	0.15
Research management	2013	1
Laboratory Animal Science (Article 9)	2013	3
Research Integrity	2014	0.3
Biomedical English Writing	2014	2
Biostatistics Methods I	2014	2
Basic R workshop	2016	1.8

(Inter) national conferences and presentations		
CBG/CGC Meeting, *poster*	2014	0.4
Society for Neuro-Oncology (SNO) Annual Meeting Miami, FL, *Poster*	2014	0.4
American Association for Cancer Research (AACR) Annual Meeting, New Orleans, LA, *poster*	2016	0.4
Erasmus MC Molecular Medicine (MolMed) Day, *oral and poster*	2014-2017	0.8

Other meetings		
Weekly Josephine Nefkens Institute (JNI) research Meetings, *oral*	2013-2017	2
Biweekly Neuro-oncology Meetings, *oral*	2013-2017	2
Monthly MolMed Oncology lectures	2013-2017	1
Bimonthly Zebrafish Meetings, *oral*	2015-2017	1

Teaching		
Supervising HLO technicians in training	2013-2017	15

ABOUT THE AUTHOR

Gao Ya was born in *Jinan, Shandong, China* on 29th November 1988. In 2007 she came to *the Netherlands* for a bachelor program in Life Sciences at the Hogeschool van Arnhem en Nijmegen. During her bachelor she went to Leiden University for an internship (supervised by Prof. Dr. Cees van den Hondel), focused on antifungal drug screening. She obtained her Bachelor of Applied Science degree in 2011 after finishing her thesis on characterizing cholinergic neurons in sleep-deprived mice at the University of Pennsylvania in the *United States* (supervised by Prof. Dr. Allan Pack). In that same year she continued her MSc study at the University of Manchester in the *United Kingdom*. During her MSc, she majored in Biochemistry and joined Prof. Dr. Jeremy Derrick's lab for structural studies of proteins involved in biosynthesis of Type IV Pilus in *Neisseria meningitides*. After completing her thesis on the role of LITAF (lipopolysaccharide-induced TNFα Factor) in ubiquitin-mediated protein degradation supervised by Prof. Dr. Phillip Woodman, she received her Master of Sciences degree in 2012. Gao Ya was inspired by disease-driven research and the challenges in cancer research has always been attractive to her. In 2013, she moved back to *the Netherlands* and joined Dr. Pim French's lab for her PhD where she did research on *IDH1* and *EGFR* mutations in gliomas. Since November 2017, she continued her research on EGFR mutations in glioblastomas and non-small-cell lung cancers as a post-doctoral fellow in the same group.